(Bergtold *et al.*, 2005; Mousavi *et al.*, 2007). These reports suggest that an antibody with enhanced binding affinity to FcγRIIa would be more rapidly eliminated from plasma by FcγRIIa-mediated uptake and degradation than wild-type IgG1, while an antibody with enhanced binding only to FcγRIIb would have a longer half-life because the antibody would be recycled back to the cell surface. Indeed, an antibody with enhanced binding to both murine FcγRII and FcγRIII (counterpart of human FcγRIIa) exhibited more rapid clearance from plasma compared with an antibody with enhanced binding only to murine FcγRII (data not shown).

These facts indicate that therapeutic IgG with S267E/L328F substitution has the potential to induce platelet aggregation and activation and to be rapidly cleared from plasma in patients with FcγRIIa^{R131} genotype. One report described that the allelic frequency of R/R131, R/H131 and H/H131 is 31, 44 and 25%, respectively, among healthy Caucasians, and 26, 43 and 31%, respectively, among healthy African Americans (Lehrnbecher *et al.*, 1999). Another report showed that in Japanese, Chinese and Asian Indian populations the R/R131 genotype occurs in 6, 6 and 31%, respectively (Osborne *et al.*, 1994). Considering the proportion of populations with R/R and R/H genotypes, enhancing the binding affinity to FcγRIIa^{R131} would have a substantial impact.

Previous studies using S267E/L328F or S267E substitution(s) have demonstrated that enhancing affinity to FcγRIIb is a promising application for therapeutic antibodies against CD19, IgE, DR5 and CD40 (Li and Ravetch, 2011, 2012; Chu *et al.*, 2012; Hammer, 2012). Consistent with these reports, V12 variant, as well as S267E/L328F variant, enhanced agonistic activity of antibody against CD137, one of TNFR superfamily molecules, compared with intact human IgG1. Since agonistic antibodies against TNFR superfamily are currently being explored for cancer immunotherapy, enhancement of the agonistic activity of these antibodies by selectively improving the binding affinity for FcγRIIb could be a promising approach. In addition, in Ba/F3 cells expressing constitutively active mutants of the receptor tyrosine kinase, Kit, ICs that crosslinked FcγRIIb and Kit inhibited growth factor-independent proliferation (Malbec and Daëron, 2012). In another report, ICs suppressed the TLR4-mediated response of DCs in rheumatoid arthritis patients through FcγRIIb. Each of these effects of FcγRIIb could be enhanced by applying Fc with enhanced affinity for FcγRIIb. Moreover, ICs significantly suppressed expression of CD40, CD80 and CD86 on FcγRIIb-overexpressing DCs, suggesting that in DCs, using ICs consisting of an antibody variant with selectively enhanced FcγRIIb affinity relative to FcγRIIa might polarize IC-triggered activating signals to inhibitory signals (Zhang *et al.*, 2011).

Conclusion

In this study, we screened antibody Fc variant which selectively enhances the binding affinity to FcγRIIb over both FcγRIIa^{R131} and FcγRIIa^{H131} by comprehensive mutagenesis. We identified a distinct substitution, P238D, that could discriminate FcγRIIb from FcγRIIa^{R131} precisely, and crystal structural analysis revealed that this substitution substantially changed the recognition interface of Fc-FcγRIIb. We further designed an antibody variant with 200-fold higher affinity for FcγRIIb than IgG1 without increasing the affinity for other active FcγRs. The variant was comparable with IgG1 in terms of pharmacokinetics and storage stability. We also showed that an antibody with increased affinity for FcγRIIa has an increased possibility of inducing platelet activation and aggregation and of being rapidly cleared from plasma. Since previous studies and our study using agonist anti-CD137 antibody suggested that increasing the binding affinity to FcγRIIb has various therapeutic applications, our engineered Fc, which enhances binding selectivity to FcγRIIb, is expected to have a significant therapeutic potential.

Supplementary data

Supplementary data are available at *PEDS* online.

Acknowledgements

We thank our colleagues at Chugai Research Institute for Medical Science, Inc. and Chugai Pharmaceutical Co., Ltd: M.Fujii, Y.Nakata, A.Maeno and S.Masujima for antibody generation; W.Hatakeyama and M.Saito for carrying out SPR analysis; M.Irie for carrying out preparation of GST-EndoF1; R.Saito for carrying out platelet aggregation assay and A.Sakamoto, M.Okamoto and M.Endo for carrying out preparation of human FcγRs.

Funding

This work was fully supported by Chugai Pharmaceutical Co., Ltd. Funding to pay the Open Access publication charges for this article was provided by Chugai Pharmaceutical Co., Ltd.

References

Bergtold,A., Desai,D.D., Gavhane,A. and Clynes,R. (2005) *Immunity*, **23**, 503–514.
Boruchov,A.M., Heller,G., Veri,M.C., Bonvini,E., Ravetch,J.V. and Young,J.W. (2005) *J. Clin. Invest.*, **115**, 2914–2923.
Boumpas,D.T., Furie,R., Manzi,S., Illei,G.G., Wallace,D.J., Balow,J.E. and Vaishnaw,A.; BG9588 Lupus Nephritis Trial Group. (2003) *Arthritis Rheum.*, **48**, 719–727.
Brekke,O.H. and Sandlie,I. (2003) *Nat. Rev. Drug Discov.*, **2**, 52–62.
Cemerski,S., Chu,S.Y., Moore,G.L., Muchhal,U.S., Desjarlais,J.R. and Szymkowski,D.E. (2012) *Immunol. Lett.*, **143**, 34–43.
Chu,S.Y., Vostiar,I., Karki,S., Moore,G.L., Lazar,G.A., Pong,E., Joyce,P.F., Szymkowski,D.E. and Desjarlais,J.R. (2008) *Mol. Immunol.*, **45**, 3926–3933.
Chu,S.Y., Horton,H.M., Pong,E., *et al.* (2012) *J. Allergy Clin. Immunol.*, **129**, 1102–1115.
Crowley,J.E., Stadanlick,J.E., Cambier,J.C. and Cancro,M.P. (2009) *Blood*, **113**, 1464–1473.
Dall'Acqua,W.F., Cook,K.E., Damschroder,M.M., Woods,R.M. and Wu,H. (2006) *J. Immunol.*, **177**, 1129–1138.
DeLano,W.L. (2002) *The PyMOL Molecular Graphics System*. Palo Alto, CA, Schrödinger, LLC.
Desai,D.D., Harbers,S.O., Flores,M., Colonna,L., Downie,M.P., Bergtold,A., Jung,S. and Clynes,R. (2007) *J. Immunol.*, **178**, 6217–6226.
Emsley,P., Lohkamp,B., Scott,W.G. and Cowtan,K. (2010) *Acta Cryst.*, **D66**, 486–501.
Evans,P. (2006) *Acta Cryst.*, **D62**, 72–82.
Grueninger-Leitch,F., D'Arcy,A., D'Arcy,B. and Chène,C. (1996) *Protein Sci.*, **5**, 2617–2622.
Hammer,O. (2012) *mAbs*, **4**, 571–577.
He,F., Hogan,S., Latypov,R.F., Narhi,L.O. and Razinkov,V.I. (2010) *J. Pharm. Sci.*, **99**, 1707–1720.
Hernández,T., de Acosta,C.M., López-Requena,A., Moreno,E., Alonso,R., Fernández-Marrero,Y. and Pérez,R. (2010) *Mol. Immunol.*, **48**, 98–108.
Heyman,B. (2003) *Immunol. Lett.*, **88**, 157–161.
Horton,H.M., Chu,S.Y., Ortiz,E.C., *et al.* (2011) *J. Immunol.*, **186**, 4223–4233.
Igawa,T., Tsunoda,H., Tachibana,T., *et al.* (2010) *Protein Eng. Des. Sel.*, **23**, 385–392.
Kabsch,W. (2010) *Acta Cryst.*, **D66**, 125–132.

Lehrnbecher,T., Foster,C.B., Zhu,S., Leitman,S.F., Goldin,L.R., Huppi,K. and Chanock,S.J. (1999) *Blood*, **94**, 4220–4232.
Leibson,P.J. (2004) *Curr. Opin. Immunol.*, **16**, 328–336.
Li,F. and Ravetch,J.V. (2011) *Science*, **333**, 1030–1034.
Li,F. and Ravetch,J.V. (2012) *Proc. Natl Acad. Sci. USA*, **109**, 10966–10971.
Maggon,K. (2007) *Curr. Med. Chem.*, **14**, 1978–1987.
Malbec,O. and Daëron,M. (2012) *Immunol. Lett.*, **143**, 28–33.
McCoy,A.J., Grosse-Kunstleve,R.W., Adams,P.D., Winn,M.D., Storoni,L.C. and Read,R.J. (2007) *J. Appl. Crystallogr.*, **40**, 658–674.
Meyer,T., Robles-Carrillo,L., Robson,T., Langer,F., Desai,H., Davila,M., Amaya,M., Francis,J.L. and Amirkhosravi,A. (2009) *J. Thromb. Haemost.*, **7**, 171–181.
Mössner,E., Brünker,P., Moser,S., *et al.* (2010) *Blood*, **115**, 4393–4402.
Mousavi,S.A., Sporstøl,M., Fladeby,C., Kjeken,R., Barois,N. and Berg,T. (2007) *Hepatology*, **46**, 871–884.
Murshudov,G.N., Skubák,P., Lebedev,A.A., Pannu,N.S., Steiner,R.A., Nicholls,R.A., Winn,M.D., Long,F. and Vagin,A.A. (2011) *Acta Cryst.*, **D67**, 355–367.
Nimmerjahn,F. and Ravetch,J.V. (2005) *Science*, **310**, 1510–1512.
Nimmerjahn,F. and Ravetch,J.V. (2008) *Nat. Rev. Immunol.*, **8**, 34–47.
Nimmerjahn,F. and Ravetch,J.V. (2012) *Cancer Immun.*, **12**, 13.
Osborne,J.M., Chacko,G.W., Brandt,J.T. and Anderson,C.L. (1994) *J. Immunol. Methods*, **173**, 207–217.
Pollreisz,A., Assinger,A., Hacker,S., *et al.* (2008) *Br. J. Dermatol.*, **159**, 578–584.
Ramsland,P.A., Farrugia,W., Bradford,T.M., *et al.* (2011) *J. Immunol.*, **187**, 3208–3217.
Richards,J.O., Karki,S., Lazar,G.A., Chen,H., Dang,W. and Desjarlais,J.R. (2008) *Mol. Cancer Ther.*, **7**, 2517–2527.
Robles-Carrillo,L., Meyer,T., Hatfield,M., *et al.* (2010) *J. Immunol.*, **185**, 1577–1583.
Scappaticci,F.A., Skillings,J.R., Holden,S.N., *et al.* (2007) *J. Natl Cancer Inst.*, **99**, 1232–1239.
Shuford,W.W., Klussman,K., Tritchler,D.D., *et al.* (1997) *J. Exp. Med.*, **186**, 47–55.
Smith,P., DiLillo,D.J., Bournazos,S., Li,F. and Ravetch,J.V. (2012) *Proc. Natl Acad. Sci. USA*, **109**, 6181–6186.
Stavenhagen,J.B., Gorlatov,S., Tuaillon,N., *et al.* (2007) *Cancer Res.*, **67**, 8882–8890.
White,A.L., Chan,H.T., Roghanian,A., *et al.* (2011) *J. Immunol.*, **187**, 1754–1763.
White,A.L., Chan,H.T., French,R.R., Beers,S.A., Cragg,M.S., Johnson,P.W. and Glennie,M.J. (2013) *Cancer Immunol Immunother.*, **62**, 941–948.
Wilson,N.S., Yang,B., Yang,A., *et al.* (2011) *Cancer Cell*, **19**, 101–113.
Winter,G. (2010) *J. Appl. Cryst.*, **43**, 186–190.
Zalevsky,J., Leung,I.W., Karki,S., Chu,S.Y., Zhukovsky,E.A., Desjarlais,J.R., Carmichael,D.F. and Lawrence,C.E. (2009) *Blood*, **113**, 3735–3743.
Zhang,C.Y. and Booth,J.W. (2010) *J. Biol. Chem.*, **285**, 34250–34258.
Zhang,Y., Liu,S., Yu,Y., Zhang,T., Liu,J., Shen,Q. and Cao,X. (2011) *Eur. J. Immunol.*, **41**, 1154–1164.

PLOS ONE

Engineered Monoclonal Antibody with Novel Antigen-Sweeping Activity *In Vivo*

Tomoyuki Igawa*, Atsuhiko Maeda, Kenta Haraya, Tatsuhiko Tachibana, Yuki Iwayanagi, Futa Mimoto, Yoshinobu Higuchi, Shinya Ishii, Shigero Tamba, Naoka Hironiwa, Kozue Nagano, Tetsuya Wakabayashi, Hiroyuki Tsunoda, Kunihiro Hattori

Research Division, Chugai Pharmaceutical Co., Ltd., Gotemba, Shizuoka, Japan

Abstract

Monoclonal antibodies are widely used to target disease-related antigens. However, because conventional antibody binds to the antigen but cannot eliminate the antigen from plasma, and rather increases the plasma antigen concentration by reducing the clearance of the antigen, some clinically important antigens are still difficult to target with monoclonal antibodies because of the huge dosages required. While conventional antibody can only bind to the antigen, some natural endocytic receptors not only bind to the ligands but also continuously eliminate them from plasma by pH-dependent dissociation of the ligands within the acidic endosome and subsequent receptor recycling to the cell surface. Here, we demonstrate that an engineered antibody, named sweeping antibody, having both pH-dependent antigen binding (to mimic the receptor-ligand interaction) and increased binding to cell surface neonatal Fc receptor (FcRn) at neutral pH (to mimic the cell-bound form of the receptor), selectively eliminated the antigen from plasma. With this novel antigen-sweeping activity, antibody without *in vitro* neutralizing activity exerted *in vivo* efficacy by directly eliminating the antigen from plasma. Moreover, conversion of conventional antibody with *in vitro* neutralizing activity into sweeping antibody further potentiated the *in vivo* efficacy. Depending on the binding affinity to FcRn at neutral pH, sweeping antibody reduced antigen concentration 50- to 1000-fold compared to conventional antibody. Thereby, sweeping antibody antagonized excess amounts of antigen in plasma against which conventional antibody was completely ineffective, and could afford marked reduction of dosage to a level that conventional antibody can never achieve. Thus, the novel mode of action of sweeping antibody provides potential advantages over conventional antibody and may allow access to the target antigens which were previously undruggable by conventional antibody.

Citation: Igawa T, Maeda A, Haraya K, Tachibana T, Iwayanagi Y, et al. (2013) Engineered Monoclonal Antibody with Novel Antigen-Sweeping Activity *In Vivo*. PLoS ONE 8(5): e63236. doi:10.1371/journal.pone.0063236

Editor: Maria Gasset, Consejo Superior de Investigaciones Cientificas, Spain

Received October 31, 2012; **Accepted** April 1, 2013; **Published** May 7, 2013

Funding: The authors have no support or funding to report.

Competing Interests: All authors are employees of Chugai Pharmaceutical Co., Ltd. T.I. and A.M. are inventors of the patents which claim pH-dependent binding antibody and sweeping antibody. This does not alter the authors' adherence to all the PLOS ONE policies on sharing data and materials.

* E-mail: igawatmy@chugai-pharm.co.jp

Introduction

Therapeutic monoclonal antibodies are now becoming an important option for treating various diseases [1,2]. Although high affinity antibodies with neutralizing activity against various antigens have been generated and shown to be therapeutically effective *in vivo*, some clinically important antigens have proved difficult to target by conventional antibody because of the huge antibody dosage required.

It has been reported that administering conventional antibodies to target soluble antigens, such as amyloid beta [3], MCP1 [4], hepcidin [5], IL6 [6], CD23 [7] and VEGF [8], results in more than 1000-fold increased antigen concentration over the baseline due to the accumulation of antibody-antigen complex in plasma. Since the half-life of the IgG antibody is very much longer than that of the antigen, the binding of antigen to antibody results in an increase in the plasma antigen concentration by reducing the clearance of the antigen [9]. The extent of increase in antigen concentration is determined by the difference in clearance between antigen and antibody-antigen complex [10]. As a striking example, administration of high affinity antibody against hepcidin, which has very rapid clearance, resulted in approximately 5,000-fold increase in plasma hepcidin concentration, requiring a huge antibody dosage of 300 mg/kg weekly to neutralize the hepcidin, which is an unrealistic dosage for therapeutic development [5]. In other cases, the baseline plasma concentration of the antigen may itself be extremely high, as in that of complement factor C5, the target antigen of eculizumab, which is in the range of μg/mL, in contrast to most therapeutic antibodies in the pg/mL or ng/mL range. Because of such high C5 concentration, eculizumab requires huge antibody dosage for efficient C5 neutralization [11], which makes eculizumab one of the highest annual dosages of the approved therapeutic antibodies. In theory, even an antibody with infinite affinity would need to be at a concentration higher than that of the total antigen to neutralize that antigen *in vivo* [12]. Therefore, when targeting soluble antigens with rapid clearance or high baseline plasma concentration, even conventional antibody with infinite affinity requires huge antibody dosage to achieve therapeutic efficacy. This impedes not only the development of subcutaneous formulations, which are important for chronic disease, but also the commercial development itself, because of increased manufacturing cost.

Since these issues stem from the fact that conventional antibody can only bind to the antigen and accumulates the antigen in plasma, engineered antibody that enables active and selective elimination of the antigen from plasma could overcome these issues. In the natural system, several cell surface endocytic receptors, such as asialoglycoprotein receptor [13], low-density lipoprotein receptor [14] and epidermal growth factor receptor [15], deliver ligands to the lysosome to eliminate the ligands from plasma. These receptors bind to the ligands at the cell surface and internalize the ligands into the cell. Since these receptors bind to the ligands pH dependently, they release the ligands in the acidic endosome, and while the released ligands are transferred to lysosome and degraded, the free receptors rapidly recycle back to the cell surface for another round of ligand elimination from plasma. Such properties make these receptors ideal for "sweeping" the ligands from the plasma. In this study, we engineered monoclonal antibody to mimic the endocytic receptor-like property so that it can exert antigen-sweeping activity and eliminate the antigen from the plasma.

We have investigated engineered monoclonal antibody to exert novel antigen-sweeping activity by simultaneously engineering both pH-dependent antigen binding, to mimic the pH-dependent receptor-ligand binding of such endocytic receptors, and increased FcRn binding affinity at neutral pH, to mimic the cell-bound form of the receptors. We demonstrate that the conversion of conventional antibody into sweeping antibody, which directly eliminates the antigen from plasma, could afford huge reduction of the antibody dosage to a level that conventional antibody even with infinite affinity cannot achieve and may allow access to target antigens which have previously been undruggable by conventional antibody.

Materials and Methods

Ethics Statement

Animal studies were performed in accordance with the Guidelines for the Care and Use of Laboratory Animals at Chugai Pharmaceutical Co., Ltd. under the approval of the company's Institutional Animal Care and Use Committee. The company is fully accredited by the Association for Assessment and Accreditation of Laboratory Animal Care International (http://www.aaalac.org).

Generation of Anti-IL-6R Antibodies with Increased Binding Affinity to FcRn at Neutral pH

pH-dependent binding antibody against human soluble IL-6 receptor (hsIL-6R) with neutralizing activity (PH-IgG1) were generated from non-pH-dependent binding antibody (NPH-IgG1) as previously described [16]. pH-dependent binding antibodies against hsIL-6R without neutralizing activity (PHX-IgG1) in BaF/gp130 assay [17] were also generated. To increase the binding affinity to either mouse FcRn (mFcRn) or human FcRn (hFcRn) at neutral pH, various Fc-engineered variants were generated by site-directed mutagenesis of human IgG1. Amino acid substitutions were introduced at the positions 251–258, 286, 288, 307–316, 428 and 433–436 in the EU numbering system which were reported to affect FcRn binding [18–26]. Mutation was comprehensively introduced at each position, and effective mutations identified were combined to generate Fc variants with increased binding affinity to FcRn at neutral pH. More than 1,000 variants were generated and assessed for their binding affinity (K_D) to recombinant mFcRn or hFcRn [18] at pH 7.0 using Biacore T200 (GE Healthcare). Each variant was captured onto a Protein L (ACTIgen) immobilized CM4 sensor chip, then FcRn was injected over the flow cell. K_D was determined using Biacore T200 Evaluation Software (GE Healthcare). Fc variants with the desired affinity to FcRn were identified. NPH-IgG1 (conventional antibody with neutralizing activity but without pH-dependent binding), PH-IgG1, PHX-IgG1 and their Fc variants were expressed transiently and purified. NPH-IgG1, PH-IgG1 and PHX-IgG1 were assessed for their K_D to recombinant hsIL-6R at pH 7.4 and pH 6.0 as previously described [16].

In vivo Study of Antibodies in Normal Mice and hFcRn Transgenic Mice Co-injection Model

All animal experiments in this study were performed in accordance with the Guidelines for the Care and Use of Laboratory Animals at Chugai Pharmaceutical Co., Ltd. In co-injection model, C57BL/6J normal mice (Charles River) or hFcRn transgenic mice (hFcRn-Tgm, B6.mFcRn−/−.hFcRn Tg line 276+/+ mouse, Jackson Laboratories) [27] were administered by single i.v. injection with hsIL-6R alone or with hsIL-6R pre-mixed with antibody. The first group received 50 μg/kg hsIL-6R but the other groups additionally received 1 mg/kg of anti-IL-6R antibodies. Total hsIL-6R plasma concentration was determined as previously described [16].

In vivo Study of Antibodies in a Normal Mice hsIL-6R Trans-signaling Model

To evaluate the effect of antibodies on hsIL-6R trans-signaling inhibition *in vivo*, C57BL/6J normal mice were initially i.v. injected with hsIL-6R [16] (250 μg/kg). Then antibodies with designated doses and MR16-1 [28] (15 mg/kg, rat anti-mouse IL-6R antibody) were administered at 2 h after the initial injection. 8 μg/kg of human IL-6 (Toray) was injected at 24 h. Blood samples were collected at 30 h after the initial injection and total hsIL-6R and serum amyloid A (SAA) plasma concentrations were determined as previously described [16].

In vivo Study of Single Doses of Antibodies in Normal Mice and hFcRn Transgenic Mice Steady-state Model

An infusion pump (alzet) filled with 92.8 μg/mL hsIL-6R was implanted under the skin on the back of C57BL/6J normal mice or hFcRn-Tgm (B6.mFcRn−/−.hFcRn Tg line 32+/+ mouse, Jackson Laboratories) [27] to prepare model mice with constant plasma concentration of hsIL-6R. Monoclonal anti-mouse CD4 antibody GK1.5 [29] was administered by i.v. injection to inhibit the production of mouse antibody against hsIL-6R by depleting CD4+ T-cells. Antibodies against hsIL-6R were administered at 1 mg/kg to normal mice or hFcRn-Tgm with or without a single i.v. injection of 1 g/kg of hIgG (Intravenous immunoglobulin, CSL Behring) to mimic endogenous human IgG.

Plasma anti-hsIL-6R antibody concentration in the presence of human IgG was determined using anti-idiotype antibody coated on ELISA 96-well plates, and detected by hsIL-6R, biotinylated anti-hIL-6R antibody (R&D Systems) and Streptavidin-PolyHRP80 (Stereospecific Detection Technologies) using peroxidase substrate. Plasma total hsIL-6R, antibody concentration in the absence of hIgG and pharmacokinetic parameters were determined as previously described [16]. The theoretical free hsIL-6R concentration was calculated from antibody concentration, total hsIL-6R concentration and the K_D of the antibody by equilibrium reaction formula.

In vivo Study of Multiple Doses of Antibodies in hFcRn Transgenic Mice Steady-state Model with High hsIL-6R Concentration

Study was performed as described in the single dose study but with 320 μg/mL hsIL-6R in the pump, and doses were administered to hFcRn-Tgm (B6.mFcRn−/−.hFcRn Tg line 32+/+ mouse, Jackson Laboratories) [27] every other day (except the first dose which was injected together with a single i.v. injection of 1 g/kg of human IgG). Total hsIL-6R plasma concentrations were determined as described above. To determine free hsIL-6R plasma concentration, samples were treated by rProtein A (GE healthcare) to remove antibody and antibody-antigen complex. Because rProtein A treatment requires 10 μL of plasma, samples of n = 3–5 were equally pooled before the treatment. Subsequently, the free hsIL-6R plasma concentrations were determined by the same method as for total hsIL-6R, and hsIL-6R neutralization percentages were obtained by calculating the percentage reduction of free hsIL-6R plasma concentration over control group.

Pharmacokinetic Analysis and Simulation using Antibody-antigen Dynamic Model

The plasma concentration–time profiles of antibodies and total hsIL-6R obtained in the study of hFcRn-Tgm steady-state model were fitted to an antibody-antigen dynamic model [30] and parameters were optimized for conventional, pH-dependent binding, and v4-type sweeping antibodies. The k_a and k_d values were from surface plasmon resonance (SPR) data. Simulation study was carried out using the obtained pharmacokinetic parameters, and antibody dosages required to neutralize 95% of the antigen (baseline 250 ng/mL (6.6 nM)) at trough by dosing once a month were obtained for each type of antibody with antigen binding affinity (K_D) of 0.001, 0.01, 0.1, 1 and 10 nM.

Results

Antigen Sweeping by pH-dependent Binding Antibody with Increased FcRn Binding at Neutral pH

In order to evaluate the effect of pH-dependent antigen binding and increased FcRn binding affinity at neutral pH on antigen pharmacokinetics, we used a non-pH-dependent binding antibody against hsIL-6R with hIgG1 constant region (NPH-IgG1) and a pH-dependency-engineered variant (PH-IgG1) (Table S1). hIgG1 has almost no detectable binding to FcRn at pH 7.4, and very weak binding at pH 7.0. In order to increase the binding affinity of PH-IgG1 to either mouse FcRn (mFcRn) or human FcRn (hFcRn) at neutral pH, various hIgG1 Fc variants with mutation(s) in the FcRn binding region (positions 251–258, 286, 288, 307–316, 428 and 433–436 in the EU numbering system) were generated by site-directed mutagenesis. More than 1000 variants were screened by binding to either mFcRn or hFcRn at pH 7.0, and hIgG1 Fc variants for *in vivo* studies were selected (Table 1). The v1 variant was used to evaluate the *in vivo* effect of pH-dependent antigen binding antibody with increased binding affinity to mFcRn at pH 7.0 by administering hsIL-6R to normal mice either on its own or in complex with NPH-IgG1, PH-IgG1 or PH-v1 (Fig. 1A). In this co-injection model, NPH-IgG1 significantly reduced the clearance of hsIL-6R because antigen-antibody complex has lower clearance than the antigen [9,10]; PH-IgG1 increased the clearance of hsIL-6R to some extent, but was still slower than hsIL-6R alone; while PH-v1 accelerated the clearance of hsIL-6R faster than hsIL-6R alone.

Since this co-injection model may not have reflected the actual therapeutic situation where antibody is exposed to plasma in which steady-state baseline concentration of soluble antigen is present, we evaluated antigen sweeping in a mouse model which maintains steady-state plasma antigen concentration. We administered NPH-IgG1, PH-IgG1 and PH-v1 into normal mice steady-state model (Fig. 1B). Consistent with the co-injection model, NPH-IgG1 significantly increased hsIL-6R plasma concentration; PH-IgG1 reduced that increase but an increase over the baseline was still observed; and PH-v1 actively eliminated hsIL-6R from the plasma and reduced the plasma hsIL-6R concentration approximately 150-fold below the baseline, demonstrating that engineered antibody with pH-dependent binding antibody and increased binding affinity to FcRn at neutral pH can eliminate the antigen form plasma *in vivo*.

Effect of Antigen Sweeping by Sweeping Antibody on Antigen Antagonism *in vivo*

To evaluate the effect of antigen sweeping by sweeping antibody on antigen antagonism *in vivo*, *in vivo* efficacy of the anti-hsIL-6R sweeping antibodies was tested in a normal mouse hsIL-6R trans-signaling model [31], which exhibits an increase in SAA dependent on hIL-6/hsIL-6R-mediated trans-signaling. We generated PHX-IgG1, a pH-dependent binding antibody against hsIL-6R without hsIL-6R neutralizing activity *in vitro* (Table S1), and its Fc variant PHX-v1 with increased binding affinity to mFcRn at neutral pH. In the first study, PHX-IgG1 and PHX-v1 were administered at antibody dosage of 30 mg/kg, and plasma concentration of hsIL-6R and SAA, as a pharmacodynamic marker of hsIL-6R antagonism, are shown (Fig. 2A,B). While PHX-IgG1 could not inhibit SAA production at all, PHX-v1 significantly inhibited SAA production *in vivo* by directly sweeping hsIL-6R from the plasma, despite having no neutralizing activity *in vitro*. In the next study, antibodies with hsIL-6R neutralizing activity, NPH-IgG1, PH-IgG1 and PH-v1, were administered at antibody dosage of 0.03 mg/kg. While NPH-IgG1 and PH-IgG1 with hsIL-6R neutralizing activity *in vitro* could not completely inhibit SAA production at this dosage, PH-v1, with both neutralizing and sweeping activity, completely inhibited SAA production (Fig. 2C,D).

Antigen Sweeping Requires Both pH-Dependent Antigen Binding and Increased FcRn Binding Affinity at Neutral pH

For clinical application of sweeping antibody, further studies of antigen sweeping were conducted using an hFcRn system. The v2 variant with increased binding affinity to hFcRn at neutral pH was generated (Table 1). As a control for v2 variant, a YTE variant previously reported as improving the half-life [19] with increased binding affinity to hFcRn at acidic pH but not significantly at neutral pH, was used. In a co-injection model, hsIL-6R was administered to hFcRn-Tgm either on its own or in complex with NPH-IgG1, PH-IgG1, PH-YTE and PH-v2 (Fig. 3A). Consistent with the study using normal mice, PH-v2 markedly accelerated the clearance of hsIL-6R faster than hsIL-6R alone in hFcRn-Tgm. On the other hand, PH-YTE exerted slightly slower clearance of hsIL-6R than PH-IgG1.

To further clarify the molecular requirement to achieve antigen sweeping, we administered NPH-IgG1, PH-IgG1, NPH-v2, PH-v2 and PH-v0 to hFcRn-Tgm steady-state model (Fig. 3B). NPH-v2, a non-pH-dependent binding antibody with increased binding affinity to hFcRn at neutral pH, increased hsIL-6R plasma concentration above the baseline to a similar level to NPH-IgG1;

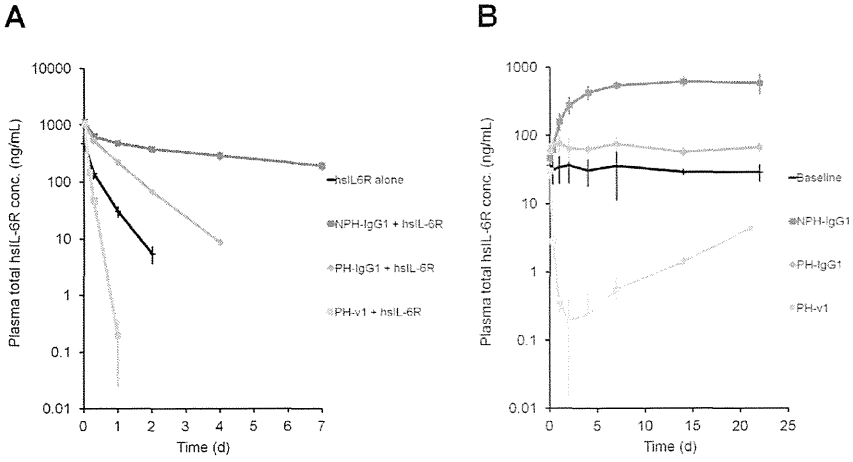

Figure 1. Antigen sweeping by pH-dependent antigen binding antibody with increased FcRn binding at neutral pH. *In vivo* study of NPH-IgG1, PH-IgG1 and PH-v1 in normal mice. Effect of antibodies on the total hsIL-6R plasma concentration was evaluated in a co-injection model and a steady-state model. In the co-injection model, hsIL-6R, hsIL-6R+NPH-IgG1, hsIL-6R+PH-IgG1 and hsIL-6R+PH-v1 were intravenously administered as single doses of 50 μg/kg for hsIL-6R and 1 mg/kg for antibody and a time profile of total hsIL-6R plasma concentration (A) is shown. Each data point represents the mean ± s.d. (n = 3 each). In the steady-state model, steady-state plasma concentration of approximately 20 ng/mL hsIL-6R was maintained using an infusion pump filled with hsIL-6R solution, and NPH-IgG1, PH-IgG1 and PH-v1 were intravenously administered as single doses of 1 mg/kg and a time profile of total hsIL-6R plasma concentration (B) is shown. Each data point represents the mean ± s.d. (n = 3 each).
doi:10.1371/journal.pone.0063236.g001

PH-v0, a pH-dependent binding antibody with no hFcRn binding [32], also increased hsIL-6R plasma concentration to a similar level to PH-IgG1, but only transiently; and only PH-v2, a pH-dependent binding antibody with increased binding affinity to hFcRn at neutral pH, actively eliminated hsIL-6R from the plasma. This clearly demonstrates that both pH-dependent antigen binding and increased binding affinity to FcRn at neutral pH are required for antigen sweeping.

Effect of Endogenous IgG Competition on Antigen Sweeping

Because mouse IgG does not bind to hFcRn [33], hFcRn-Tgm has substantially no endogenous IgG competing with sweeping antibody for hFcRn, which might not reflect the clinical situation in which there is high endogenous human IgG (hIgG) concentration [20]. To evaluate the effect of endogenous IgG on antigen sweeping, NPH-IgG1, PH-IgG1 and PH-v2 alone or together with

Table 1. *Mutations and FcRn binding affinity of hIgG1 Fc variants.*

Fc variant	K_D (nM) at pH7.0		K_D (nM) at pH6.0		Mutations
	mouse FcRn	human FcRn	mouse FcRn	human FcRn	
IgG1	3918	88000	237	1377	–
v1	52	NT	3	NT	I332V/N434Y
v2	NT	155	NT	6	M252W/N434W
v3	NT	288	NT	15	M252Y/N434Y
v4	NT	120	NT	8	M252Y/N286E/N434Y
v5	NT	77	NT	5	M252Y/T307Q/Q311A/N434Y
v6	NT	35	NT	3	M252Y/V308P/N434Y
v0	no binding	no binding	no binding	no binding	I253A

Binding affinity (K_D) of IgG1 and v1 to mFcRn at pH 7.0 and pH 6.0, binding affinity (K_D) of IgG1, v2-v6 and v0 to hFcRn at pH 7.0 and pH 6.0, and mutations introduced in the Fc region are shown. Mutation sites in the Fc region are described in EU numbering. NT, not tested.
doi:10.1371/journal.pone.0063236.t001

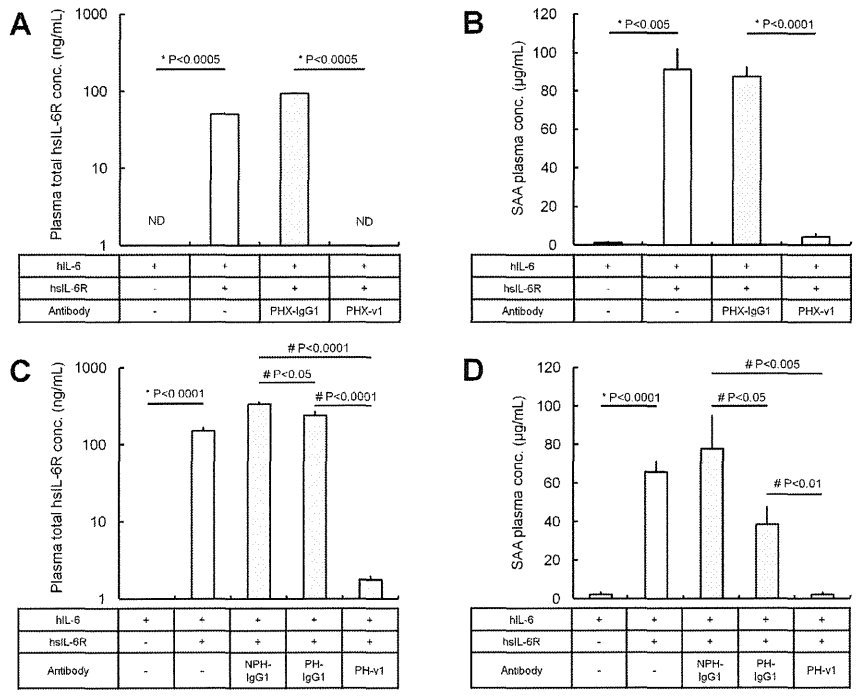

Figure 2. *In vivo* study of sweeping antibodies in a normal mice hsIL-6R trans-signaling model. Effect of antibodies on the total hsIL-6R plasma concentration and SAA plasma concentration (as a marker for hsIL-6R antagonism) were evaluated. hsIL-6R was intravenously administered as a single dose of 250 μg/kg. At 2 h, non-neutralizing antibodies PHX-IgG1 and PHX-v1 were intravenously administered as single doses of 30 mg/kg (A, B), and neutralizing antibodies NPH-IgG1, PH-IgG1 and PH-v1 were intravenously administered as single doses of 0.03 mg/kg (C, D). At 24 h, hIL-6 was intravenously administered as a single dose of 8 μg/kg. Total hsIL-6R plasma concentration (A, C) and SAA plasma concentration (B, D) at 30 h is shown. Each data represents the mean ± s.d. for total hsIL-6R plasma concentration and the mean ± s.e. for SAA plasma concentration (n = 3–7 each). ND, not detected (below 0.195 ng/mL). Statistical significance was determined by t-test (*) or Tukey's multiple comparison test (#) for total hsIL-6R and SAA plasma concentration.
doi:10.1371/journal.pone.0063236.g002

1 g/kg of hIgG, *which mimics endogenous* IgG, *were administered* to hFcRn-Tgm steady-state model. hsIL-6R sweeping by PH-v2 was attenuated when hIgG as endogenous IgG was present (Fig. S1).

Effect of hFcRn Binding Affinity at Neutral pH on Antigen Sweeping in Human FcRn Transgenic Mice

Since FcRn binding at neutral pH is required for antigen sweeping, it is assumed that binding affinity (K_D) to FcRn at neutral pH would affect the antigen sweeping profile. In addition, previous studies have shown that increasing FcRn binding affinity at neutral pH either increased or did not affect the antibody clearance [21–24]. In order to assess the effect of FcRn binding affinity at neutral pH on antigen sweeping and antibody *pharmacokinetics, Fc variants (v3-v6) with various binding affinity* to hFcRn at pH 7.0 were generated (Table 1).

Antigen sweeping and antibody pharmacokinetics of NPH-IgG1, PH-IgG1 and its Fc variants were evaluated in hFcRn-Tgm steady-state model in the presence of hIgG (Fig. 4A,B, Table S2). Compared to IgG1, the v3 variant, with K_D 288 nM at pH 7.0, slightly prolonged the antibody pharmacokinetics; moreover, PH-v3 reduced total hsIL-6R plasma concentration to a similar level as baseline concentration. Notably, *the v4 variant, with* K_D 120 nM at pH 7.0, reduced total hsIL-6R plasma concentration below the baseline level while the antibody pharmacokinetics was maintained. Total hsIL-6R plasma concentration of PH-v4 was 50-fold lower than NPH-IgG1 while the antibody plasma concentration was comparable. The study using the v5 and v6 variants with, respectively, K_D 77 and 35 nM at pH 7.0 has demonstrated that variants with stronger hFcRn binding affinity exhibited more

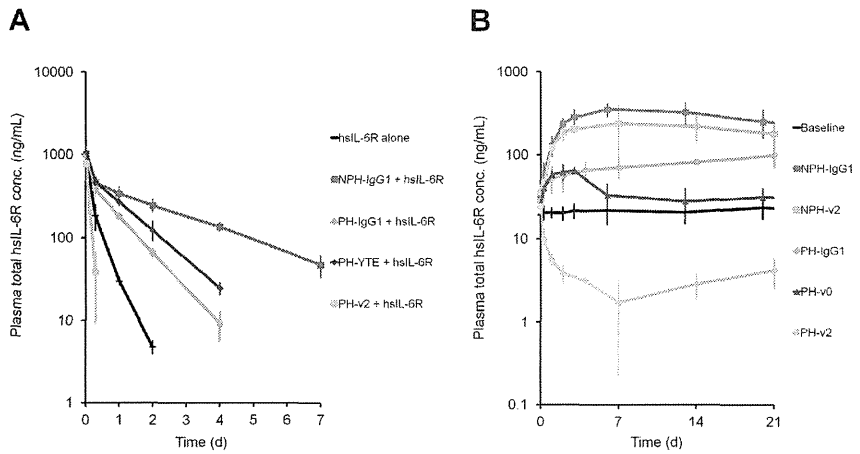

Figure 3. Characterization of sweeping antibody in hFcRn-Tgm. (A) *In vivo* study of NPH-IgG1, PH-IgG1, PH-YTE and PH-v2 in hFcRn-Tgm. Effect of antibodies on the total hsIL-6R plasma concentration was evaluated in a co-injection model. hsIL-6R, hsIL-6R+NPH-IgG1, hsIL-6R+PH-IgG1, hsIL-6R+PH-YTE and hsIL-6R+PH-v2 were intravenously administered as single doses of 50 μg/kg for hsIL-6R and 1 mg/kg for antibody and a time profile of total hsIL-6R plasma concentration is shown. Each data point represents the mean ± s.d. (n = 3 each). (B) Effect of pH-dependent antigen binding and increased binding affinity to FcRn at neutral pH on antigen sweeping in hFcRn-Tgm steady-state model with hsIL-6R plasma concentration of approximately 20 ng/mL. NPH-IgG1, NPH-v2, PH-IgG1, PH-v2 and PH-v0 were intravenously administered as single doses of 1 mg/kg. Time profile of total hsIL-6R plasma concentration is shown. Each data point represents the mean ± s.d. (n = 3 each).
doi:10.1371/journal.pone.0063236.g003

extensive antigen sweeping and lower minimum total hsIL-6R plasma concentration, but had increased antibody clearance and a shorter duration of antigen sweeping (faster recovery to baseline). Specifically, the v6 variant reduced total hsIL-6R plasma concentration approximately 1000-fold compared to NPH-IgG1, while the antibody clearance was increased only by 4-fold.

Sweeping Antibody Antagonizes High Concentration Antigen where Conventional Antibody is Ineffective

The v6-type sweeping antibody with hFcRn binding affinity of 35 nM provided short-lasting but extensive 1000-fold reduction of antigen plasma concentration compared to conventional antibody. To understand its therapeutic advantage, NPH-IgG1, PH-IgG1 and PH-v6 at doses of 0.01 mg/kg were administered to hFcRn-Tgm steady-state model with high plasma hsIL-6R concentration (250 ng/mL) every other day in the presence of hIgG (Fig. 5 A, B). Multiple dosing of NPH-IgG1 and PH-IgG1 achieved no hsIL-6R neutralization throughout the study because molar hsIL-6R concentration was higher than that of antibody (molar antibody concentration was approximately 5-fold lower than the total antigen concentration immediately after the first administration); however, PH-v6 gradually reduced the total hsIL-6R plasma concentration, enabling a neutralization of hsIL-6R at Day 8.

Discussion

In this study, we have demonstrated that simultaneous engineering of pH-dependent antigen binding and increased FcRn binding affinity at neutral pH actively eliminated the antigen from the plasma, creating "sweeping antibody". Importantly, both pH-dependent antigen binding and increased FcRn binding affinity at neutral pH was required for antigen sweeping, mimicking the function of the ligand-sweeping endocytic receptors that we previously mentioned.

When targeting soluble antigen with monoclonal antibody, conventional antibody (NPH-IgG1) remains bound to the soluble antigen within the acidic endosome (Fig. S2A) and thereby inhibits the antigen degradation by lysosome, resulting in accumulation of the antigen in the plasma. We have recently reported that engineered antibody with pH-dependent antigen binding (PH-IgG1), named recycling antibody, dissociates the soluble antigen in the acidic endosome and the dissociated antigen is then transferred to lysosome and degraded (Fig. S2B) [16]. However, our current study demonstrates that pH-dependent antigen binding alone could not actively eliminate the antigen from plasma. This is because intact IgG1 does not bind to FcRn on the cell surface at neutral pH [25], and the antibody-antigen complex is only marginally taken up into the cell by pinocytosis, which limits the rate of antigen degradation.

Previous studies have demonstrated that Fc-engineering to increase the binding affinity to FcRn at acidic pH improved the endosomal recycling efficiency and prolonged the pharmacokinetics of the antibody [20,25,26]. However, a simultaneous increase of binding affinity at neutral pH did not prolong [21,22], or even shortened [23,24], the pharmacokinetics because of inefficient antibody release from FcRn back to plasma after transporting it back to the cell surface, providing no therapeutic merit. Increasing FcRn binding affinity at neutral pH would anchor the antibody to the cell surface, similarly to an endocytic receptor, and enhance cellular uptake of antibody-antigen complex by FcRn-mediated

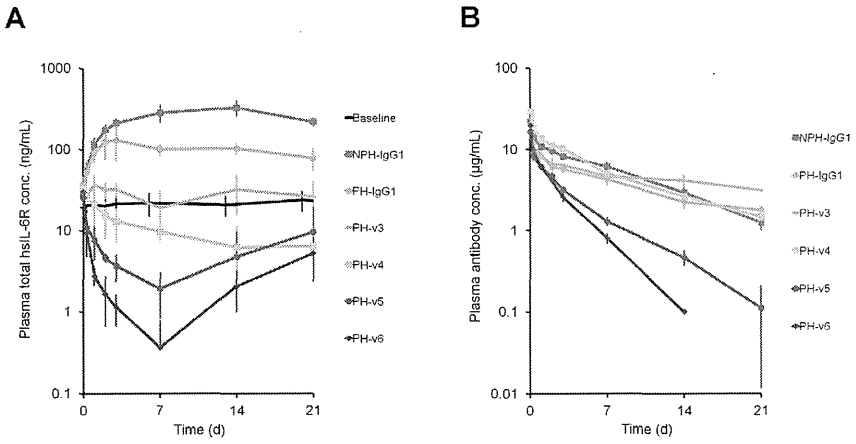

Figure 4. Effect of hFcRn binding affinity at neutral pH on antigen sweeping profile in hFcRn-Tgm. (A, B) Effect of FcRn binding affinity at pH 7.0 on antigen sweeping and antibody pharmacokinetics in hFcRn-Tgm steady-state model with hsIL-6R concentration of approximately 20 ng/mL in the presence of human IgG. NPH-IgG1, PH-IgG1, PH-v3, v4, v5 and v6 were intravenously administered as single doses of 1 mg/kg with 1 g/kg of hIgG. Time profiles of total hsIL-6R plasma concentration (A) and antibody plasma concentration (B) are shown. Each data point represents the mean ± s.d. (n = 3–6 each).
doi:10.1371/journal.pone.0063236.g004

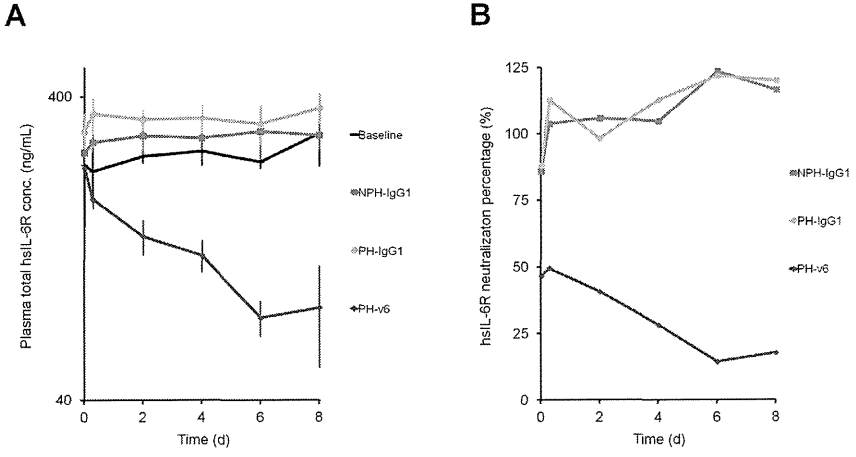

Figure 5. Effect of sweeping antibody on high plasma concentration antigen. Effect of NPH-IgG1, PH-IgG1 and PH-v6 on a hFcRn-Tgm steady-state model with high hsIL-6R concentration of approximately 250 ng/mL in the presence of human IgG. NPH-IgG1, PH-IgG1 and PH-v6 were intravenously administered as multiple doses of 0.01 mg/kg every other day. Molar baseline hsIL-6R concentration (6.6 nM) is 5-fold higher than antibody concentration at 15 min (1.3 nM). Time profiles of total hsIL-6R plasma concentration (A) and free hsIL-6R percentage over control (B) are shown. Each data point represents the mean ± s.d. for total hsIL-6R concentration (n = 3–5 each). Free hsIL-6R percentage over control is determined from the pooled plasma sample of n = 3–5 each.
doi:10.1371/journal.pone.0063236.g005

endocytosis. However, our study demonstrated that antibody with increased FcRn binding affinity at neutral pH without pH-dependent antigen binding (NPH-v2) could not actively eliminate the antigen from plasma because the antigen is also recycled back to plasma by FcRn in the antibody-antigen complex.

Combining a pH-dependent antigen binding with increased FcRn binding at only acidic pH (PH-YTE) attenuated rather than accelerated antigen clearance compared to pH-dependent antigen-binding antibody with wild type IgG1 (PH-IgG1), probably because the improved endosomal recycling efficiency [19] also applied to the antigen that remained bound to the antibody. In addition, non-FcRn binding Fc (PH-NB) could not actively eliminate the antigen from plasma because, similar to PH-IgG1, the uptake of antibody-antigen complex into the cell was marginal.

Antigen sweeping was only achieved by the combination of pH-dependent antigen binding with increased FcRn binding affinity at neutral pH (PH-v2). These studies support the following mechanism of sweeping antibody, mimicking the process of rapid ligand sweeping by endocytic receptors [13–15] (Fig. S2C): (i) increasing binding affinity to FcRn at neutral pH anchors the antibody to the cell surface and provides FcRn-mediated cellular uptake of antibody-antigen complex, (ii) pH-dependent dissociation of antibody-antigen complex enables selective degradation of the antigen, (iii) FcRn-mediated recycling of the free antibody to the cell surface enables another round of the cycle. Because this cycle has a rapid turnover rate and FcRn is broadly expressed in the body, sweeping antibody can effectively eliminate the antigen from plasma.

As our results show, this antigen-sweeping activity can be successfully applied either to antibody which has no *in vitro* hsIL-6R neutralizing activity (PHX-v1) to create *in vivo* inhibition of hsIL-6R/hIL-6-mediated trans-signaling or to convert conventional antibody with *in vitro* activity (NPH-IgG1) into sweeping antibody (PH-v1) to further potentiate the *in vivo* signaling inhibition. This study demonstrated that *in vivo* efficacy of sweeping antibody required no *in vitro* biological activity, indicating that sweeping antibody could antagonize multi-epitope antigen (antigen with multiple functional epitope) or toxic antigen with no functional epitope, which cannot be antagonized with a conventional antibody, by directly eliminating the antigen from plasma. Moreover, this study also demonstrated that conventional antibody with biological activity *in vitro* can be further potentiated *in vivo* by engineering the antibody into sweeping antibody, indicating that engineering conventional antibody into sweeping antibody could be an alternative approach to enhancing the therapeutic efficacy of conventional antibody.

Since sweeping antibody would compete with endogenous IgG to bind to FcRn, it was assumed that endogenous IgG would affect the efficiency of antigen sweeping. A similar phenomenon has been reported for antibody-dependent cellular cytotoxicity mediated by Fc gamma receptor binding, which was significantly inhibited by the presence of endogenous hIgG [34]. As expected, antigen sweeping in hFcRn-Tgm was significantly attenuated in the presence of hIgG when hIgG concentration was maintained at an average of 10 mg/mL (reflecting the clinical situation where endogenous hIgG is approximately 10 mg/mL [20]). This demonstrates that endogenous IgG is an important factor in the efficacy of sweeping antibody when considering clinical applications. It has been reported that IgG with increased FcRn binding at neutral pH (Abdeg) accelerates the clearance of endogenous IgG by blocking FcRn [35]. However, we did not observe accelerated clearance of hIgG in the presence of v4-type sweeping antibody (data not shown). Since reported Abdeg (with FcRn binding affinity of 7.4 nM at pH 7.2) accelerated the clearance of endogenous IgG at a dose of approximately 8 mg/kg, it is expected that v4-type sweeping antibody (with FcRn binding affinity of 120 nM at pH 7.0 significantly lower than Abdeg) would not accelerate the clearance of endogenous IgG at a therapeutically relevant dosage, although a high dosage of v6-type sweeping antibody (with stronger FcRn binding affinity of 35 nM at pH 7.0) may have some effect on the clearance of endogenous IgG.

The effect of hFcRn binding affinity at neutral pH on the antigen sweeping profile and antibody pharmacokinetics was investigated by evaluating Fc variants v3 to v6 in hFcRn-Tgm in the presence of hIgG. The results clearly demonstrate that both antigen sweeping and antibody pharmacokinetics depend on hFcRn binding affinity at neutral pH. By increasing the binding affinity at neutral pH, the extent of antigen sweeping (reflected by minimum total hsIL-6R plasma concentration (Table S2)) was enhanced but the duration of antigen sweeping was shortened and antibody clearance was increased. Compared to conventional antibody (NPH-IgG1), all sweeping antibody exhibited stronger reduction of free antigen plasma concentration, which determines the *in vivo* efficacy as a therapeutic antibody, and the extent and the duration of free antigen reduction depended on hFcRn binding affinity (Fig. S3).

Sweeping antibody with moderate hFcRn binding affinity at neutral pH provides moderate but long-acting antigen sweeping. Specifically, compared to conventional antibody (NPH-IgG1), sweeping antibody with hFcRn binding affinity of 120 nM (PH-v4) maintains a similar antibody plasma concentration and provides long-lasting approximately 50-fold reduction of total antigen plasma concentration. Importantly, this demonstrates that the antigen, *not* the antibody, is selectively *eliminated from* the plasma. To systematically understand the therapeutic advantage of this v4-type sweeping antibody, modeling and simulation [30] was conducted based on the experimental result of the hFcRn-Tgm study (Fig. S4A, Table S3). The simulation was conducted to calculate the dosage required to neutralize 95% of hsIL-6R (baseline 250 ng/mL) by once-a-month dosing using conventional, pH-dependent antigen binding, and v4-type sweeping antibodies with different binding affinity to hsIL-6R (Fig. S4B). In the simulation study, the dosage of conventional antibody cannot be lowered below 45 mg/kg even with infinite affinity, whereas sweeping antibody with only 0.1 nM affinity can be effective at 1.4 mg/kg. This demonstrates that v4-type sweeping antibody provides more than 30-fold reduction of dosage over conventional antibody even with infinite affinity, a level which can never be achieved with conventional antibody.

On the other hand, sweeping antibody with hFcRn binding affinity below 80 nM provides short-lasting but extensive reduction of antigen plasma concentration compared to conventional antibody. Specifically, sweeping antibody with hFcRn binding affinity of 35 nM (PH-v6) reduces antigen concentration approximately 1000-fold compared to conventional antibody, while the antibody clearance is increased only 4-fold. To understand the therapeutic advantage of v6-type sweeping antibody, antibodies were tested under conditions in which an excess molar amount of antigen was present in plasma, mimicking the therapeutic situation where antigen is present at a high concentration. This excess amount of antigen, which, as expected, conventional antibody (NPH-IgG1) or pH-dependent binding antibody (PH-IgG1) could not antagonize, was antagonized by sweeping antibody (PH-v6) by reducing the plasma antigen concentration below the baseline. This study demonstrated that sweeping antibody could antagonize high concentration antigen against which conventional or pH-

dependent antigen binding antibody, even with infinite affinity, would be completely ineffective.

We believe that sweeping antibody, an engineered monoclonal antibody with novel antigen-sweeping activity, provides potential advantages over conventional antibody that can only bind to the antigen and accumulates the antigen in plasma. First, sweeping antibody could be applied to high concentration antigens or antigens with rapid clearance which conventional antibodies, even with infinite affinity, have previously had difficulty in targeting. Second, by directly eliminating the antigen from plasma, sweeping antibody could be applied to antagonize multi-epitope antigen or toxic antigens without functional epitope, which cannot be simply antagonized by a conventional antibody. These two points suggest that sweeping antibody may expand the target antigen space of therapeutic monoclonal antibody to include target antigens which were previously undruggable by conventional monoclonal antibody. Third, sweeping antibody could provide an alternative approach to affinity maturation against the antigen by reducing the plasma antigen concentration to potentiate the efficacy of conventional antibody [36]. Fourth, sweeping antibody could provide a significant advantage over conventional antibody (even *assuming infinite affinity*) *in dosing by enabling the convenience of* subcutaneous and less frequent injections, or in manufacturing by reducing the cost. Since changing the binding affinity to hFcRn generates antibodies with different extent and duration of antigen sweeping, antigen-sweeping profiles can be readily customized. We have applied sweeping antibody technology to various antigens such as IL6, IgA, soluble plexin A1, soluble CD4 and other antigens. We have identified pH-dependent antibodies against each of these antigens and engineered them to bind to FcRn at neutral pH. All of these antibodies demonstrated similar antigen sweeping effect that is shown in this study using hsIL-6R (data not shown). These results suggest that sweeping antibody can be broadly applicable to various antigens.

Supporting Information

Figure S1 Effect of high concentration hIgG on antigen sweeping in hFcRn-Tgm. NPH-IgG1, PH-IgG1 and PH-v2 were intravenously administered as single doses of 1 mg/kg either with or without 1 g/kg of hIgG to hFcRn-Tgm with steady-state hsIL-6R concentration of approximately 20 ng/mL. Time profile of total hsIL-6R plasma concentration is shown. Each data point represents the mean ± s.d. (n = 3 each).
(TIF)

Figure S2 Proposed mode of action of sweeping antibody in comparison with conventional and pH-dependent binding antibody. (A) Conventional antibody bound to soluble antigen is non-specifically taken up by pinocytosis, and binds to FcRn in acidic endosome. Antibody-antigen complex is recycled back to the cell surface and released from FcRn back to plasma. (B) pH-dependent binding antibody (recycling antibody) *bound to soluble antigen is non-specifically taken up by* pinocytosis, and binds to FcRn in acidic endosome, while antigen is dissociated from the antibody, transferred into lysosome and degraded. Antibody is recycled back to the cell surface by FcRn, released from FcRn back to plasma and binds to another antigen, allowing single antibody to bind to antigen multiple times. (C) Sweeping antibody bound to soluble antigen is rapidly taken up by FcRn-mediated endocytosis. In acidic endosome, antibody binds to FcRn, and antigen is dissociated from the antibody, transferred into lysosome and degraded. Antibody is recycled back to the cell surface and either released from FcRn back to plasma or stays bound to FcRn on the cell surface to bind to another antigen. Rapid FcRn-mediated uptake allows enhanced lysosomal antigen degradation rate.
(TIF)

Figure S3 Antigen sweeping profile of antibodies with different hFcRn binding affinity at neutral pH in hFcRn-Tgm. *Effect of FcRn binding affinity at pH 7.0 on antigen* sweeping and antibody pharmacokinetics in hFcRn-Tgm with steady-state hsIL-6R concentration of approximately 20 ng/mL in the presence of human IgG. NPH-IgG1, PH-IgG1, PH-v3, v4, v5 and v6 were intravenously administered as single doses of 1 mg/kg with 1 g/kg of hIgG. Theoretical free hsIL-6R plasma concentration was calculated from plasma antibody concentration, total hsIL-6R concentration and binding affinity to hsIL-6R. Time profile of theoretical free hsIL-6R plasma concentration is shown.
(TIF)

Figure S4 Modeling and simulation of sweeping antibody. (A) Antibody-antigen dynamic model of sweeping antibody. Antibody is injected intravenously to the central compartment and distributed to the peripheral compartment. Antibody binds to the antigen in the central compartment. Antibody, antigen and antibody-antigen complex are eliminated from the central compartment. Effect of pH-dependent binding and increased binding affinity to FcRn is reflected in the elimination rate of antibody-antigen complex. Parameters used in this model are k_{synthe} (rate constant of antigen synthesis), $C_{antigen,baseline}$ (baseline concentration of antigen), $k_{el,antigen}$ (elimination rate constant of antigen), $Vd1_{antigen}$ (volume of distribution of antigen), $k_{12,antigen}$ (transfer rate constant of antigen from central to peripheral compartment), $k_{21,antigen}$ (transfer rate constant of antigen from peripheral to central compartment), $k_{el,mab}$ (elimination rate constant of antibody), $Vd1_{mab}$ (volume of distribution of antibody), $k_{12,mab}$ (transfer rate constant of antibody from central to peripheral compartment), $k_{21,mab}$ (transfer rate constant of antibody from peripheral to central compartment) and $k_{el,complex}$ (elimination rate constant of antigen in complex with antibody). Note that antibody in complex with antigen is eliminated at the rate of $k_{el,mab}$. (B) *Simulation of required dosage to neutralize* antigen (baseline concentration 250 ng/mL) by 95% at trough with dosing once a month using conventional antibody (non-pH dependent binding IgG1 antibody), pH-dependent binding IgG1 antibody and v4-type sweeping antibody with different binding affinity to the antigen. Relationship between the antigen binding affinity (K_D) and the antibody dosage required to achieve once monthly dosing is shown.
(TIF)

Table S1 Binding affinity of the anti-IL-6R IgG1 antibodies.
(TIF)

Table S2 Antibody clearance and minimum or maximum total hsIL-6R plasma concentration for tested antibodies.
(TIF)

Table S3 Fitted pharmacokinetic parameters in antibody-antigen dynamic model.
(TIF)

Acknowledgements

We thank colleagues in Chugai Research Institute for Medical Science, Inc, and Chugai Pharmaceutical Co. Ltd., Y. Kawase and H. Tateishi for breeding hFcRn-Tgm; M. Hirabayashi, M. Kinoshita, Yuichiro Ochiai, K. Koguchi, H. Sano, Yuichi Ochiai, T. Sakamoto, M. Kawaharada, T. Yokoyama and T. Nishimura for carrying out *in vivo* studies; M. Fujii, S. Masujima and A. Takara for antibody generation; and W. Hatakeyama, M. Saito and Y. Okura for carrying out SPR and *in vitro* analysis.

Author Contributions

Provided direction and guidance: HT K. Hattori. Conceived and designed the experiments: TI. Performed the experiments: AM K. Haraya TT YI KN YH SL. Analyzed the data: K. Haraya TT YI FM. Contributed reagents/materials/analysis tools: NH ST TW. Wrote the paper: TI.

References

1. Chan AC, Carter PJ (2010) Therapeutic antibodies for autoimmunity and inflammation. Nature Rev Immunol 10: 301–316.
2. Weiner LM, Surana R, Wang S (2010) Monoclonal antibodies, versatile platforms for cancer immunotherapy. Nature Rev Immunol 10: 317–327.
3. Davda JP, Hansen RJ (2010) Properties of a general PK/PD model of antibody-ligand interactions for therapeutic antibodies that bind to soluble endogenous targets. MAbs: 2, 576–588.
4. Haringman JJ, Gerlag DM, Smeets TJ, Baeten D, van den Bosch F, et al. (2006) A randomized controlled trial with an anti-CCL2 (anti-monocyte chemotactic protein 1) monoclonal antibody in patients with rheumatoid arthritis. ARTHRITIS and RHEUMATISM 54: 2387–2392.
5. Xiao JJ, Krzyzanski W, Wang YM, Li H, Rose MJ, et al. (2010) Pharmacokinetics of anti-hepcidin monoclonal antibody Ab 12H9m and hepcidin in cynomolgus monkeys. AAPS J 12: 646–657.
6. Martin PL, Cornacoff J, Prabhakar U, Lohr T, Treacy G, et al. (2005) Preclinical Safety and Immune-Modulating Effects of Therapeutic Monoclonal Antibodies to Interleukin-6 and Tumor Necrosis Factor-alpha in Cynomolgus Macaques. J Immunotoxicol 3: 131–139.
7. Byrd JC, O'Brien S, Flinn IW, Kipps TJ, Weiss M, et al. (2007) Phase I study of lumiliximab with detailed pharmacokinetic and pharmacodynamic measurements in patients with relapsed or refractory chronic lymphocytic leukemia. Clin Cancer Res 13: 4448–4455.
8. Jayson GC, Mulatero C, Ranson M, Zweit J, Jackson A, et al. (2005) Phase I investigation of recombinant anti-human vascular endothelial growth factor antibody in patients with advanced cancer. Eur J Cancer 41: 555–563.
9. Finkelman FD, Madden KB, Morris SC, Holmes JM, Boiani N, et al. (1993) Anti-cytokine antibodies as carrier proteins. Prolongation of in vivo effects of exogenous cytokines by injection of cytokine-anti-cytokine antibody complexes. J Immunol 151: 1235–1244.
10. Davis CB, Tobia LP, Kwok DC, Oishi CM, Kheterpal N, et al. (1999) Accumulation of Antibody-Target Complexes and the Pharmacodynamics of Clotting after Single Intravenous Administration of Humanized Anti-Factor IX Monoclonal Antibody to Rats. Drug Delivery 6: 171–179.
11. Zareba KM (2007) Eculizumab, A novel therapy for paroxysmal nocturnal hemoglobinuria. Drugs Today (Barc) 43: 539–46.
12. Rathanaswami P, Roalstad S, Roskos L, Su QJ, Lackie S, et al. (2005) Demonstration of an in vivo generated sub-picomolar affinity fully human monoclonal antibody to interleukin-8. Biochem Biophys Res Commun 334: 1004–1013.
13. Feinberg H, Torgersen D, Drickamer K, Weis WI (2000) Mechanism of pH-dependent N-acetylgalactosamine binding by a functional mimic of the hepatocyte asialoglycoprotein receptor. J Biol Chem 275: 35176–35184.
14. Yamamoto T, Chen HC, Guigard E, Kay CM, Ryan RO (2008) Molecular studies of pH-dependent ligand interactions with the low-density lipoprotein receptor. Biochemistry 47: 11647–11652.
15. French AR, Tadaki DK, Niyogi SK, Lauffenburger DA (1995) Intracellular trafficking of epidermal growth factor family ligands is directly influenced by the pH sensitivity of the receptor/ligand interaction. J Biol Chem 270: 4334–4340.
16. Igawa T, Ishii S, Tachibana T, Maeda A, Higuchi Y, et al. (2010) Antibody recycling by engineered pH-dependent antigen binding improves the duration of antigen neutralization. Nat Biotechnol 28: 1203–1207.
17. Jostock T, Mullberg J, Ozbek S, Atreya R, Blinn G, et al. (2001) Soluble gp130 is the natural inhibitor of soluble interleukin-6 receptor transsignaling responses. Eur J Biochem 268: 160–167.
18. Dall'Acqua WF, Woods RM, Ward ES, Palaszynski SR, Patel NK, et al. (2002) Increasing the affinity of a human IgG1 for the neonatal Fc receptor:biological consequences. J Immunol 169: 5171–5180.
19. Dall'Acqua WF, Kiener PA, Wu H (2006) Properties of human IgG1s engineered for enhanced binding to the neonatal Fc receptor (FcRn). J Biol Chem 281: 23514–23524.
20. Petkova SB, Akilesh S, Sproule TJ, Christianson GJ, Al Khabbaz H, et al. (2006) Enhanced half-life of genetically engineered human IgG1 antibodies in a humanized FcRn mouse model, potential application in humorally mediated autoimmune disease. Int Immunol 18: 1759–1769.
21. Yeung YA, Leabman MK, Marvin JS, Qiu J, Adams CW, et al. (2009) Engineering human IgG1 affinity to human neonatal Fc receptor, impact of affinity improvement on pharmacokinetics in primates. J Immunol 182: 7663–7671.
22. Datta-Mannan A, Witcher DR, Tang Y, Watkins J, Wroblewski VJ (2007) Monoclonal antibody clearance. Impact of modulating the interaction of IgG with the neonatal Fc receptor. J Biol Chem 282: 1709–1717.
23. Deng R, Loyet KM, Lien S, Iyer S, DeForge LE, et al. (2010) Pharmacokinetics of humanized monoclonal anti-tumor necrosis factor-{alpha} antibody and its neonatal Fc receptor variants in mice and cynomolgus monkeys. Drug Metab Dispos 38: 600–605.
24. Dall'Acqua WF, Kiener PA, Wu H (2006) Properties of human IgG1s engineered for enhanced binding to the neonatal Fc receptor (FcRn). J Biol Chem. 281: 23514–23524.
25. Hinton PR, Xiong JM, Johlfs MG, Tang MT, Keller S, et al. (2006) An engineered human IgG1 antibody with longer serum half-life. J Immunol 176: 346–356.
26. Zalevsky J, Chamberlain AK, Horton HM, Karki S, Leung IW, et al. (2010) Enhanced antibody half-life improves in vivo activity. Nat Biotechnol 28: 157–159.
27. Roopenian DC, Christianson GJ, Sproule TJ (2010) Human FcRn transgenic mice for pharmacokinetic evaluation of therapeutic antibodies. Methods Mol Biol 602: 93–104.
28. Okazaki M, Yamada Y, Nishimoto N, Yoshizaki K, Mihara M (2002) Characterization of anti-mouse interleukin-6 receptor antibody. Immunol Lett 84: 231–240.
29. Rashid A, Auchincloss H Jr, Sharon J (1992) Comparison of GK1.5 and chimeric rat/mouse GK1.5 anti-CD4 antibodies for prolongation of skin allograft survival and suppression of alloantibody production in mice. J Immunol 148: 1382–1388.
30. Betts AM, Clark TH, Yang J, Treadway JL, Li M, et al. (2010) The application of target information and preclinical pharmacokinetic/pharmacodynamic modeling in predicting clinical doses of a Dickkopf-1 antibody for osteoporosis. J Pharmacol Exp Ther 333: 2–13.
31. Ozbek S, Peters M, Breuhahn K, Mann A, Blessing M, et al. (2001) The designer cytokine hyper-IL-6 mediates growth inhibition and GM-CSF-dependent rejection of B16 melanoma cells. Oncogene 20: 972–979.
32. Deng R, Meng YG, Hoyte K, Lutman J, Lu Y, et al. (2012) Subcutaneous bioavailability of therapeutic antibodies as a function of FcRn binding affinity in mice. MAbs 4: 101–109.
33. Ober RJ, Radu CG, Ghetie V, Ward ES (2001) Differences in promiscuity for antibody-FcRn interactions across species, implications for therapeutic antibodies. Int Immunol 13: 1551–1559.
34. Preithner S, Elm S, Lippold S, Locher M, Wolf A, et al. (2006) High concentrations of therapeutic IgG1 antibodies are needed to compensate for inhibition of antibody-dependent cellular cytotoxicity by excess endogenous immunoglobulin G. Mol Immunol 43: 1183–1193.
35. Vaccaro C, Zhou J, Ober RJ, Ward ES (2005) Engineering the Fc region of immunoglobulin G to modulate in vivo antibody levels. Nat Biotechnol 23: 1283–1288.
36. Finch DK, Sleeman MA, Moisan J, Ferraro F, Botterell S, et al. (2011) Whole-molecule antibody engineering: generation of a high-affinity anti-IL-6 antibody with extended pharmacokinetics. J Mol Biol 411: 791–807.

OPEN ACCESS Freely available online

Identification and Multidimensional Optimization of an Asymmetric Bispecific IgG Antibody Mimicking the Function of Factor VIII Cofactor Activity

Zenjiro Sampei, Tomoyuki Igawa*, Tetsuhiro Soeda, Yukiko Okuyama-Nishida, Chifumi Moriyama, Tetsuya Wakabayashi, Eriko Tanaka, Atsushi Muto, Tetsuo Kojima, Takehisa Kitazawa, Kazutaka Yoshihashi, Aya Harada, Miho Funaki, Kenta Haraya, Tatsuhiko Tachibana, Sachiyo Suzuki, Keiko Esaki, Yoshiaki Nabuchi, Kunihiro Hattori

Research Division, Chugai Pharmaceutical Co., Ltd., Gotemba, Shizuoka, Japan

Abstract

In hemophilia A, routine prophylaxis with exogenous factor VIII (FVIII) requires frequent intravenous injections and can lead to the development of anti-FVIII alloantibodies (FVIII inhibitors). To overcome these drawbacks, we screened asymmetric bispecific IgG antibodies to factor IXa (FIXa) and factor X (FX), mimicking the FVIII cofactor function. Since the therapeutic potential of the lead bispecific antibody was marginal, FVIII-mimetic activity was improved by modifying its binding properties to FIXa and FX, and the pharmacokinetics was improved by engineering the charge properties of the variable region. Difficulties in manufacturing the bispecific antibody were overcome by identifying a common light chain for the anti-FIXa and anti-FX heavy chains through framework/complementarity determining region shuffling, and by pI engineering of the two heavy chains to facilitate ion exchange chromatographic purification of the bispecific antibody from the mixture of byproducts. Engineering to overcome low solubility and deamidation was also performed. The multidimensionally optimized bispecific antibody hBS910 exhibited potent FVIII-mimetic activity in human FVIII-deficient plasma, and had a half-life of 3 weeks and high subcutaneous bioavailability in cynomolgus monkeys. Importantly, the activity of hBS910 was not affected by FVIII inhibitors, while anti-hBS910 antibodies did not inhibit FVIII activity, allowing the use of hBS910 without considering the development or presence of FVIII inhibitors. Furthermore, hBS910 could be purified on a large manufacturing scale and formulated into a subcutaneously injectable liquid formulation for clinical use. These features of hBS910 enable routine prophylaxis by subcutaneous delivery at a long dosing interval without considering the development or presence of FVIII inhibitors. We expect that hBS910 (investigational drug name: ACE910) will provide significant benefit for severe hemophilia A patients.

Citation: Sampei Z, Igawa T, Soeda T, Okuyama-Nishida Y, Moriyama C, et al. (2013) Identification and Multidimensional Optimization of an Asymmetric Bispecific IgG Antibody Mimicking the Function of Factor VIII Cofactor Activity. PLoS ONE 8(2): e57479. doi:10.1371/journal.pone.0057479

Editor: Peter J. Lenting, Institut National de la Santé et de la Recherche Médicale, France

Received October 24, 2012; **Accepted** January 21, 2013; **Published** February 28, 2013

Funding: Chugai Pharmaceutical Co., Ltd. supported and funded the research described in this report. The funders authorized our decision to publish, but had no role in study design, data collection and analysis, or preparation of the manuscript.

Competing Interests: All authors are employees of Chugai Pharmaceutical Co., Ltd. which is conducting the clinical study of hBS910 (ACE910). TS, T. Kojima and KH are inventors of the patents and patent applications which claim FVIII-mimetic bispecific antibodies to FIXa and FX. ZS, TI, TS, YON, CM, AM, T. Kojima, T. Kitazawa and KY are inventors of the patent application which claims hBS910, the investigational drug. These do not alter the authors' adherence to all the PLOS ONE policies on sharing data and materials.

* E-mail: igawatmy@chugai-pharm.co.jp

Introduction

Hemophilia A is caused by an X-linked inherited dysfunction of coagulation factor VIII (FVIII). Patients with severe hemophilia A, who have plasma FVIII levels of less than 1% of normal, typically experience bleeding events several times a month [1]. Routine supplementation with exogenous human FVIII to maintain FVIII levels at 1% of normal or above is effective for reducing joint bleeding events and improving joint status and health-related quality of life in hemophilia A patients [2]. However, there are two major drawbacks to this prophylactic usage of exogenous FVIII. The first drawback is the necessity of frequent intravenous administration: three intravenous injections weekly of FVIII are necessary because of its low subcutaneous bioavailability and its short plasma half-life [3,4,5]. The second drawback is the development of inhibitory anti-FVIII alloantibodies, known as "inhibitors" [6]. Once FVIII inhibitors have developed, routine supplementation with exogenous FVIII will be no longer effective and the usage of exogenous FVIII for treating on-going bleeds is restricted. In such cases, alternative agents, such as activated factor VII and activated prothrombin complex concentrate, which are more expensive and have less stable hemostatic effects, need to be used to control bleeding [7,8]. Therefore, a new agent that resolves these drawbacks of exogenous FVIII is awaited in the field of the bleeding prophylaxis of severe hemophilia A.

Monoclonal antibodies have become an important therapeutic option in numerous diseases and are expected to play a greater role in the future of disease treatment [9,10]. Various monoclonal antibodies have been generated [11]; these not only include those with antagonistic activity but also those with agonistic activity [12], catalytic activity [13], and allosteric activity [14]. Antibody engineering technologies to generate bispecific antibodies have been extensively studied due to the huge potential of these antibodies for therapeutic applications [15]. Bispecific antibodies can be applied to simultaneously target two disease related antigens, retarget effector cells against the target cell [16], and co-ligate two different antigens on the same cell [17].

FVIII is cleaved by thrombin or factor Xa (FXa), and the resultant factor VIIIa (FVIIIa) presents a heterotrimeric structure consisting of the A1 subunit, the A2 subunit, and the light chain [18]. Simultaneous binding of FVIIIa to FIXa and FX by the light chain and the A2 subunit, and by the A1 subunit, respectively, contributes to FVIII cofactor activity which places FIXa and FX into proximity, and also allosterically enhances the catalytic rate constant of FIXa [19,20,21,22,23] (Fig. 1A).

Considering this function of FVIII and the versatilities of antibodies, we hypothesized that a bispecific antibody recognizing FIXa with one arm and FX with the other arm could mimic the FVIII cofactor activity by placing FIXa and FX in spatially appropriate positions, and by allosterically enhancing the catalytic activity of FIXa (Fig. 1B) [23]. We have recently reported a recombinant humanized bispecific antibody to FIXa and FX, termed hBS23, which exerted coagulation activity in FVIII-deficient plasma, even in the presence of FVIII inhibitors, and showed *in vivo* hemostatic activity in a cynomolgus monkey model of acquired hemophilia A, and had high subcutaneous bioavailability and a 2-week half-life in cynomolgus monkey [23]. Although the pharmacological concept of FVIII-mimetic bispecific antibody was clearly demonstrated in this report, the detail of this anti-FIXa/FX asymmetric bispecific IgG antibody identification was not described, and moreover, it required further optimization in several ways before the clinical use of such an agent in humans.

For therapeutic development, optimization of the bispecific antibody by molecular engineering to enable large-scale manufacturing of the bispecific antibody at clinical grade would be required. Although a variety of molecular formats for bispecific antibodies have been studied, including single-chain diabody, tandem scFv, IgG-scFv, DVD-Ig, CrossMab, and dual-binding Fab [24], we selected an asymmetric bispecific IgG format because it is the only format that can recognize FIXa and FX with each arm and has a long half-life and a native IgG structure. However, recombinant production of this format is challenging in comparison to the other formats because it consists of two different heavy chains and two different light chains which would result in the secretion of a mixture of ten different combinations of heavy and light chains [25]. Purification of one desired bispecific antibody from a mixture including nine miss-paired byproducts is nearly impossible. Engineering technologies to resolve such a difficulty have been previously reported. First, identification of a common light chain by phage display as the partner of the two heavy chains can reduce the number of heavy and light combinations to three: one heterodimeric bispecific antibody and two homodimeric

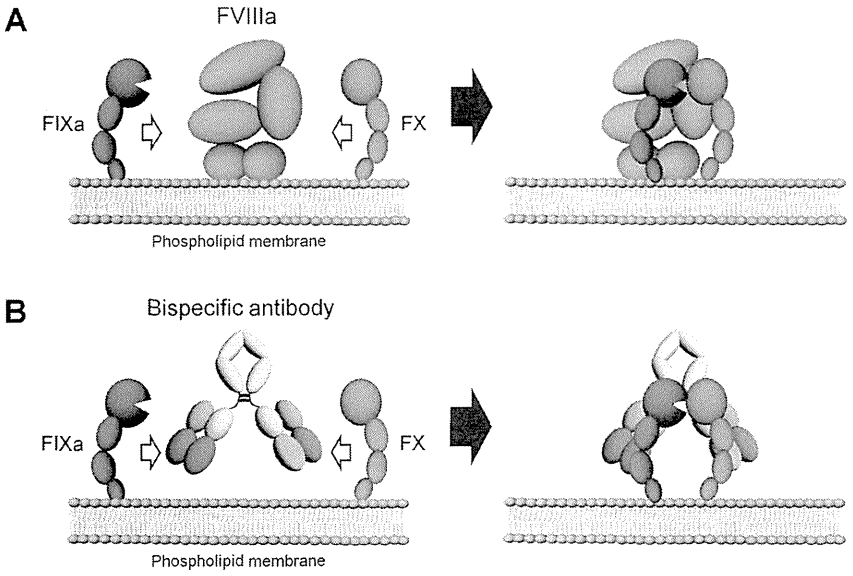

Figure 1. Schematic illustrations of cofactor actions of FVIIIa and a bispecific antibody promoting the interaction between FIXa and FX. (A) FVIIIa forms a complex with FIXa and supports the interaction between FIXa and FX through its binding ability to both factors on the phospholipid membrane. (B) A bispecific antibody binding to FIXa and FX would promote the interaction between FIXa and FX and exert FVIII-mimetic activity on the phospholipid membrane.
doi:10.1371/journal.pone.0057479.g001

monospecific antibodies [26]. *However, selection of a common* light chain with potent FVIII-mimetic activity based on the binding affinity by phage display was not feasible for our bispecific antibody, because higher binding affinities was considered not to lead to higher activity. To date, alternative approach to obtain common light chain has not been reported. Second, engineering the C_H3 domain to facilitate Fc heterodimerization can minimize the amount of homodimeric byproducts [25,26]. Nevertheless, the efficiency of heterodimerization is not complete; therefore, a small amount of homodimeric byproduct is formed, which needs to be removed in the downstream purification process. However, because the biophysical properties of the homodimeric byproducts are often similar to those of the target bispecific antibody, purifying the target bispecific antibody on a large scale for clinical applications is still challenging. To date, technologies to address this issue have not been reported. Therefore, improving the manufacturability of this type of FVIII-mimetic antibody by molecular engineering is required for therapeutic application.

Moreover, for maximizing the therapeutic potential of FVIII-mimetic bispecific antibody, optimization to increase the FVIII-mimetic activity of the bispecific antibody, prolong the half-life, improve the physicochemical properties of the antibody and reduce the immunogenicity of the humanized antibody would be required. This would enable more effective and long-term prophylaxis with stronger hemostatic effect for hemophilia A patients by a subcutaneous formulation with a longer dosing interval.

In this paper, we report molecular identification and multidimensional optimization of a FVIII-mimetic bispecific antibody which can be used for clinical application. At the start of this study, we examined bispecific combinations of large number of monoclonal anti-FIXa and anti-FX antibodies, and identified the lead anti-FIXa/FX bispecific IgG antibody having FVIII-mimetic activity. Then, this lead bispecific antibody was subjected to multidimensional optimization processes [27] to improve both its therapeutic potential and manufacturability. We successfully generated a humanized bispecific IgG antibody having sufficient FVIII-mimetic activity for prophylactic use even in the presence of FVIII inhibitors, high subcutaneous bioavailability with an approximately 3-week plasma half-life in cynomolgus monkeys, and minimal immunogenicity risk. In addition, molecular engineering enabled purification on a large manufacturing scale and formulation into a liquid formulation of 150 mg/mL for subcutaneous delivery. We expect that this anti-FIXa/FX bispecific antibody mimicking FVIII cofactor activity will provide significant benefit for managing bleeding events in severe hemophilia A patients.

Results

Research Flow of Identification and Multidimensional Optimization of Lead FVIII-mimetic anti-FIXa/FX Bispecific Antibody

Figure 2 shows the flow of the screening process to identify the lead bispecific antibody with a common light chain (BS15). BS15 was generated by combinatorial screening of bispecific antibodies composed of anti-FIXa and anti-FX antibodies derived from *immunization, followed by screening of common light chains* and then framework/complementarity determining region (FR/CDR) shuffling.

Figure 3 represents the multidimensional optimization flow to generate the bispecific antibody with the most appropriate properties for clinical application (hBS910) from the lead bispecific antibody (BS15). BS15 was firstly humanized to generate hBS1, *followed by engineering to improve* FVIII-*mimetic* activity (hBS106), improve pharmacokinetics (hBS128 and hBS228), enable purification of target bispecific antibody (hBS366 and hBS376), improve solubility (hBS560), remove deamidation site (hBS660), and reduce immunogenicity risk (deimmunization) to generate a multidimensionally optimized bispecific antibody (hBS910). Through this multidimensional optimization process, the numbers of variable region variants that we have generated for anti-FIXa heavy chain, anti-FX heavy chain and common light chain were approximately 500, 300 and 400, respectively, and the number of bispecific IgG antibodies that we have prepared and evaluated is approximately 2,400. Supplementary table S1 represents the number of mutations which were introduced into hBS1 to generate bispecific antibodies described in this report.

Identification of Lead Anti-FIXa/FX Bispecific Antibody with FVIII-mimetic Activity

Approximately 200 monoclonal antibodies against FIXa or FX were obtained from animals immunized with either human FIXa or FX. Approximately 40,000 bispecific IgG antibodies that comprised different combinations of anti-FIXa and anti-FX antibodies in each arm were expressed. Although the expression product of two different heavy chain and two different light chain genes consists of a mixture of ten different species with different heavy and light chain combinations, including the one desired bispecific antibody and the nine miss-paired antibodies (miss-paired antibody includes two homodimeric antibodies with a correct heavy and light chain pair), Fc heterodimerization mutations would theoretically enable expression of an antibody mixture containing at least approximately 20% of the target bispecific antibody (see methods for detail) [25]. A total number of 94 bispecific antibodies, or combinations of anti-FIXa heavy chain and anti-FX heavy chain, which had FVIII-mimetic activity were successfully identified by an enzymatic assay. Heavy chain combinations were selected from the point of high FVIII-mimetic activity, not from the point of the similarity of the cognate light chain.

Next, in order to identify a common light chain for the different heavy chains to FIXa and FX, the selected heavy chain combinations were expressed with either one of cognate light chains. Out of 188 light chain commonized bispecific antibodies, the most potent one, termed c1, which consisted of rat anti-FIXa V_H and mouse anti-FX V_H chimerized with human IgG_4 and rat anti-FIXa V_L chimerized with human κ (c1L), was selected for the next step.

Finally, in order to design a more potent common light chain, we performed FR/CDR shuffling. Since the cognate light chain for the selected anti-FX V_H (c2L) was not effective as a common light chain at all (data not shown), we tried to seek another effective common light chain with a high homology to c2L. From our antibody source, we identified a light chain (c3L) whose CDR sequence had >85% homology to that of c2L, and found out that it was effective as a common light chain for the selected two heavy chains. Therefore, we decided to use c3L for FR/CDR shuffling, too. Then, CDRs of c1L, c2L and c3L were shuffled among each other and grafted onto the FRs of c1L and c3L to generate twenty four light chain variants (supplementary Fig. S2A). Twenty four light chain variants were expressed with the two heavy chains, and the most potent common light chain, BS15L, a mouse–rat hybrid V_L chimerized with human κ, was identified (supplementary Fig. S2B). Thus, the light chain communized bispecific antibody with BS15L was selected as the lead chimeric bispecific IgG antibody (termed BS15).

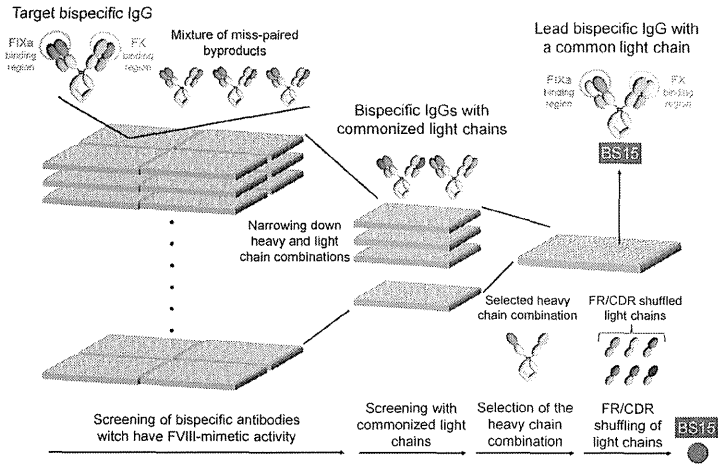

Figure 2. Flow of process to identify the lead bispecific antibody (BS15). BS15 was identified by combinatorial screening of bispecific antibodies, followed by screening of common light chains and then FR/CDR shuffling.
doi:10.1371/journal.pone.0057479.g002

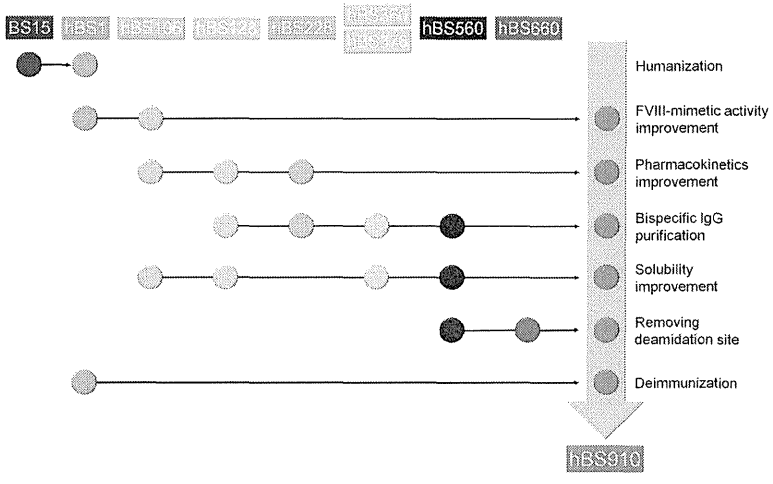

Figure 3. Multidimensional optimization flow to generate the bispecific antibody with most appropriate properties (hBS910). hBS910 was generated through multidimensional optimization with various antibody engineering technologies.
doi:10.1371/journal.pone.0057479.g003

Humanization of Lead Chimeric Bispecific Antibody

The lead chimeric bispecific IgG antibody, BS15, was subjected to humanization. CDRs of the anti-FIXa heavy chain, the anti-FX heavy chain and the common light chain were grafted onto homologous human antibody FRs, which were the FRs of V_H3, V_H1 and $V_κ1$ subfamilies respectively, by using a conventional CDR grafting approach [28]. A humanized bispecific IgG_4 antibody, termed hBS1, was successfully generated while maintaining FVIII-mimetic activity (supplementary Fig. S3).

Improving FVIII-mimetic Activity of the Bispecific Antibody

Although the humanized bispecific antibody hBS1 enhanced FX activation dose-dependently, demonstrating FVIII-mimetic activity, its therapeutic potential was marginal and its FVIII-mimetic activity needed to be improved for therapeutic application. Therefore, we explored mutations in the CDRs of hBS1 to improve the FVIII-mimetic activity, and we identified several effective mutations in the CDRs of the three chains. Following extensive studies to identify effective combinations of mutations that additively or synergistically improved FVIII-mimetic activity, we successfully generated hBS106. hBS106 demonstrated marked improvement of FVIII-mimetic activity over hBS1, including maximum activity, in the enzymatic assay (Fig. 4A).

During the course of subsequent optimization of hBS106 from the point of other aspects, FVIII-mimetic activity was monitored for each mutation so that the mutation would not compromise the activity. Moreover, further screening for mutations to further improve the activity was performed in parallel with other optimizations. Finally, we successfully generated hBS910, whose activity was even higher than that of hBS106 (Fig. 4A).

Improving Pharmacokinetics of the Bispecific Antibody

To assess the pharmacokinetics of hBS106, the variant with improved FVIII-mimetic activity, the time course of the plasma concentration of this antibody (Fig. 4B) and its pharmacokinetic parameters (supplementary Table S2) were determined in mice. Clearance of hBS106 (67 mL/day/kg) was unexpectedly larger than the clearance of human IgG_4 antibody reported in mice after subcutaneous injection (3–20 mL/day/kg) [29].

A homology model of hBS106 was used to explore the molecular features responsible for the poor pharmacokinetics, and a positive charge cluster was identified on the surface of Fv of the anti-FIXa arm (supplementary Fig. S4). To remove this cluster, we initially attempted subjecting lysine and arginine residues in the cluster to mutagenesis. However, these residues were found to be indispensable for the FVIII-mimetic activity (data not shown). Therefore, we explored the introduction of negatively charged residues near the cluster to neutralize the positive charge, and we identified a Tyr30Glu mutation in the common light chain that achieved this without any reduction in FVIII-mimetic activity. With hBS128, a variant of hBS106 with the single Tyr30Glu mutation, we observed improved plasma concentration and an approximately 4-fold improvement in the clearance compared to hBS106. Furthermore, the isoelectric point (pI) of hBS128 was lowered by introducing multiple mutations in the variable regions. hBS228, a variant of hBS128 with lowered pI, demonstrated further improved plasma concentration and approximately 2-fold improvement in clearance compared to hBS128 (Fig. 4B, supplementary Table S2). During the course of subsequent optimization of hBS228, we constantly made an effort to further improve the pharmacokinetics of the bispecific antibody.

Isoelectric Point Engineering to Facilitate Purification of the Target Bispecific Antibody

Having a common light chain reduces the number of pairs of heavy and light chains to three, and engineering the C_H3 domain enables preferential secretion of heterodimerized heavy chains. However, it is still difficult to completely prevent miss-paired homodimerization in large-scale production. Therefore, a downstream purification process to remove homodimeric byproducts is essential for pharmaceutical development. Ion exchange chromatography (IEC) is the major purification process by which to remove impurities after Protein A purification. The retention of IgG antibodies by IEC is determined by the electrostatic charge of the antibody molecule, which can be measured as its pI. Therefore, the pIs of hBS128 and hBS228, variants with improved pharmacokinetics, and pIs of their homodimeric byproducts were determined by cIEF (Fig. 5A). For both hBS128 and hBS228, the pIs of the bispecific antibody and the homodimeric byproducts

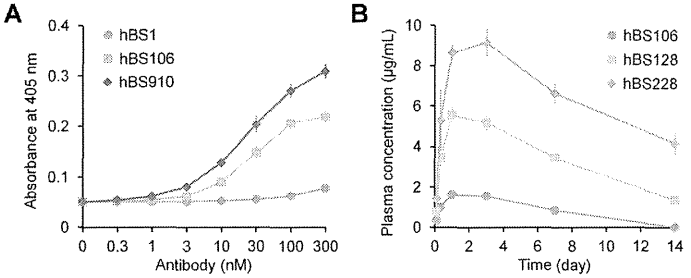

Figure 4. Improvement of therapeutic potential of the bispecific antibody. (A) Improving FVIII-mimetic activity of the bispecific antibody. Effect of hBS1 (circles), hBS106 (squares), and hBS910 (diamonds) on FX activation in the presence of FIXa, FX, and synthetic phospholipid is shown. The Y-axis indicates the absorbance at 405 nm of the chromogenic substrate assay (in many cases, the bars depicting s.d. are shorter than the height of the symbols). (B) Improving pharmacokinetics of the bispecific antibody. Time profiles of plasma concentration of hBS106 (circles), hBS128 (squares), and hBS228 (diamonds) in mice after subcutaneous injection at a dose of 1 mg/kg are shown. All the data were collected in triplicate and are expressed as mean ± s.d.
doi:10.1371/journal.pone.0057479.g004

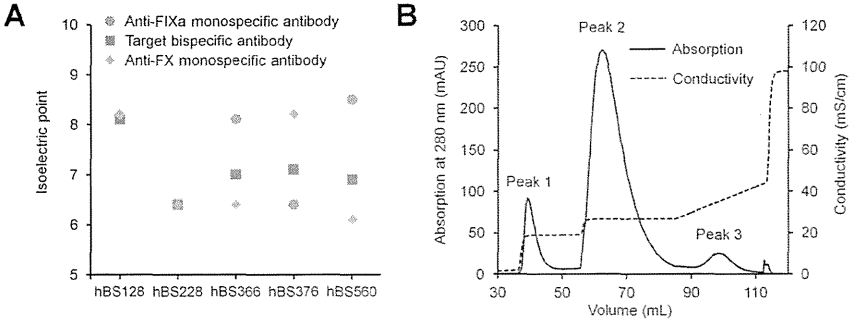

Figure 5. Isoelectric point engineering to facilitate purification of the target bispecific antibody. (A) Isoelectric points of target bispecific (squares) antibodies and homodimeric byproducts (anti-FIXa monospecific antibodies (circles) and anti-FX monospecific antibodies (diamonds)) determined by cIEF. (B) Cation exchange purification chromatogram of the target bispecific antibody of hBS560 from its homodimeric byproducts with step-wise elution with different NaCl concentrations. Peak 1, anti-FX homodimeric antibody; Peak 2, target bispecific antibody; Peak 3, anti-FIXa homodimeric antibody. Each peak area of peak 1, peak 2 and peak 3 was 9.9%, 85.7% and 4.4%, respectively.
doi:10.1371/journal.pone.0057479.g005

were very close to each other, indicating that purification of the bispecific antibody hBS128 or hBS228 from the mixture of homodimeric byproducts is not feasible.

To facilitate the purification of the bispecific antibody, we implemented pI engineering into either one of the heavy chain variable regions to increase the pI difference between the bispecific antibody and the homodimeric byproducts. We successfully generated two variants, hBS366 (pI of the anti-FX heavy chain is lowered) and hBS376 (pI of the anti-FIXa heavy chain is lowered), in which FVIII-mimetic activity was maintained. The difference in the pI between the bispecific antibody and homodimeric byproducts markedly increased (Fig. 5A).

hBS366 was further optimized from the point of solubility (detail in the next paragraph), to generate hBS560. The target molecular form of hBS560 (heterodimeric bispecific antibody) was well separated from the two homodimeric byproducts by using cation exchange chromatography with step-wise elution (Fig. 5B). During the course of subsequent optimization of hBS560, the pI difference between the two heavy chains was carefully maintained. The multidimensionally optimized variant hBS910 was capable of being purified on a large production scale (2500-liter fermentation).

Improving Solubility Properties of the Bispecific Antibody

hBS106, a variant with improved FVIII-mimetic activity, had unexpectedly low solubility, exhibiting either precipitation or liquid–liquid phase separation [30] (supplementary Fig. S5). This lack of solubility was partially due to the positive charge cluster, since the Tyr30Glu mutation described above markedly improved the solubility. However, for hBS376, the variant whose anti-FIXa heavy chain pI was lowered, at concentrations of 4 and 40 mg/mL, precipitation and phase separation still occurred in phosphate buffer of pH 5.5 to 7.0 and NaCl of 100 mM or less (Fig. 6A).

To improve the solubility of hBS376, mutations in the variable regions of hBS376 were explored. Several effective mutations including substitutions of hydrophobic residues into hydrophilic residues were identified, and their combinations successfully generated hBS560. Precipitation and phase separation of hBS560, the variant with improved solubility, was markedly suppressed and occurred only below 40 mM NaCl (Fig. 6A). The solubility of hBS560 was more than 100 mg/mL. During the course of subsequent optimization of hBS560, the effect of mutations on the solubility was constantly monitored and we made further efforts on improving the solubility. We successfully generated hBS910, a multidimensionally optimized variant, which did not exhibit precipitation or phase separation under the conditions tested (Fig. 6A). Furthermore, hBS910 could be concentrated up to at least 200 mg/mL.

Removing Deamidation Site in the CDR of the Bispecific Antibody

An accelerated stability study revealed that hBS560 exhibited asparagine deamidation in the third complementarity-determining region of the heavy chain (HCDR3) (Asn99) of the anti-FIXa arm after incubation at 40 C for 2 weeks, as shown by the increase in the acidic peak in the cation exchange chromatography analysis (Fig. 6B) [31], and reduction of FVIII-mimetic activity was observed (data not shown). A single mutation of Asn99 to another amino acid to remove this deamidation site was not feasible due to the loss of FVIII-mimetic activity and solubility. Subsequently, a double mutation was explored, and hBS660, in which a His98Arg and Asn99Glu double mutation was introduced to hBS560, was identified to maintain the FVIII-mimetic activity. hBS660 showed no increase in the acidic peak after incubation, demonstrating that the deamidation site was removed (Fig. 6B). During the course of subsequent optimization of hBS660, deamidation was carefully monitored, and successfully generated hBS910, a multidimensionally optimized variant, which did not exhibit deamidation.

Deimmunization of Humanized Bispecific Antibody by Removing T-cell Epitopes

During the course of multidimensional optimization of hBS1, the effects of each mutation on immunogenicity were evaluated by Epibase (Lonza), an *in silico* T-cell epitope prediction system [32]. Any mutation that was predicted to increase the potential

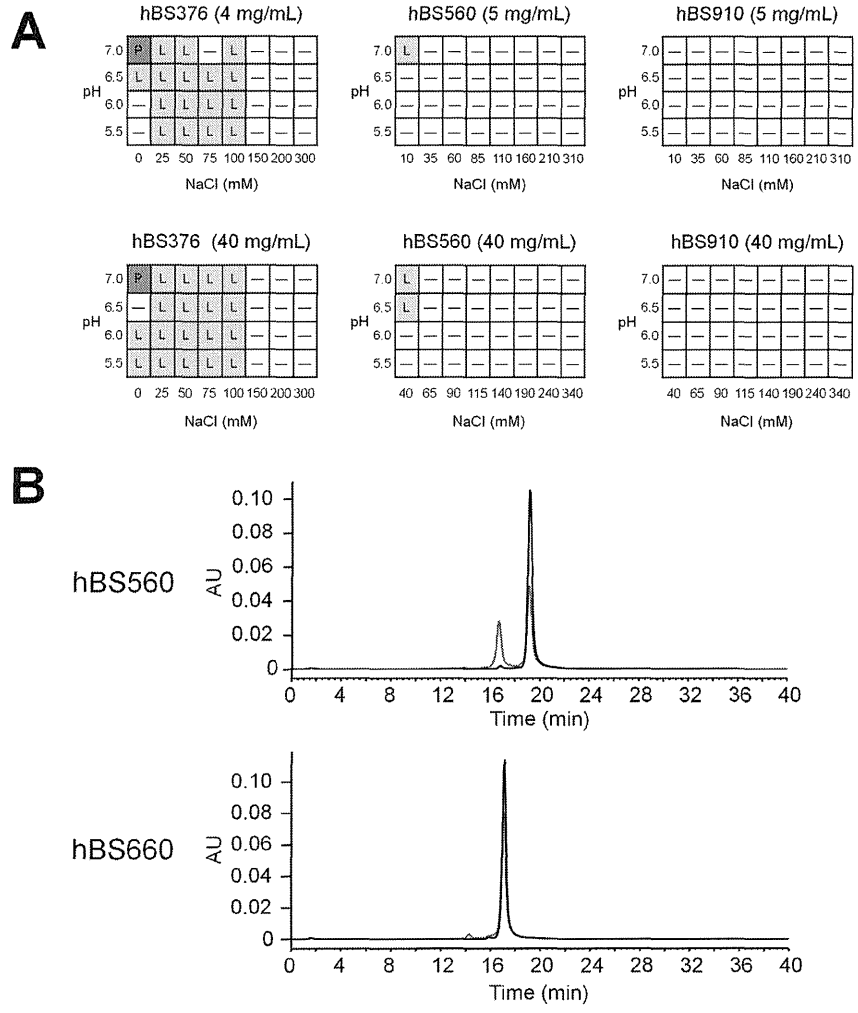

Figure 6. Improvement of pharmaceutical properties of bispecific antibodies. (A) Antibody solution profiles of hBS376 and hBS560 at different antibody concentrations, pH, and NaCl concentrations. The antibody solution under each condition was photographed and the state determined (P, precipitation; L, liquid–liquid phase separation; –, clear liquid). (B) Cation exchange chromatography of hBS560 and hBS660 before (black) and after incubation at 40°C for 2 weeks (red). Acidic peak indicating deamidation at HCDR3 increased after incubation at 40°C for 2 weeks for hBS560. No marked increase of acidic peak was observed for hBS660.
doi:10.1371/journal.pone.0057479.g006

immunogenicity risk was avoided as much as possible. Simultaneously, to generate a bispecific antibody with minimum immunogenicity risk, any mutation that was predicted to decrease the potential immunogenicity risk by reducing the number of T-cell epitopes was screened.

The immunogenicity risk score of hBS910, the multidimensionally optimized variant, was markedly decreased compared to the lead chimeric antibody (BS15) and its humanized version (hBS1), and was comparable to trastuzumab and palivizumab which are non-immunogenic in clinical (supplementary Fig. S6A). Moreover, EpiMatrix (EpiVax), another *in silico* immunogenicity prediction system [33,34], also predicted that the sequence of hBS910 was minimally immunogenic (supplementary Fig. S6B).

Therapeutic Potential of the Multidimensionally Optimized Bispecific Antibody, hBS910

To examine the therapeutic potential of hBS910, its FVIII-mimetic activity was compared with human FVIII by using thrombin generation assay (TGA) [23,35,36] in commercially available human FVIII-deficient plasma which was derived from a single donor with severe hemophilia A without FVIII inhibitors (Fig. 7A). hBS910 dose-dependently increased peak height (defined as the peak concentration of free thrombin) in the same manner as recombinant human FVIII (rhFVIII). The thrombin generation activity of hBS910 was also observed even in plasma of a hemophilia A donor who has FVIII inhibitors, whereas 1 IU/mL of rhFVIII did not exhibit any effects (data not shown). On the other hand, while polyclonal anti-idiotype antibodies to the anti-FIXa Fab or anti-FX Fab of hBS910 completely inhibited the activity of hBS910, they did not interfere with rhFVIII activity at all (data not shown).

To assess the potential for subcutaneous delivery with a long dosing interval, hBS910 was intravenously and subcutaneously administrated to cynomolgus monkeys, and the time course of the antibody plasma concentration and pharmacokinetic parameters were obtained (Fig. 7B, supplementary Table S3). The subcutaneous bioavailability was sufficiently high (86%) and the plasma half-life was approximately 3 weeks. Moreover, hBS910 could be formulated into a 150 mg/mL liquid formulation for subcutaneous delivery in the clinical setting without any significant aggregation or degradation during storage.

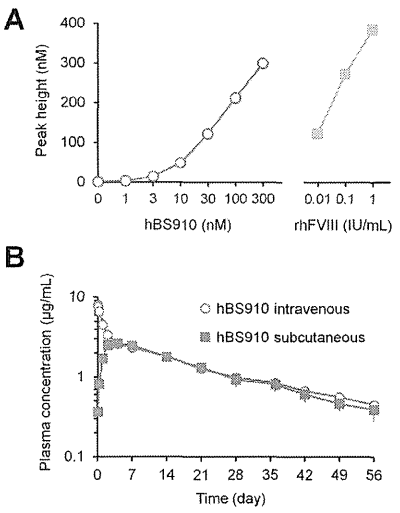

Figure 7. Therapeutic potential of multidimensionally optimized bispecific antibody, hBS910. (A) FVIII-mimetic activity of hBS910 in thrombin generation assay (TGA). Effect of hBS910 (circles) or recombinant human FVIII (squares) on thrombin generation in FVIII-deficient plasma is shown. The reaction was triggered by FXIa, synthetic phospholipid, and Ca^{2+}. The Y-axis indicates the peak height, a thrombin generation parameter (in many cases, the bars depicting s.d. are shorter than the height of the symbols). Data were collected in triplicate for each plasma lot and are expressed as mean ± s.d. (B) Pharmacokinetics of hBS910 in cynomolgus monkeys. Time profiles of plasma concentration of hBS910 after intravenous (circles) or subcutaneous (squares) injection are shown.
doi:10.1371/journal.pone.0057479.g007

Discussion

The lead bispecific antibody was identified from approximately 40,000 different bispecific antibodies. Bispecific antibodies meeting the criteria for FVIII cofactor activity were extremely rare (<0.3%). This seems reasonable since such a bispecific antibody requires simultaneous binding to the appropriate epitope of both FIXa and FX in order to place these two factors into a spatially appropriate position and precisely bring the catalytic site of FIXa close to the cleavage site of FX. Requirement of simultaneous binding to FIXa and FX by a single bispecific antibody was supported by the fact that only a bispecific antibody, and neither monospecific antibodies nor a mixture of them, exhibited FVIII-mimetic activity (supplementary Fig. S7).

Generally, the biological activity of antagonistic antibodies can be improved by increasing the binding affinity to the target antigen [37,38]. The biological activity of agonistic antibodies, on the other hand, is reported to be inversely correlated with the affinity to the antigen, presumably due to the necessity to dissociate from the antigen to repeatedly induce agonistic signals to the target [39]. In the case of our bispecific antibody, the antibody needs to bind to both FIXa and FX with sufficient affinity to promote the interaction between the factors, while after FX activation by FIXa, FXa needs to be rapidly dissociated from the antibody to proceed to the subsequent coagulation reaction and to enable the antibody to turn over. Therefore, we assumed that a simple increase in the binding affinity to both FIXa and FX would not necessarily improve the FVIII-mimetic activity. Consequently, generation of variants that had improved activity required screening of a large number of variants in which mutations had been introduced via structure-based or random mutagenesis. These mutations were mainly introduced to the residues that were predicted to directly or indirectly contact the antigen by the homology modeling of the lead antibody or experimentally identified to affect FVIII-mimetic activity.

To gain insights into the mechanisms underlying the improvement in activity, kinetic analyses of hBS1, hBS106, and hBS910 (bispecific antibodies each with different FVIII-mimetic activity) binding to FIXa and FX were performed by SPR analysis (supplementary Fig. S8A, B). However, because the kinetic parameters of these antibodies were differently affected by the fitting conditions of the sensorgrams, we were not able to obtain meaningful kinetic parameters with which to compare these antibodies. Nevertheless, the binding properties of these antibodies

were obviously different, and these changes might have contributed to the improvement in activity. It appears that the binding affinity of hBS910 to FIXa is weaker than hBS1 and hBS106, and hBS910 has faster association and dissociation rate for FX. Although this tendency might result in rapid turnover of FX activation by the bispecific antibody and explain the highest FVIII-mimetic activity of hBS910, it does not explain the large difference of FVIII-mimetic activity between hBS1 and hBS106. Since bispecific antibody needs to strictly place catalytic site of FIXa to the cleavage site of FX and may require allosteric effect on FIXa in order to mimic the function of FVIII, it can be postulated that the improved FVIII-mimetic activity of hBS106 compared to hBS1 may be derived not only from the changes in the binding kinetics but also from the subtle changes in the binding epitope, binding angle or allosteric effect caused by the mutations introduced.

The FVIII-mimetic activity of 30 nM hBS910 was equivalent to rhFVIII activity at 0.01 IU/mL (1% of normal level), and the activity of 300 nM hBS910 was greater than rhFVIII activity at 0.1 IU/mL (10% of normal level) in the TGA using human FVIII-deficient plasma. The activity was also observed even in the presence of FVIII inhibitors, which is reasonable considering the lack of homology between the sequences of hBS910 and FVIII. Recently, we have demonstrated that FVIII-mimetic bispecific antibody, termed hBS23, exerts hemostatic activity *in vivo* in acquired hemophilia A model using cynomolgus monkey, which was considered sufficient for routine prophylaxis [23]. hBS23 is one of the FVIII-mimetic activity improved variants obtained during the multidimensional optimization to generate hBS910, and has similar FVIII-mimetic activity as hBS106. Kinetic analysis [23] of hBS23 and hBS910 demonstrated that hBS910 showed two times the effect on increasing k_{cat}/K_m compared to hBS23 (unpublished data). In human FVIII-deficient plasma, hBS910 required only two third of plasma concentration to exhibit the equivalent activity to hBS23 in the TGA, suggesting that hBS910 has 1.5 times the activity to promote thrombin burst (unpublished data). When compared with FVIII, this *in vivo* hemostatic effect was consistent with its *in vitro* activity in TGA. Thus, the above results clearly demonstrate that hBS910, which is more potent than hBS23, could exert FVIII-mimetic activity in hemophilia A patients sufficient to achieve routine prophylaxis regardless of the presence of FVIII inhibitors. The amino acid sequence of hBS23 is described in our patent as an antibody name Q153-G4k/J142-G4h/L180-k, and that of hBS910 is described in the patent [Igawa T, Sampei Z, Kojima T, Soeda T, Muto A, et al. Multi-specific antigen-binding molecule having alternative function to function of blood coagulation factor VIII. WO/2012/067176].

It is highly desirable that our bispecific antibody be able to be administered subcutaneously with a long interval between doses. The poor pharmacokinetics of hBS106 in mice was partially attributed to the large positive charge cluster, and the single Tyr30Glu mutation to neutralize this charge cluster markedly improved the pharmacokinetics. Such a charge cluster may increase non-specific binding to the extracellular matrix which would increase the clearance of the molecule. Recently, it was reported that antibodies with lower pI have better pharmacokinetics, and engineering antibodies to lower the pI improved their pharmacokinetics [29]. This approach was successfully applied to our bispecific antibody. hBS910 exhibited a plasma half-life of approximately 3 weeks in cynomolgus monkeys, which is longer than the half-lives of hBS23 (approximately 2 weeks) [23] and other humanized or fully human IgG antibodies [40,41], presumably due to the benefit of pI engineering. Since the half-lives of IgG antibodies are generally longer in humans than in cynomolgus monkeys [42], we expect that hBS910 would have a half-life of at least 3 weeks in humans, which is overwhelmingly longer than that of exogenous FVIII (0.5 days) [4]. Furthermore, hBS910 exhibited 86% subcutaneous bioavailability, consistent with that of other IgG antibodies [24,43,44], providing a huge advantage over exogenous FVIII which requires intravenous administration [5]. This high subcutaneous bioavailability and long half-life of hBS910 strongly supports the feasibility of routine prophylaxis by subcutaneous administration with a long dosing interval.

We utilized an *in silico* T-cell epitope prediction system, Epibase, to minimize the number of T-cell epitopes present in the bispecific antibody. The immunogenicity risk of hBS910 was predicted not only by Epibase but also by EpiMatrix to be comparable with that of non-immunogenic antibodies. Considering that up to 30% of patients develop inhibitors against exogenous FVIII [45], immunogenicity is an important issue in the routine prophylaxis of hemophilia A. Although the true immunogenicity of hBS910 needs to be evaluated clinically, it is noteworthy that two different *in silico* systems predicted hBS910 to be non-immunogenic. However, the possibility that a small number of patients could develop anti-hBS910 antibodies cannot be ruled out. In case hBS910 becomes ineffective owing to development of anti-hBS910 antibodies, it is important that they do not cross-react with FVIII so that exogenous FVIII treatment remains as an alternative. In addition to the fact that there is no homology between the amino acid sequences of hBS910 and FVIII, the risk of such cross-reactivity was found to be negligible because polyclonal anti-idiotype antibodies against hBS910 did not inhibit the thrombin generation activity of FVIII. This demonstrates that the development of anti-hBS910 antibodies would not compromise the use of exogenous human FVIII therapy.

No recombinant bispecific IgG antibody has yet reached the market. One of the reasons is the difficulty in large-scale manufacturing at clinical grade. Identification of a common light chain is an important step for manufacturing asymmetric bispecific IgG antibodies. A previous study utilized a phage display library to identify a common light chain for the two heavy chains against different antigens [26]. However, since high-affinity binding to FIXa or FX would not necessarily result in high FVIII-mimetic activity, selection of a common light chain with potent activity based on the binding affinity by phage display was not feasible. We successfully identified a potent common light chain by a novel FR/CDR shuffling approach. Since we were able to obtain the common light chain (BS15L) that had much better potency than the parental light chain (c1L) from the initial twenty four light chain variants, we did not perform further shuffling of FRs. Because residues in the FR often affects antigen binding of the antibody, we propose that shuffling of both CDRs and FRs would be an efficient and general approach to identify potent common light chains for bispecific antibodies. This novel approach enables incorporation of the beneficial residues from each CDR and FR into a common light chain. Although it might be not suitable for screening common light chain against large panels of heavy chains, this approach can be generally applicable for identification of a common light chain for the selected pair of heavy chains without using a library display system. In our other asymmetric bispecific antibodies with the same molecular format, common light chains for two different heavy chains could be successfully identified by this approach. In some cases, it was possible to directly identify humanized common light chain by performing CDR shuffling on the human FRs. This could be a more efficient approach since it abbreviates the following humanization process. However, since FR residues are often important for antigen binding property, we took more cautious approach in this FVIII-mimetic bispecific antibody, and performed CDR shuffling on its cognate FRs to identify a potent common light chain, followed by humanization of the identified common light chain.

Although the heavy chain heterodimerization efficiency depended on the expression balance of each heavy chain, our Fc heterodimerization mutations achieved approximately 85% efficiency for hBS560 in the system of unoptimized expression balance (Fig. 5B). Nevertheless, expression of a small amount of monospecific homodimeric antibodies is inevitable even with Fc heterodimerization mutations. In the case of our bispecific antibody, byproducts are anti-FIXa and anti-FX bivalent monospecific antibodies. These byproducts are not simply impurities with no activity, but they have the potential to competitively inhibit the activity of the bispecific antibody by bivalent binding to the factors. Therefore, homodimeric byproducts need to be removed as much as possible by a downstream process. However, the only molecular difference between a homodimeric byproduct and the bispecific antibody is the heavy chain variable region of one arm. Since antibody variable regions generally have similar sequences except for the CDRs, it was assumed that separation of such byproducts from the bispecific antibody by IEC would be difficult. Therefore, we took the advantage of pI engineering, and engineered the heavy chain variable region to increase the pI difference between the bispecific antibody and the byproducts, thereby improving the separation by IEC. pI engineered hBS910 could be actually purified from 2500-liter fermentation by Protein A and IEC using conventional antibody purification processes. Such a novel pI engineering approach would be generally applicable to facilitate the purification of bispecific IgG antibodies.

To realize subcutaneous delivery in a clinical setting, bispecific antibodies need to be formulated into a high concentration (i.e. >100 mg/mL) since the volume that can be subcutaneously injected is generally limited to less than 1.5 mL [46]. However, hBS376 exhibited phase separation even at 4 mg/mL. Phase separation of antibody solutions into an upper phase with low antibody concentration and a lower phase with high antibody concentration not only precludes high concentration formulation but also makes downstream purification processes difficult [30]. It has been recently reported that low solubility of antibodies has been overcome by introducing specific mutations into the molecular surface [47], but mutations to prevent phase separation have not been reported. We demonstrated that phase separation of hBS376 could also be eliminated by introducing multiple mutations into the molecular surface. hBS910 exhibited no phase separation under the conditions tested, and could be concentrated up to at least 200 mg/mL without any issue.

Since FVIII is unstable under liquid formulation, all the marketed FVIII agents are distributed as lyophilized formulation, and therefore require reconstitution before injection. Liquid formulation allows injection without this process, and thus would be much more convenient for the patients. However, monoclonal antibodies stored in aqueous solution often undergo deamidation of the asparagine residues in the CDRs resulting in reduction of the biological activity of the antibody, which was the case for hBS560 [31]. Although the general strategy is to remove the deamidation site by mutating the asparagine residue itself to another amino acid, this strategy was not feasible in the case of hBS560. A simultaneous double mutation approach enabled storage of hBS910 at 40°C for 2 weeks without reduction of activity. Consequently, hBS910 could be stably stored in a patient-friendly 150 mg/mL liquid formulation, which would enable approximately 3 mg/kg subcutaneous delivery in humans (1.5 mL injection for a 75 kg patient). Considering the FVIII-mimetic activity determined by TGA and the pharmacokinetics in cynomolgus monkeys, such a formulation would provide effective prophylaxis by subcutaneous delivery with a long dosing interval.

In conclusion, we have generated a novel humanized anti-FIXa/FX bispecific IgG antibody, hBS910, through a process of identifying the lead candidate from approximately 40,000 bispecific combinations, followed by a multidimensional optimization process to improve both the therapeutic potential and the manufacturability. hBS910 overcomes the two major drawbacks of routine prophylaxis by exogenous FVIII. First, while exogenous FVIII requires frequent intravenous administration, hBS910 can be subcutaneously administered with a long dosing interval. Second, while the development of FVIII inhibitors is a critical issue for exogenous FVIII, our study suggests that hBS910 can be used without fear of developing FVIII inhibitors and can be used in patients who have already developed FVIII inhibitors. We believe that hBS910, with its multidimensionally optimized profile, will provide significant improvement in the quality of life of hemophilia A patients by reducing not only bleeding but also the burden on the patients themselves, their parents, and all medical staff. Potential of hBS910 (investigational drug name; ACE910) in hemophilia A patient is currently being evaluated in clinical study.

Materials and Methods

Ethics Statement

Animal studies were performed in accordance with the Guidelines for the Care and Use of Laboratory Animals at Chugai Pharmaceutical Co., Ltd. under the approval of the company's Institutional Animal Care and Use Committee. The company is fully accredited by the Association for Assessment and Accreditation of Laboratory Animal Care International (http://www.aaalac.org). Details of cynomolgus monkey care and maintenance, including shelter and availability of food, water, and environmental enrichment are as follows. Identification of individuals; individual animals were identified by microchip number. Each cage was identified by a cage number indicated on the cage rack. cage type; a stainless steel cage, housing density; 1 animal/cage, temperature; 18 C to 28 C, relative humidity; 35% to 75%, air change frequency; at least 10 times per h, illumination timing; 12 h per day, from 7:00 am to 7:00 pm, feed; cynomolgus monkeys were daily provided approximately 100 g of solid chow (Certified Primate Diet 5048, Japan SLC) and supplementary foods (1/2 peeled banana or 50 g of sweet potato) and drinking water; animal room tap water, provided ad libitum using the automatic water supply system. The studies involved injection of the agents and collection of blood samples which did not require procedures that would cause more than slight or momentary pain or distress to the animals. All injections and blood collection were conducted by trained and qualified primate therapeutic staff in Chugai Pharmaceutical. Provisions were made in the approved protocol for veterinary intervention in the case of any distress or morbidity from the injected agent; however no adverse events occurred during the studies or during the recovery period. Therefore, no scarification of the animals was conducted.

Generation of Anti-FIXa/FX Bispecific Antibodies

Approximately 200 monoclonal antibodies to FIXa or FX were obtained from FIXa or FX immunized mice, rats, and rabbits. The V_H and V_L of those antibodies were then combined with engineered human IgG_2 or IgG_4 that included mutations to facilitate Fc heterodimerization. These engineered human IgG_2 or IgG_4, which included the knobs-into-holes mutations [26], were generated by introducing the same substitutions as those of IgG_1 knobs-into-holes to the corresponding positions of IgG_2 and IgG_4

heavy chains, and were used through the screening for the lead identification. Anti-FIXa/FX bispecific were generated by HEK293 cells co-transfected with mixture of four plasmids encoding anti-FIXa heavy and light chain and anti-FX heavy and light chain (supplementary Fig. S1). At the screening step for lead identification, we used knobs-into-holes mutations which could achieve at least 90% efficiency of the two heavy chain heterodimerization. If the assembly of a heavy chain with two light chains occurs with equal probability, 25% of heavy chain heterodimeric antibodies will have the correct heavy and light chain pair [25]. Theoretically, in the supernatant of transfected cells, this would result in at least approximately 20% (90% ×25% = 22.5%) of antibodies to be the target bispecific antibody, and less than 3% (10% ×25% = 2.5%) of antibodies to be homodimeric antibodies with a correct heavy and light chain pair. Transfected cells were cultured in 96-well culture plates, and either filtrated culture supernatants or Protein A purified antibodies were used for evaluation. We also generated bispecific antibodies with a common light chain, anti-FIXa monospecific IgG consisting of anti-FIXa heavy chain and a common light chain, and anti-FX monospecific IgG consisting of anti-FX heavy chain and a common light chain by the method described above. The engineered human IgG_4 including the knobs-into-holes mutations was used during the early stage of the multidimensional optimization, and a different engineered IgG_4 including electrostatic steering mutations [25] was used during the late stage optimization. By using the engineered IgG_4, approximately 85–95% of the Protein A purified antibody would be the target bispecific antibody and the rest would be homodimeric antibodies. For the detailed characterization of hBS910, homodimeric antibodies were removed by ion exchange chromatography.

Screening Bispecific Antibodies for FVIII-mimetic Activity (Enzymatic Assay)

The ability of each antibody to enhance FIXa-catalized FXa generation was evaluated in an enzymatic assay with purified human coagulation factors (Enzyme Research Laboratories). The FXa generation reaction was performed in the presence of 1 nM human FIXa, 140 nM human FX, 20 μM synthetic phospholipid (10% phosphatidylserine, 60% phosphatidylcholine and 30% phosphatidylethanolamine; Avanti Polar Lipids) prepared as previously described [48], and antibodies at room temperature for 2 min in TBS containing 5 mM $CaCl_2$, 1 mM $MgCl_2$ and 0.1% (wt/vol) BSA (pH 7.6). The reaction was stopped by the addition of EDTA at appropriate time points. The activity of the FXa generated was determined by absorbance at 405 nm after the addition of chromogenic substrate S-2222 (Chromogenix). Data were collected in triplicate.

FR/CDR Shuffling of the Light Chains

CDRs of three light chains (c1L, c2L and c3L) were shuffled among each other then grafted onto the FRs of either c1L or c3L to generate light chain variants (supplementary Fig. S2A). Since c2L and c3L had identical CDR1 and CDR2 sequences, we generated twenty four light chains (twelve CDR combinations in two FRs) including parental c1L and c3L. Light chain variant genes were generated by assembly PCR, and the twenty four bispecific antibodies with these light chains were prepared as described above. FVIII-mimetic activity of each antibody was evaluated in APTT assay with standard techniques using APTT reagent (Sysmex) and FVIII deficient plasma (Sysmex).

Pharmacokinetic Study of Bispecific Antibodies in Mice

1 mg/kg doses of each bispecific antibody were administered to C57BL/6J normal mice (Charles River) by single subcutaneous injection ($n = 3$ for each group). Blood samples were collected at an appropriate time after each administration. Plasma concentration of bispecific antibodies was determined by human IgG-specific ELISA. Pharmacokinetic parameters were calculated by WinNonlin Professional software (Pharsight).

Determination of Isoelectric Point (pI) by Capillary Isoelectric Focusing (cIEF)

cIEF analyses of antibodies were performed with a PA800 plus Pharmaceutical Analysis System and 32 Karat software (Beckman Coulter) as described in the cIEF application guide (PN A78788AA). Briefly, antibody solutions (approximately 1 mg/mL in PBS) were diluted 1:25 with cIEF master mix solution containing cIEF gel, urea, Pharmalyte 3–10, arginine, iminodiacetic acid, and pI markers. A neutral capillary was preconditioned by rinsing with urea solution, and samples were injected and focused. The pI of each of the antibodies was determined from the pI markers.

Separation of Bispecific Antibodies by Cation Exchange Chromatography

Using an AKTAexplorer 10S (GE Healthcare), two HiTrap SP FF 1 mL columns (GE Healthcare) were connected in tandem and equilibrated by 20 mM sodium phosphate, pH 6.0. The elution buffer contained an appropriate concentration of NaCl in this equilibration buffer. The load sample was first prepared from culture supernatant using MabSelect Sure (GE Healthcare), and was then dialyzed with equilibration buffer. The sample antibody solution was applied to the HiTrap SP FF column at 1.5 mg/mL resin. After washing with equilibration buffer, antibodies were eluted with 10 column volumes (CV) of equilibration buffer containing 150 mM NaCl and then with 15 CV of 220 mM NaCl buffer in a stepwise manner, and finally with 15 CV of NaCl buffer in a linear gradient to 450 mM.

Solubility Analysis of Bispecific Antibodies

Stock solutions of bispecific antibodies were prepared by dialysis against water or 50 mM NaCl solutions, followed by ultrafiltration concentration. Samples were prepared by adding formulation stock solution to antibody stock solution using a Hydra II Plus One liquid-handling robot (Matrix). After centrifugation, 1 μL of each sample was stored in an Intelli-Plate 96-2 (Art Robbins) at 20°C for 1 day, and then images of each well were taken by Rock Imager 54 (Formulatrix). The state of each antibody solution was determined as either a clear solution, precipitation, or liquid–liquid phase separation.

Accelerated Stability Study of Bispecific Antibodies

Solutions of bispecific antibodies were dialyzed against PBS, pH 7.4 (Sigma). 1 mg/mL of each antibody solution was stored at 40°C for 2 weeks and then analyzed by cation exchange chromatography (IEC) using BioPro SP columns (YMC) at room temperature. The mobile phase (A) was 20 mM sodium phosphate, pH 5.8, and the mobile phase (B) was 20 mM sodium phosphate and 500 mM NaCl, pH 5.8.

In silico Evaluation of Immunogenicity of the Variable Region of Bispecific Antibodies

T-cell epitope prediction of the bispecific antibody variants and immunogenicity risk scores of antibodies were provided by Epibase (Lonza). Immunogenicity scales of antibodies were provided by EpiMatrix (EpiVax).

Thrombin Generation Assay (TGA)

Calibrated automated thrombography [35] was employed using a 96-well plate fluorometer (Thermo Fisher Scientific) equipped with a 390/460 filter set, a dispenser, and the analyzing software (Thrombinoscope software version 3.0.0.29; Thrombinoscope) to measure thrombograms. Briefly, each concentration of bispecific antibody or rhFVIII (Bayer Healthcare) was added to FVIII-deficient plasma (<1% FVIII activity) either without inhibitors or with inhibitors against FVIII (George King Bio-Medical). Each concentration of bispecific antibody or rhFVIII was also added to plasma containing polyclonal rabbit anti-idiotype antibodies against anti-FIXa Fab or anti-FX Fab (300 μg/mL each). Into each well was dispensed 80 μL of the plasma, to which was then added 20 μL of the triggering solution containing 0.47 nM human FXIa (Enzyme Research Laboratories) and 20 μM synthetic phospholipid but no Ca^{2+}. For calibration, 20 μL of Thrombin Calibrator (Thrombinoscope) was added instead of the triggering solution. 20 μL of FluCa-reagent prepared from FluCa-kit (Thrombinoscope) was dispensed to initiate the reaction. The thrombograms and peak height were analyzed by the software. Data were collected in triplicate.

Pharmacokinetic Study of hBS910 in Cynomolgus Monkeys

A single dose of 0.3 mg/kg of hBS910 was intravenously or subcutaneously administered to male cynomolgus monkeys ($n = 3$ for each group). Blood samples were collected at an appropriate time after each administration. Plasma concentration of bispecific antibodies was determined by human IgG-specific ELISA. Pharmacokinetic parameters were calculated by WinNonlin Professional software (Pharsight).

Kinetic Analysis of Bispecific Antibodies Binding to FIXa and FX Using Surface Plasmon Resonance

Kinetic analysis of bispecific antibodies was performed by surface plasmon resonance (SPR) using a Biacore T200 system (GE Healthcare). MabSelect SuRe Ligand (Recombinant Protein A; GE Healthcare) was immobilized onto a CM4 sensor chip (GE Healthcare). Then, anti-FIXa or anti-FX monospecific antibodies were injected into flow cell 2 to be captured. Natalizumab (Biogen-Idec Inc.) as a control human IgG_4 antibody was also injected into flow cell 1 to be captured. Then, 0, 80, 160, 320, 640, or 1,280 nM human FIXa or FX dissolved in running buffer (10 mM HEPES [pH 7.4], 150 mM NaCl, 0.05% surfactant P20, 2.5 mM $CaCl_2$) was injected at a flow rate of 30 μL/min to monitor the association phase for 120 s and the dissociation phase for 30 s.

Supporting Information

Figure S1 Generation of anti-FIXa/FX bispecific antibodies. Heavy chain variable regions (V_H) of anti-FIXa or anti-FX antibodies were fused with engineered human IgG_2 or IgG_4 constant region having mutations to facilitate Fc heterodimerization. Light chain variable regions (V_L) were fused with human κ or λ constant region. Bispecific antibodies were generated by expression with two pairs of genes, anti-FIXa and anti-FX heavy chain and light chain genes (or a common light chain gene).
(PDF)

Figure S2 FR/CDR shuffling of the light chain. (A) CDRs of three light chains (c1L, c2L and c3L) were shuffled among each other and grafted onto the FRs of c1L and c3L. Each light chain variant was expressed with the selected anti-FIXa and anti-FX heavy chains. (B) Effects of bispecific antibodies (67 nM) with light chain variants on APTT assay in FVIII-deficient plasma are shown. The Y-axis indicates the APTT (s). All the data were collected in duplicate and are expressed as mean.
(PDF)

Figure S3 Effect of humanization of the lead chimeric antibody (BS15) on FVIII-mimetic activity. Effect of chimeric antibody BS15 (circles) or humanized antibody hBS1 (squares) on FX activation in the presence of FIXa, FX, and synthetic phospholipid. The Y-axis indicates the 405 nm absorbance at 120 min of chromogenic development in the chromogenic substrate assay. All the data were collected in triplicate and are expressed as mean ± s.d (in many cases, the bars depicting s.d. are shorter than the height of the symbols).
(PDF)

Figure S4 Positive charge cluster and Tyr30Glu mutation on anti-FIXa Fv of hBS106. The positive charge cluster consists of arginine or lysine residues at Kabat position 60, 61, and 95 in the heavy chain and Kabat positions 24, 27, 31, 53, 54, 61, and 66 in the light chain of hBS106. Tyrosine located at Kabat position 30 in the light chain was mutated to glutamic acid to neutralize the positive charge cluster. Blue, red and gray colored surface indicates positively charged, negatively charged and neutral protein surface, respectively. Red and green line indicates heavy and light chain, respectively.
(PDF)

Figure S5 Precipitation and liquid–liquid phase separation of bispecific antibody solution. Micro CCD camera images of states of bispecific antibody solution showing a clear solution, precipitation, and liquid–liquid phase separation.
(PDF)

Figure S6 *In silico* prediction of immunogenicity of bispecific antibodies. (A) Immunogenicity risk score of BS15, hBS1, hBS910, trastuzumab, and palivizumab predicted by Epibase. (B) Immunogenicity scale of hBS910 and other marketed monoclonal antibodies by EpiMatrix. In both prediction systems, higher score indicates higher risk of immunogenicity in human.
(PDF)

Figure S7 Necessity of bispecific binding to FIXa and FX for FVIII-mimetic activity. Effect of the bispecific antibody (hBS910) (circles), monospecific anti-FIXa antibody (squares), monospecific anti-FX antibody (triangles), or a mixture of the two monospecific antibodies (diamonds) on FX activation in the presence of FIXa, FX, and synthetic phospholipid. The Y-axis indicates the 405 nm absorbance at 30 min of chromogenic development in the chromogenic substrate assay. All the data were collected in triplicate and are expressed as mean ± s.d (in many cases, the bars depicting s.d. are shorter than the height of the symbols). Monospecific antibodies against FIXa or FX antibodies or the mixture of them did not exhibit any detectable activity even at 120 min of chromogenic development.
(PDF)

Figure S8 Surface plasmon resonance analysis of bispecific antibodies binding to FIXa and FX. Sensorgrams of hBS1, hBS106, and hBS910 binding to FIXa (A) and FX (B) at a concentration of 80 nM, 160 nM, 320 nM, 640 nM, and 1280 nM.
(PDF)

Acknowledgments

We thank our colleagues at Chugai Research Institute for Medical Science, Inc. and Chugai Pharmaceutical Co. Ltd., K. Nagano, H. Sano, T. Sakamoto, T. Matsuura, R. Takemoto, M. Hiranuma and H. Kitamura for carrying out *in vivo* studies; M. Fujii, Y. Nakata, H. Ishida and F. Isomura for antibody generation; S. Ohtsu for carrying out the physicochemical study; and M. Yoshida for carrying out the cIEF analysis.

Author Contributions

Provided direction and guidance: YN. Provided the hypothesis of the bispecific antibody, directed and organized the program: K. Hattori. Conceived and designed the experiments: TI T. Kojima T. Kitazawa. Performed the experiments: ZS TI TS YON CM TW ET AM KY AH MF K. Haraya TT SS KE. Wrote the paper: ZS TI.

References

1. Geraghty S, Dunkley T, Harrington C, Lindvall K, Maahs J, et al. (2006) Practice patterns in haemophilia A therapy - global progress towards optimal care. Haemophilia 12: 75–81.
2. Manco-Johnson MJ, Abshire TC, Shapiro AD, Riske B, Hacker MR, et al. (2007) Prophylaxis versus episodic treatment to prevent joint disease in boys with severe hemophilia. N Engl J Med 357: 535–544.
3. Ragni MV, Fogarty PJ, Josephson NC, Neff AT, Raffini LJ, et al. (2012) Survey of current prophylaxis practices and bleeding characteristics of children with severe haemophilia A in US haemophilia treatment centres. Haemophilia 18: 63–68.
4. Bjorkman S, Oh M, Spotts G, Schroth P, Fritsch S, et al. (2012) Population pharmacokinetics of recombinant factor VIII: the relationships of pharmacokinetics to age and body weight. *Blood* 119: 612–618.
5. Shi Q, Kuether EL, Schroeder JA, Fahs SA, Montgomery RR (2012) Intravascular recovery of VWF and FVIII following intraperitoneal injection and differences from intravenous and subcutaneous injection in mice. Haemophilia 18: 639–646.
6. Berntorp E, Shapiro AD (2012) Modern haemophilia care. Lancet 379: 1447–1456.
7. Astermark J, Donfield SM, DiMichele DM, Gringeri A, Gilbert SA, et al. (2007) A randomized comparison of bypassing agents in hemophilia complicated by an inhibitor: the FEIBA NovoSeven Comparative (FENOC) Study. Blood 109: 546–551.
8. Leissinger C, Gringeri A, Antmen B, Berntorp E, Biasoli C, et al. (2011) Anti-inhibitor coagulant complex prophylaxis in hemophilia with inhibitors. N Engl J Med 365: 1684–1692.
9. Chan AC, Carter PJ (2010) Therapeutic antibodies for autoimmunity and inflammation. Nat Rev Immunol 10: 301–316.
10. Weiner LM, Surana R, Wang S (2010) Monoclonal antibodies: versatile platforms for cancer immunotherapy. Nat Rev Immunol 10: 317–327.
11. Beck A, Wurch T, Bailly C, Corvaia N (2010) Strategies and challenges for the next generation of therapeutic antibodies. Nat Rev Immunol 10: 345–352.
12. Liu Z, Stoll VS, Devries PJ, Jakob CG, Xie N, et al. (2007) A potent erythropoietin-mimicking human antibody interacts through a novel binding site. Blood 110: 2408–2413.
13. Mayorov AV, Amara N, Chang JY, Moss JA, Hixon MS, et al. (2008) Catalytic antibody degradation of ghrelin increases whole-body metabolic rate and reduces refeeding in fasting mice. Proc Natl Acad Sci U S A 105: 17487–17492.
14. Bhaskar V, Goldfine ID, Bedinger DH, Luu A, Kuan HF, et al. (2012) A fully human, allosteric monoclonal antibody that activates the insulin receptor and improves glycemic control. Diabetes 61: 1263–1271.
15. Songsivilai S, Lachmann PJ (1990) Bispecific antibody: a tool for diagnosis and treatment of disease. Clin Exp Immunol 79: 315–321.
16. Baeuerle PA, Kufer P, Bargou R (2009) BiTE: Teaching antibodies to engage T-cells for cancer therapy. Curr Opin Mol Ther 11: 22–30.
17. *Jackman J, Chen Y, Huang A, Moltat B, Scheer JM, et al. (2010) Development* of a two-part strategy to identify a therapeutic human bispecific antibody that inhibits IgE receptor signaling. J Biol Chem 285: 20850–20859.
18. Fay PJ, Haidaris PJ, Smudzin TM (1991) Human factor VIIIa subunit structure. Reconstruction of factor VIIIa from the isolated A1/A3-C1-C2 dimer and A2 subunit. J Biol Chem 266: 8957–8962.
19. Fay PJ, Koshibu K (1998) The A2 subunit of factor VIIIa modulates the active site of factor IXa. J Biol Chem 273: 19049–19054.
20. Lapan KA, Fay PJ (1997) Localization of a factor X interactive site in the A1 subunit of factor VIIIa. J Biol Chem 272: 2082–2088.
21. Lapan KA, Fay PJ (1998) Interaction of the A1 subunit of factor VIIIa and the serine protease domain of factor X identified by zero-length cross-linking. Thromb Haemost 80: 418–422.
22. Lenting PJ, Donath MJ, van Mourik JA, Mertens K (1994) Identification of a binding site for blood coagulation factor IXa on the light chain of human factor VIII. J Biol Chem 269: 7150–7155.
23. Kitazawa T, Igawa T, Sampei Z, Muto A, Kojima T, et al. (2012) A bispecific antibody to factors IXa and X restores factor VIII hemostatic activity in a hemophilia A model. Nat Med 18: 1570–1574.
24. Kontermann R (2012) Dual targeting strategies with bispecific antibodies. MAbs 4: 182–197.
25. Klein C, Sustmann C, Thomas M, Stubenrauch K, Croasdale R, et al. (2012) Progress in overcoming the chain association issue in bispecific heterodimeric IgG antibodies. MAbs 4: 653–663.
26. Merchant AM, Zhu Z, Yuan JQ, Goddard A, Adams CW, et al. (1998) An efficient route to human bispecific IgG. Nat Biotechnol 16: 677–681.
27. Igawa T, Tsunoda H, Kuramochi T, Sampei Z, Ishii S, et al. (2011) Engineering the variable region of therapeutic IgG antibodies. MAbs 3: 243–252.
28. Jones PT, Dear PH, Foote J, Neuberger MS, Winter G (1986) Replacing the complementarity-determining regions in a human antibody with those from a mouse. Nature 321: 522–525.
29. Igawa T, Tsunoda H, Tachibana T, Maeda A, Mimoto F, et al. (2010) Reduced elimination of IgG antibodies by engineering the variable region. Protein Eng Des Sel 23: 385–392.
30. Mason BD, Zhang L, Remmele RL, Jr., Zhang J (2011) Opalescence of an IgG2 monoclonal antibody solution as it relates to liquid-liquid phase separation. J Pharm Sci 100: 4587–4596.
31. Vlasak J, Bussat MC, Wang S, Wagner-Rousset E, Schaefer M, et al. (2009) Identification and characterization of asparagine deamidation in the light chain CDR1 of a humanized IgG1 antibody. Anal Biochem 392: 145–154.
32. *Van Walle I, Gansemans Y, Parren PW, Stas P, Lasters I* (2007) Immunogenicity screening in protein drug development. Expert Opin Biol Ther 7: 405–418.
33. De Groot AS, McMurry J, Moise L (2008) Prediction of immunogenicity: in silico paradigms, ex vivo and in vivo correlates. Curr Opin Pharmacol 8: 620–626.
34. Weber CA, Mehta PJ, Ardito M, Moise L, Martin B, et al. (2009) T cell epitope: friend or foe? Immunogenicity of biologics in context. Adv Drug Deliv Rev 61: 965–976.
35. Hemker HC, Giesen P, Al Dieri R, Regnault V, de Smedt E, et al. (2003) Calibrated automated thrombin generation measurement in clotting plasma. Pathophysiol Haemost Thromb 33: 4–15.
36. Shima M, Matsumoto T, Ogiwara K (2008) New assays for monitoring haemophilia treatment. Haemophilia 14 Suppl 3: 83–92.
37. Maynard JA, Maassen CB, Leppla SH, Brasky K, Patterson JL, et al. (2002) Protection against anthrax toxin by recombinant antibody fragments correlates with antigen affinity. Nat Biotechnol 20: 597–601.
38. Johnson S, Griego SD, Pfarr DS, Doyle ML, Woods R, et al. (1999) A direct comparison of the activities of two humanized respiratory syncytial virus monoclonal antibodies: MEDI-493 and RSHZ19. J Infect Dis 180: 35–40.
39. Lacy SE, DeVries PJ, Xie N, Fung E, Lesniewski RR, et al. (2008) The potency of erythropoietin-mimic antibodies correlates inversely with affinity. J Immunol 181: 1282–1287.
40. Lin YS, Nguyen C, Mendoza JL, Escandon E, Fei D, et al. (1999) Preclinical pharmacokinetics, interspecies scaling, and tissue distribution of a humanized monoclonal antibody against vascular endothelial growth factor. J Pharmacol Exp Ther 288: 371–378.
41. Benincosa LJ, Chow FS, Tobia LP, Kwok DC, Davis CB, et al. (2000) Pharmacokinetics and pharmacodynamics of a humanized monoclonal antibody to factor IX in cynomolgus monkeys. J Pharmacol Exp Ther 292: 810–816.
42. Deng R, Iyer S, Theil FP, Mortensen DL, Fielder PJ, et al. (2011) Projecting human pharmacokinetics of therapeutic antibodies from nonclinical data: what have we learned? MAbs 3: 61–66.
43. Vugmeyster Y, Xu X, Theil FP, Khawli LA, Leach MW (2012) Pharmacokinetics and toxicology of therapeutic proteins: Advances and challenges. World J Biol Chem 3: 73–92.
44. Richter WF, Bhansali SG, Morris ME (2012) Mechanistic determinants of biotherapeutics absorption following SC administration. AAPS J 14: 559–570.
45. Fischer K, Lewandowski D, Marijke van den Berg H, Janssen MP (2012) Validity of assessing inhibitor development in haemophilia PUPs using registry data: the EUHASS project. Haemophilia 18: e241–246.
46. Shire SJ, Shahrokh Z, Liu J (2004) Challenges in the development of high protein concentration formulations. J Pharm Sci 93: 1390–1402.
47. Pepinsky RB, Silvian L, Berkowitz SA, Farrington G, Lugovskoy A, et al. (2010) Improving the solubility of anti-LINGO-1 monoclonal antibody L33 by isotype switching and targeted mutagenesis. Protein Sci 19: 954–966.
48. Okuda M, Yamamoto Y (2004) Usefulness of synthetic phospholipid in measurement of activated partial thromboplastin time: a new preparation procedure to reduce batch difference. Clin Lab Haematol 26: 215–223.

REPORT

mAbs 5:2, 229–236; March/April 2013; © 2013 Landes Bioscience

Novel asymmetrically engineered antibody Fc variant with superior FcγR binding affinity and specificity compared with afucosylated Fc variant

Futa Mimoto, Tomoyuki Igawa,* Taichi Kuramochi, Hitoshi Katada, Shojiro Kadono, Takayuki Kamikawa, Meiri Shida-Kawazoe and Kunihiro Hattori

Research Division; Chugai Pharmaceutical Co., Ltd.; Tokyo, Japan

Keywords: antibody engineering, ADCC, A/I ratio, Fc engineering, FcγR

Abbreviations: ADCC, antibody-dependent cell-mediated cytotoxicity; T_M, melting temperature; mAb, monoclonal antibody; NK, natural killer; ITAM, immunoreceptor tyrosine-based activation motif; ITIM, immunoreceptor tyrosine-based inhibition motif; SPR, surface plasmon resonance; PBMC, peripheral blood mononuclear cells; FcγR, Fc gamma receptor

Fc engineering is a promising approach to enhance the antitumor efficacy of monoclonal antibodies (mAbs) through antibody-dependent cell-mediated cytotoxicity (ADCC). Glyco- and protein-Fc engineering have been employed to enhance FcγR binding and ADCC activity of mAbs; the drawbacks of previous approaches lie in their binding affinity to both FcγRIIIa allotypes, the ratio of activating FcγR binding to inhibitory FcγR binding (A/I ratio) or the melting temperature (T_M) of the C_H2 domain. To date, no engineered Fc variant has been reported that satisfies all these points. Herein, we present a novel Fc engineering approach that introduces different substitutions in each Fc domain asymmetrically, conferring optimal binding affinity to FcγR and specificity to the activating FcγR without impairing the stability. We successfully designed an asymmetric Fc variant with the highest binding affinity for both FcγRIIIa allotypes and the highest A/I ratio compared with previously reported symmetrically engineered Fc variants, and superior or at least comparable in vitro ADCC activity compared with afucosylated Fc variants. In addition, the asymmetric Fc engineering approach offered higher stability by minimizing the use of substitutions that reduce the T_M of the C_H2 domain compared with the symmetric approach. These results demonstrate that the asymmetric Fc engineering platform provides best-in-class effector function for therapeutic antibodies against tumor antigens.

Introduction

Monoclonal antibodies (mAbs) have enormous potential as anticancer therapeutics. MAbs promote elimination of tumor cells by Fab-dependent and Fc-dependent mechanisms, such as interference with signaling pathways, apoptosis induction, complement-dependent cytotoxicity, antibody-dependent cell-mediated phagocytosis and antibody-dependent cell-mediated cytotoxicity (ADCC).

ADCC is induced when effector cells are recruited by the Fc domain engaging with a member of the Fcγ receptor family, which is comprised in humans of FcγRI, FcγRIIa, FcγRIIb, FcγRIIc, FcγRIIIa and FcγRIIIb isoforms. FcγRI, FcγRIIa, FcγRIIc and FcγRIIIa are activating receptors characterized by the immunoreceptor tyrosine-based activation motif (ITAM), and FcγRIIb is the only inhibitory receptor characterized by ITIM. The receptors are expressed on a variety of immune cells, such as NK cells, monocytes, macrophages and dendritic cells.[1]

Increasing affinity for FcγR enhances ADCC, so Fc engineering is considered to be a promising means of increasing the antitumor potency of mAbs.[2] Previous reports described that follicular lymphoma patients treated with rituximab had, on average, significantly prolonged progression-free survival if they possessed two copies of the high-affinity FcγRIIIa allele, FcγRIIIa$^{V/V158}$.[3,4] This result suggests that the efficacy of rituximab is mediated by FcγRIIIa-expressing cells, such as NK cells, and that higher affinity to FcγRIIIa improves the efficacy. Several strategies have been employed to enhance the FcγR binding of mAbs. The first strategy was engineering the glycan moiety attached to Asn297 residue in the Fc domain. Afucosylated IgG1 antibody, which is a mAb without fucose in the N-linked glycan at Asn297, binds to FcγRIIIa with higher affinity and mediates superior ADCC compared with wild-type fucosylated IgG1 antibody.[5,6] The second strategy was introducing amino acid substitutions into the Fc domain. mAbs with triple substitutions, S239D/A330L/I332E, bind to FcγRIIIa with higher affinity and have shown superior

*Correspondence to: Tomoyuki Igawa; Email: igawatmy@chugai-pharm.co.jp
Submitted: 12/05/12; Revised: 12/27/12; Accepted: 12/31/12
http://dx.doi.org/10.4161/mabs.23452

ADCC activity than wild-type IgG.[7] In addition to enhancing the binding to activating FcγRs, minimizing the interaction with inhibitory FcγR, namely FcγRIIb, is another strategy to enhance the potential of the antibody.[8] Enhanced cancer elimination was observed in FcγRIIb knockout mice compared with that observed in mice expressing FcγRIIb when they were treated with anti-Her2/neu mAb or anti-E-cadherin mAb,[9,10] demonstrating that the ratio of activating FcγR binding to inhibitory FcγR binding (A/I ratio) is an important factor determining the therapeutic efficacy of antitumor antibody.[11] mAb with five substitutions, L235V/F243L/R292P/Y300L/P396L, showed enhanced binding to FcγRIIIa, but not to FcγRIIb, which improved the A/I ratio.[8] In terms of improving the selectivity for a specific FcγR, antibody variants with selectively enhanced binding for FcγRI were reported.[12]

Although these glyco- and protein-engineering approaches have successfully enhanced the effector function of mAbs, each technology has issues to overcome. First, afucosylated antibodies bind with lower affinity to FcγRIIIa^{F158} than to FcγRIIIa^{V158}. As a consequence, the resulting ADCC mediated by NK cells bearing the lower-affinity FcγRIIIa allotype is lower than that mediated by NK cells bearing the higher-affinity allotype, suggesting that afucosylated Fc may not achieve maximum ADCC activity for patients having the lower-affinity allotype.[13] Second, because activating and inhibitory FcγRs have high homology, the S239D/A330L/I332E variant also increased binding affinity against inhibitory FcγRIIb, which would be undesirable for achieving maximum antitumor efficacy considering the A/I ratio. Moreover, the T_M in the C_H2 domain of the S239D/A330L/I332E variant was significantly reduced (by more than 20°C), which could be an issue when the variant is developed as a pharmaceutical product.[14] Third, although the L235V/F243L/R292P/Y300L/P396L variant did not increase the binding affinity against inhibitory FcγRIIb, it had only 10-fold increased binding affinity to FcγRIIIa, which is substantially less than the S239D/A330L/I332E variant, thereby achieving only a moderate A/I ratio.

To date, neither glyco- nor protein-engineering has been able to overcome all these issues. Ideal therapeutic use requires an antibody Fc variant that has higher binding affinity to both FcγRIIIa^{F158} and FcγRIIIa^{V158} and better stability of the C_H2 domain, but that does not increase binding affinity to inhibitory FcγRIIb to maintain a higher A/I ratio. To overcome these issues, in this study we focused on the fact that homodimeric and symmetric Fc domain recognizes monomeric FcγR asymmetrically, which was previously revealed by the structural analysis of Fc fragment with FcγR.[15] Considering that Fc and FcγR interact asymmetrically, we hypothesized that asymmetric Fc engineering would make it possible to design a novel Fc variant with improved affinity against both low- and high-affinity FcγRIIIa allotypes, enhancing ADCC activity compared with previously known protein- or glyco-engineering. In addition, asymmetric Fc engineering would result in fewer substitutions or avoidance of the need for stability-reducing substitutions to minimize the reduction of the T_M of the C_H2 domain. Moreover, asymmetric Fc engineering would allow us to optimize the Fc-FcγR interaction more precisely so as not to increase binding affinity to inhibitory FcγRIIb and to have a higher A/I ratio by discriminating activating FcγRs from inhibitory FcγR.

We designed antibody variants with an asymmetrically engineered Fc domain (asym-mAb) by introducing different substitutions in each Fc domain. Comprehensive mutagenesis in the C_H2 domain has identified several substitutions that increase the binding affinity for FcγRs more strongly when they are introduced in one Fc domain than in both chains. We successfully designed an asym-mAb with hthigher affinity for both FcγRIIIa allotypes and superior or at least comparable ADCC than the previously reported symmetrically engineered antibody (sym-mAb), without increasing the affinity for FcγRIIb or substantially reducing the stability of the antibody. Our results demonstrated a novel approach for optimizing the interaction between Fc and FcγR and confirmed the advantage of that approach when applied therapeutically.

Results

Comparing the binding affinity for FcγRIIIa of asym-mAb and sym-mAb. We screened a set of over 1,000 asym- and sym-mAbs, each with a single substitution in the lower hinge and C_H2 domain, for binding to human FcγRIIIa^{F158} to identify substitutions that enhance FcγRIIIa binding only when they were introduced in one Fc domain. The effect of substitutions in both sym- and asym-mAbs was evaluated using surface plasmon resonance (SPR). We identified several unique substitutions to meet our criteria (binding affinity of asym-mAb > that of sym-mAb). Of them, we selected three single substitutions, L234Y, G236W and S298A, and designed a variant with L234Y/G236W/S298A (YWA) substitutions, to investigate whether asymmetric Fc engineering has any advantages over symmetric Fc engineering. As an example of symmetric Fc engineering, we utilized S239D/A330L/I332E (DLE) substitutions, which were previously reported to increase affinity to FcγRIIIa.[7] We prepared five variants: hemi-DLE variant, variant with DLE substitutions in only one Fc domain; homo-DLE variant, variant with DLE in both Fc domains; hemi-YWA variant, variant with YWA substitutions in only one Fc domain; homo-YWA variant, variant with YWA in both Fc domains and DLE/YWA variant with DLE in one Fc domain and YWA in the other Fc domain. We evaluated the affinity for FcγRIIIa^{F158} of each variant (**Table 1**). The representative sensorgrams are depicted in **Figure S1**.

First, we compared homo- and hemi-DLE variants to evaluate the effect of DLE substitutions in symmetric Fc engineering or asymmetric Fc engineering. The homo-DLE variant increased the affinity for FcγRIIIa 255-fold compared with control mAb1, which only has substitutions to facilitate heterodimerization of two heavy chains, while the hemi-DLE variant increased it only 30-fold. Next, we evaluated the other substitutions, YWA. The homo-YWA variant reduced the affinity 0.47-fold, but the hemi-YWA variant increased it 5.0-fold. YWA substitutions showed a distinctly different effect on the Fc-FcγRIIIa interaction when introduced in one Fc domain than when introduced in both Fc domains. The DLE/YWA variant showed the highest affinity among evaluated variants, even higher than the homo-DLE variant.

Table 1. *Affinity for FcγRIIIa^{F158} and T_M of antibody variants*

Fc variants	Substitutions in heavy chain A	Substitutions in heavy chain B	K_D (μmol/L)	Fold	T_M (°C)	ΔT_M (°C)
control mAb1	-	-	1.4 ± 0.3	1	68	-
hemi-YWA	-	L234Y/G236W/S298A	0.28 ± 0.04	5.0	68	0
hemi-DLE	S239D/A330L/I332E	-	0.046 ± 0.009	30	60	-8
homo-YWA	L234Y/G236W/S298A	L234Y/G236W/S298A	3.0 ± 0.6	0.47	68	0
homo-DLE	S239D/A330L/I332E	S239D/A330L/I332E	0.0055 ± 0.0005	255	48	-20
DLE/YWA	S239D/A330L/I332E	L234Y/G236W/S298A	0.0042 ± 0.0003	333	59	-9

$K_D = K_D$ for FcγRIIIa^{F158}. *Fold* = K_D (control mAb1)/K_D (Fc variants). T_M means T_M of the C_H2 domain. $\Delta T_M = T_M$ (Fc variants) - T_M (control mAb1). K_D was represented as mean ± SD (n = 3).

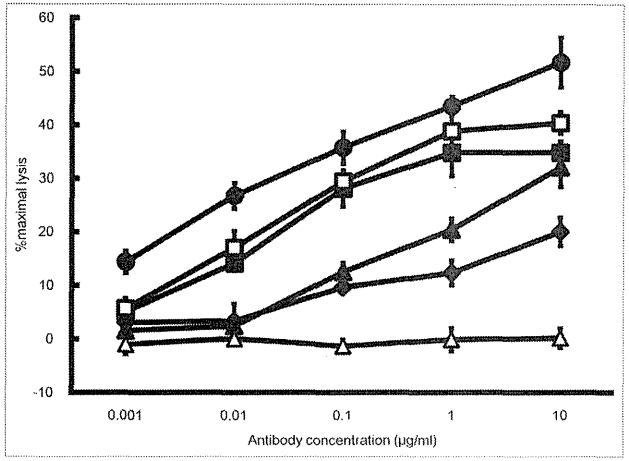

Figure 1. ADCC comparison of asym-mAbs and sym-mAbs. ADCC was determined by percent lysis of SK-Hep-1 cells expressing tumor antigen X at varying concentrations of antibody Fc variants to tumor antigen X using PBMC as effector cells. Mean ± SD of triplicate wells. Black diamond, control mAb1; white square, homo-DLE; black square, hemi-DLE; white triangle, homo-YWA; black triangle, hemi-YWA and black circle, DLE/YWA.

ADCC of antibody variants with asymmetrically engineered Fc. The cellular cytotoxicity of asym-mAb and sym-mAb to tumor antigen X with enhanced FcγRIIIa binding was evaluated using SK-Hep-1 cells expressing tumor antigen X and human PBMC (**Fig. 1**). Homo- and hemi-DLE variants showed higher ADCC than control mAb1, while ADCC of the homo-DLE variant was slightly higher than that of hemi-DLE. On the other hand, the homo-YWA variant showed no detectable ADCC, but the hemi-YWA showed higher ADCC than control mAb1. In ADCC assay, YWA substitutions showed this opposite effect whether they were introduced in both Fc domains or in only one Fc domain. The DLE/YWA variant with the highest FcγRIIIa binding showed the highest ADCC. These results from the ADCC assay were consistent with those obtained in the kinetic analyses of the variants.

Thermostability and accelerated stability study of antibody variants with asymmetrically engineered Fc. T_M of the C_H2 domain of hemi-DLE, homo-DLE, hemi-YWA, homo-YWA and DLE/YWA variants was measured by thermal shift assay (**Table 1**). The T_M of the C_H2 domain of hemi-DLE variant decreased by 8°C from control mAb1 and that of homo-DLE by 20°C. On the other hand, the T_M of hemi-YWA and homo-YWA variants was not significantly reduced, and that of the DLE/YWA variant decreased to the same degree as that of hemi-DLE variant.

After storage for two and four weeks at 40°C at a concentration of 1 mg/ml, the reduction of a monomer peak of each antibody in size-exclusion chromatography was compared

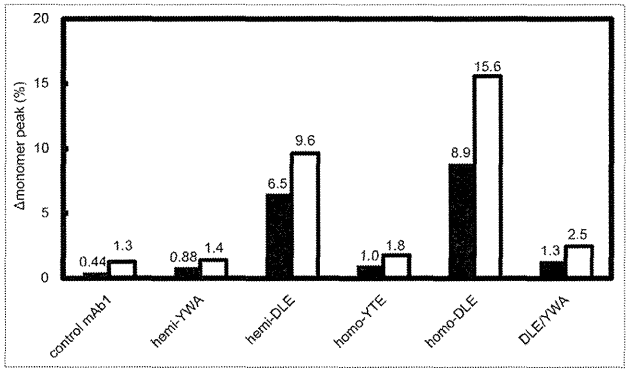

Figure 2. Stability of antibody Fc variants in accelerated stability study. Percentage of the reduction of a monomer peak (Δmonomer peak (%)) of each variant after storage at 40°C in size-exclusion chromatography is shown. Black and white bars represent the average reduction in monomer peaks after 2-week and 4-week storage, respectively. Each experiment was performed twice and individual data were shown in **Table S2**.

(**Fig. 2**). The monomer peak of hemi-DLE variant decreased ~10% after 4-week storage and that of homo-DLE decreased 16%. The same tendency was observed after 2-week storage. On the other hand, the reduction of monomer peaks of other variants, including DLE/YWA, was comparable with that of control mAb1.

Further optimization of asymmetrically engineered Fc. We further designed more potent asym-mAbs with higher binding affinity to active FcγRs. Further optimization to enhance FcγRIIIa binding was performed based on the result of comprehensive mutagenesis. As a result, we obtained asym-mAb1 containing L234Y/L235Q/G236W/S239M/H268D/D270E/S298A substitutions in one Fc domain and D270E/K326D/A330M/K334E substitutions in the other. We also prepared the reported protein- and glyco-engineered Fc variants to compare their affinity for FcγRs with asym-mAb1. Protein-engineered Fc variants were prepared by control mAb2, an antibody with only substitutions to facilitate heterodimerization of the two heavy chains. Afucosylated IgG1, afucosyl mAb and the homo-DLE variant were prepared as antibodies with enhanced FcγRIIIa binding, and the homo-L235V/F243L/R292P/Y300L/P396L (VLPYLL) variant was also prepared as an antibody with a high A/I ratio, without increased affinity for FcγRIIb.[8] Their increase of affinity for human FcγRs, A/I ratio and the reduction of T_M in C_H2 domain are shown in **Table 2**. K_D and T_M in C_H2 domain of these variants are summarized in **Table S1**.

Compared with the afucosyl mAb, homo-DLE variant and homo-VLPYLL variant, asym-mAb1 demonstrated greatly enhanced affinity for FcγRIIIa. Asym-mAb1 increased affinity for FcγRIIIa^{F158} by 2000-fold and for FcγRIIIa^{V158} by 1000-fold. On the other hand, the afucosyl mAb, homo-DLE variant and homo-VLPYLL variant enhanced affinity for FcγRIIIa^{F158} only by 18-, 286- and 63-fold and affinity for FcγRIIIa^{V158} only by 45-, 126- and 33-fold, respectively. As for the binding to FcγRIIb, the affinity for FcγRIIb of asym-mAb1 and of VLPYLL variant was comparable with that of control mab2.

Asym-mAb1 also demonstrated the highest A/I ratio. Asym-mAb1 increased A/I ratio for FcγRIIIa^{F158} 2000-fold and for FcγRIIIa^{V158} 1000-fold, while the afucosyl mAb, homo-DLE variant and homo-VLPYLL variant enhanced A/I ratio for FcγRIIIa^{F158} only by 7.7-, 43- and 119-fold and that for FcγRIIIa^{V158} only by 20-, 18- and 59-fold, respectively.

Homo-DLE variant reduced the T_M in C_H2 domain by 21°C, while other engineered Fc variants reduced it only by less than 10°C.

ADCC of further optimized asym-mAb. ADCC activity of the optimized asym-mAb was compared with that of afucosyl mAb using human PBMC obtained from four different donors. Asym-mAb1 showed remarkably greater ADCC activity than IgG1, and comparable or slightly higher ADCC activity compared with afucosyl mAb, as shown in **Figure 3 (A, B, C and D)**.

Discussion

Despite the fact that the Fc domain recognizes FcγRs asymmetrically with two distinct interfaces,[15] previous approaches for modifying Fc-FcγR interaction, such as alanine scanning mutagenesis, a protein structure design algorithm and a yeast surface displayed random mutant library screening, focused on modifying the Fc domain in a symmetric manner,[7,8,16] making it difficult to identify substitutions that enhance FcγR binding when they are introduced in only one Fc domain. We investigated such substitutions by comparing single-substituted asymmetric variants and the corresponding symmetric variants in comprehensive mutagenesis and combined the substitutions, L234Y, G236W and S298A, with the desired property that we identified through the investigation.

Table 2. Relative affinity for FcγRs and T_M in the C_H2 domain of Fc variants

Fc variants	FcγRIa	FcγRIIa^{R131}	FcγRIIa^{H131}	FcγRIIb	FcγRIIIa^{F158}		FcγRIIIa^{V158}		ΔT_M(°C)
	Fold K_D	Fold K_D	Fold K_D	Fold K_D	Fold K_D	Fold A/I	Fold K_D	Fold A/I	
afucosyl mAb	0.53	1.8	0.85	2.3	18	7.7	45	20	-2
homo-DLE	3.4	2.9	1.4	6.7	286	43	126	18	-21
homo-VLPYLL	0.36	0.32	2.2	0.54	63	119	33	59	-1
asym-mAb1	1.0	2.6	4.9	1.0	2167	2188	1054	1032	-6

Fold $K_D = K_D$ (control)/K_D (Fc variants). A/I = (K_D for FcγRIIb)/(K_D for FcγRIIIa^{F158}) or (K_D for FcγRIIb)/(K_D for FcγRIIIa^{V158}). Fold A/I = A/I (Fc variants)/A/I (control). $\Delta T_M = T_M$ in C_H2 domain (control) - T_M in C_H2 domain (Fc variants). In calculating the parameters of afucosyl mAb and protein-engineered Fc variants, those of IgG1 and control mAb2 were used as a control, respectively.

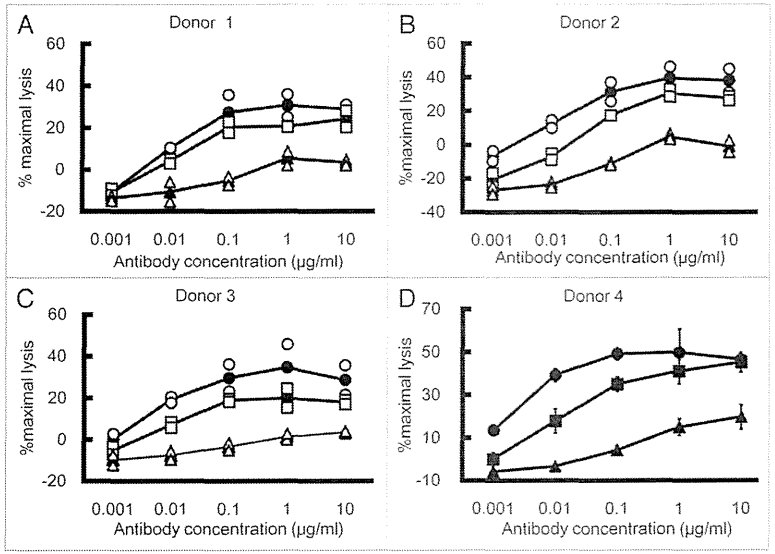

Figure 3. ADCC of antibody Fc variants. ADCC of IgG1, afucosyl mAb and asym-mAb1 was determined by percent lysis of DLD-1 cells expressing tumor antigen Y opsonized at varying concentrations of antibody Fc variants to tumor antigen Y using PBMC obtained from four different donors as effector cells with 10 mg/ml human IgG (A, B and C) or without it (D). Triangle, IgG1; square, afucosyl mAb and circle, asym-mAb1. (**A, B and C**) Open markers indicate individual data and closed makers with lines indicate average (n = 2). (**D**) Mean ± SD of triplicate wells.

We evaluated the FcγR binding and ADCC of homo-YWA, hemi-YWA, homo-DLE, hemi-DLE and DLE/YWA variants. In a previous analysis, DLE substitutions were thought to improve FcγR interaction mainly in one Fc domain.[7] In our results, hemi- and homo-DLE variant enhanced affinity for FcγRIIIa by 30- and 255-fold, respectively, compared with the wild-type antibody. While DLE substitutions in one Fc domain enhanced the binding affinity 30-fold, the gain of affinity by DLE substitution when introduced in the other Fc domain was only 8.5-fold, suggesting that DLE substitutions in each Fc domain contribute positively, but to differing degrees, to enhancing the binding affinity for FcγRIIIa. In contrast to DLE substitutions, YWA substitutions showed a distinct effect. While hemi-YWA variant enhanced affinity for FcγRIIIa 5.0-fold, homo-YWA variant substantially reduced the affinity. This result implies that YWA substitutions stabilize the interaction in one of the two interfaces with FcγRIIIa, but substantially destabilize the interaction in the other interface. The sum of the interactions in each Fc domain was not energetically beneficial, and, as a result, when YWA substitutions were introduced in both Fc domains, they substantially reduced the binding affinity to

FcγRIIIa. Although the hemi-YWA variant has enhanced binding affinity for FcγRIIIa, the binding affinity was weaker than that of the hemi-DLE variant. These results indicate that YWA substitutions are less potent than DLE substitutions both in hemi-manner and homo-manner; however, the DLE/YWA variant unexpectedly exhibited even higher affinity for FcγRIIIa than homo-DLE variant, suggesting that DLE and YWA enhance FcγRIIIa binding synergistically (not just additively) by stabilizing each of the Fc-FcγRIIIa interfaces simultaneously in a distinct structural environment. Importantly, although the homo-DLE variant was the most potent Fc variant reported to date, the effect of DLE/YWA variant demonstrated that Fc-FcγRIIIa interactions could be further optimized by the novel asymmetric engineering approach. Consistent with the affinity for FcγRIIIa, the DLE/YWA variant exerted stronger ADCC activity than homo-DLE. Among the evaluated variants, higher ADCC showed a general correlation with higher affinity for FcγRIIIa. This correlation demonstrates that asymmetrically engineered Fc could interact with FcγRIIIa expressed on effector cells in a similar manner to symmetrically engineered Fc.

DLE substitutions were reported to decrease T_M of the C_H2 domain by more than 20°C in a homo-DLE variant.[14] In our analysis, the homo-DLE variant did reduce the T_M by 20°C, but the hemi-DLE variant reduced it by only 8°C, less than half of the reduction by homo-DLE. On the other hand, even when YWA substitutions were introduced in both Fc domains, they did not decrease the T_M, and the DLE/YWA variant showed almost the same reduction in T_M as hemi-DLE. These results suggest that substitutions in each Fc domain reduce the T_M of the C_H2 domain independently and that the net reduction is the sum of them. To further clarify the storage stability of asym-mAb, we investigated the storage stability of each variant under accelerated conditions. The monomer peak of the homo-DLE variant was reduced by 16% after 4 weeks of accelerated storage, while that of hemi-DLE was reduced by about 10%, suggesting that DLE substitutions additively reduced the storage stability of the variants. On the other hand, the reduction in monomer peaks of homo-YWA, hemi-YWA and even DLE/YWA variants was comparable with that of wild-type antibody. These studies demonstrate that asymmetric engineering cannot only offer Fc variants with superior ADCC activity compared with the symmetric one, but can also offer Fc variants with higher stability.

By further optimizing the Fc domain in an asymmetric manner, we successfully generated asym-mAb1 variant. During the optimization of the DLE/YWA variant to generate asym-mAb1, we removed DLE substitutions because, despite the fact that DLE substitution significantly contributes to the increased binding affinity to FcγRIIIa, DLE substitutions even in one of the Fc domains significantly reduced the T_M of the C_H2 domain. To the best of our knowledge, asym-mAb1 binds to $FcγRIIIa^{F158}$ and $FcγRIIIa^{V158}$ with the highest affinity among any reported Fc engineered mAbs (K_D = 1.2 nM and 0.37 nM, respectively). Consistent with this increased binding affinity to FcγRIIIa, asym-mAb1 demonstrated significantly higher ADCC activity than IgG1, and comparable or slightly superior ADCC activity compared with afucosyl mAb. Asym-mAb1 showed slightly superior ADCC activity than afucosyl mAb in some donors, who might have lower-affinity FcγRIIIa genotype. Notably, asym-mAb1 increased FcγRIIIa binding affinity 1000-fold while maintaining inhibitory FcγRIIb binding comparable with wild-type IgG1. We assumed that this selectivity against FcγRIIb binding was achieved by fine-tuning each Fc-FcγR interaction, resulting in an A/I ratio of 1000 to 2000, which is far superior to the other Fc variants. Moreover, the T_M of the C_H2 domain in asym-mAb1 was 64°C, significantly higher than that of the homo-DLE variant and, though it is slightly lower than wild-type IgG, high enough for pharmaceutical development (**Table S1**). These results demonstrate that our novel asymmetric engineering provides an antibody Fc variant that has the strongest binding affinity for both $FcγRIIIa^{F158}$ and $FcγRIIIa^{V158}$ with no increased binding affinity to inhibitory FcγRIIb and with high stability of the C_H2 domain.

Although asym-mAb1 has a human FcγR binding property superior to other Fc variants, it is challenging to precisely evaluate and compare the therapeutic effects of these Fc-engineered antibody in human using an in vivo pre-clinical murine model system. This is because the structural diversity and expression patterns of murine FcγRs do not correspond to those of human FcγRs.[1] As expected, asym-mAb1 and other Fc variants bound to murine FcγRs with a different specificity and affinity (data not shown), making it impossible to predict their efficacy in human based on results from the murine model. It would be possible to predict the effect mediated by human FcγRIIIa by using human FcγRIIIa-transgenic mice as previously described, but it is still difficult to evaluate the effect mediated through other FcγRs, including the therapeutic advantage of superior A/I ratio.[17] A mouse whose FcγRs were replaced with human FcγRs was recently developed. This mouse recapitulated the unique expression pattern and the functions of human FcγRs that are mediated by human IgG[18] and might enable us to evaluate the effect of our asymmetrically engineered antibody in human more accurately.

Asymmetric bispecific IgG antibody, which binds to different antigens with each arm, was recently reported to be valuable in the field of hemophilia A[19] and approaches to overcome the problems involved in manufacturing this type of IgG antibody has been recently reviewed.[20] Cancer-targeting bispecific antibodies, although not in IgG form, have been investigated to enhance efficacy by targeting two different tumor antigens.[21] Since asymmetric bispecific IgG antibodies targeting two different tumor antigens inevitably require hetero-dimerization of the two heavy chains, our asymmetrically engineered Fc could be applied to such bispecific antibodies without any difficulty. Bispecific IgG antibody is a promising antibody format for next-generation antibody therapeutics, and our novel asymmetrically engineered Fc can be easily applied to the format to achieve maximum anti-tumor efficacy.

In conclusion, we demonstrated that asymmetric Fc engineering provides more effective optimization of the Fc-FcγR interaction and identified an asymmetric Fc variant with the highest binding affinity for both FcγRIIIa allotypes, the highest A/I ratio, and slightly higher ADCC activity than previously reported symmetric Fc variants. In addition, asymmetric Fc engineering minimized the use of substitutions that reduce the T_M of the C_H2 domain. Therefore, our asymmetric Fc engineering platform provides best-in-class effector function for maximizing the therapeutic potential of either monospecific or bispecific IgG antibodies against tumor antigens.

Materials and Methods

Preparation of antibodies. The antibody variants used in the experiments were expressed transiently in FreeStyle™ 293 cells (Invitrogen) transfected with plasmids encoding heavy and light chains and purified from culture supernatants using rProtein A Sepharose 4 Fast Flow or rProtein G Sepharose 4 Fast Flow (GE Healthcare). Site-directed mutagenesis of the constant regions of mAbs was performed using QuikChange Site-Directed Mutagenesis Kit (Stratagene) or In-Fusion HD Cloning Kit (Clontech) and the sequence was confirmed by DNA sequencing. The substitutions to facilitate Fc heterodimerization were introduced to obtain asym-mAbs consisting of different heavy chains.[20] Asym-mAbs were generated by Freestyle™ 293 cells transfected with three plasmids encoding a light chain and two different heavy chains. Sym-mAbs were generated by Freestyle™ 293 cells transfected with plasmids encoding a light chain and a heavy chain. Afucosylated antibody was prepared as previously described.[22]

Construction, expression and purification of FcγRs. The sequence information of genes encoding the extracellular region of human FcγRs was obtained from the National Center for Biotechnology Information (NCBI) and the genes were synthesized. FcγRs were fused with 6x His-tag at the C terminus. Vectors containing FcγRs were transfected into FreeStyle™ 293 cells (Invitrogen). Media were harvested and receptors were purified using cation exchange chromatography, nickel affinity chromatography and size exclusion chromatography. Instead of cation exchange chromatography, anion exchange chromatography was used to purify FcγRIa.

Comprehensive mutagenesis of the Fc domain of IgG1 and evaluation of its binding. Sym-mAb and corresponding asym-mab against tumor antigen X, each with a single substitution in only one heavy chain, were prepared for comprehensive mutagenesis assay. They were designed by substituting each of the residues 234–239, 265–271, 285, 296, 298, 300 and 324–337 (EU numbering) in the lower hinge and C_H2 domain with other 18 amino acids excluding cysteine. The Fc variants were expressed in 6-well cell culture plate (Becton, Dickinson and Company) transiently in FreeStyle™ 293 cells (Invitrogen) and purified from the culture supernatants using rProtein A Sepharose 4 Fast Flow or rProtein G Sepharose 4 Fast Flow (GE Healthcare) in a 96-well format. The concentrations of purified the Fc variants were determined by NanoDrop 8000 (Thermo Scientific). The binding activity of those variants to $FcγRIIIa^{158F}$ was quantified by a Biacore instrument. The variants were captured on the CM5 sensor chip (GE Healthcare) on which antigen peptide was immobilized, followed by injection of FcγRs. The binding of each antibody to each FcγR was normalized by the captured amount of each variant on the sensor chip and was expressed as a percentage of that of the antibody without the substitutions.

Kinetic analysis by surface plasmon resonance. The kinetic analysis of antibody variants for human FcγRs was monitored by SPR using a Biacore instrument (GE Healthcare), as previously described.[23] A recombinant protein L (ACTIGEN) was immobilized on CM5 sensor chip (GE Healthcare) using a standard primary amine-coupling protocol. Antibody variants were captured on the chip, followed by injection of FcγRs.

Thermal shift assay. T_M of the C_H2 domain of an antibody was measured as previously described.[24] The SYPRO orange dye (Invitrogen) was diluted into phosphate buffered saline (PBS; Sigma-Aldrich), before being added to the 0.3 mg/ml protein solutions. Fluorescence measurements were employed using a real-time polymerase chain reaction (RT-PCR) instrument, Rotor-Gene Q (QIAGEN). Rotor-Disc 72 was used with 20 μL of solution per well. The fluorescence emission was collected at 555 nm with a fixed excitation wavelength at 470 nm. During the measurement, the temperature was increased from 30°C to 99°C at a heating rate of 4°C/min.

Stability study under accelerated conditions. Antibodies were dialyzed against PBS and diluted to 1 mg/ml. The antibody solutions were stored at 40°C and analyzed before the treatment and after 2 weeks and 4 weeks. A monomer peak area of each antibody was analyzed with size-exclusion chromatography TSK-GEL G3000SWXL column (TOSOH) by SEC-HPLC with UV detection (Waters). The percentage of reduction from initial monomer peak area was calculated and reported using Empower Waters software.

ADCC assay. Cytotoxicity of antibody against antigen X and antigen Y was measured using a standard 4-h ^{51}Cr release assay and calcein-AM release assay, respectively.[6,25,26] Peripheral blood mononuclear cells (PBMC) were purified from whole human blood of healthy donors and used as effector cells. For ^{51}Cr-release assay, we used SK-Hep-1 cells transfected with tumor antigen X as target cells. Target cells were labeled with 1.85 MBq of ^{51}Cr at 37°C for 1 h in a CO_2 incubator. For calcein-AM release assay, DLD-1 cells expressing tumor antigen Y were labeled with calcein solution at 37°C for 2 h in a CO_2 incubator. 10 mg/ml human IgG (Sanglopor, CSL Behring K.K.) was added to mimic endogenous IgG in human. The number of tumor antigen X expressed on the cell surface was 9.8×10^4 per cell and that of tumor antigen Y was 3.7×10^5 per cell.

Antibody solution was mixed with target cells (1×10^4 cells) and then effector cells were added to the solution at 50:1 PBMC/target cell ratio. The solution was incubated in a CO_2 incubator at 37°C for 4 h. Supernatant was harvested and its radioactivity (in ^{51}Cr release assay) or the fluorescence emitted from its released calcein (in calcein-AM release assay) was quantified. Calculating the percentage of specific cell lysis from experiments was done using the following equation: % specific lysis = 100 × (mean experimental release - mean spontaneous release) ÷ (mean maximal release - mean spontaneous release). "Mean experimental release" is radioactivity in ^{51}Cr release assay or fluorescent emission in calcein-AM release assay of the supernatant from the reaction solution with antibody variants. "Mean spontaneous release" is radioactivity in ^{51}Cr release assay or fluorescent emission in calcein-AM release assay of the supernatant from the reaction solution without anvtibody. "Mean maximal release" is measured from the prepared supernatant by lysing the target cells with 2% NP-40.

Disclosure of Potential Conflicts of Interest

The authors have no conflicts of interests to disclose.

Acknowledgments

We thank our colleagues at Chugai Research Institute for Medical Science, Inc. and Chugai Pharmaceutical Co. Ltd., M. Fujii, Y. Nakata, A. Maeno and S. Masujima for antibody generation; M. Saito for carrying out SPR analysis and A. Sakamoto, M. Okamoto and M. Endo for carrying out preparation of human FcγRs. This work was fully supported by Chugai Pharmaceutical Co. Ltd.

Supplemental Materials

Supplemental materials may be found here:
www.landesbioscience.com/journals/mabs/article23452

References

1. Bruhns P. Properties of mouse and human IgG receptors and their contribution to disease models. Blood 2012; 119:5640-9; PMID:22535666; http://dx.doi.org/10.1182/blood-2012-01-380121
2. Scott AM, Allison JP, Wolchok JD. Monoclonal antibodies in cancer therapy. Cancer Immun 2012; 12:14; PMID:22896759
3. Cartron G, Dacheux L, Salles G, Solal-Celigny P, Bardos P, Colombat P, et al. Therapeutic activity of humanized anti-CD20 monoclonal antibody and polymorphism in IgG Fc receptor FcgammaRIIIa gene. Blood 2002; 99:754-8; PMID:11806974; http://dx.doi.org/10.1182/blood.V99.3.754
4. Weng WK, Levy R. Two immunoglobulin G fragment C receptor polymorphisms independently *predict response to rituximab in patients with follicular lymphoma*. J Clin Oncol 2003; 21:3940-7; PMID:12975461; http://dx.doi.org/10.1200/JCO.2003.05.013
5. Shields RL, Lai J, Keck R, O'Connell LY, Hong K, Meng YG, et al. Lack of fucose on human IgG1 N-linked oligosaccharide improves binding to human Fcgamma RIII and antibody-dependent cellular toxicity. J Biol Chem 2002; 277:26733-40; PMID:11986321; http://dx.doi.org/10.1074/jbc.M202069200
6. Shinkawa T, Nakamura K, Yamane N, Shoji-Hosaka E, Kanda Y, Sakurada M, et al. The absence of fucose but not the presence of galactose or bisecting N-acetylglucosamine of human IgG1 complex-type oligosaccharides shows the critical role of enhancing antibody-dependent cellular cytotoxicity. J Biol Chem 2003; 278:3466-73; PMID:12427744; http://dx.doi.org/10.1074/jbc.M210665200
7. Lazar GA, Dang W, Karki S, Vafa O, Peng JS, Hyun L, et al. Engineered antibody Fc variants with enhanced effector function. Proc Natl Acad Sci U S A 2006; 103:4005-10; PMID:16537476; http://dx.doi.org/10.1073/pnas.0508123103
8. Stavenhagen JB, Gorlatov S, Tuaillon N, Rankin CT, Li H, Burke S, et al. Fc optimization of therapeutic antibodies enhances their ability to kill tumor cells in vitro and controls tumor expansion in vivo via low-affinity activating Fcgamma receptors. Cancer Res 2007; 67:8882-90; PMID:17875730; http://dx.doi.org/10.1158/0008-5472.CAN-07-0696
9. Clynes RA, Towers TL, Presta LG, Ravetch JV. Inhibitory Fc receptors modulate in vivo cytotoxicity against tumor targets. Nat Med 2000; 6:443-6; PMID:10742152; http://dx.doi.org/10.1038/74704
10. Green SK, Karlsson MC, Ravetch JV, Kerbel RS. Disruption of cell-cell adhesion enhances antibody-dependent cellular cytotoxicity: implications for antibody-based therapeutics of cancer. Cancer Res 2002; 62:6891-900; PMID:12460904
11. Nimmerjahn F, Ravetch JV. Fcgamma receptors: old friends and new family members. Immunity 2006; 24:19-28; PMID:16413920; http://dx.doi.org/10.1016/j.immuni.2005.11.010
12. Jung ST, Reddy ST, Kang TH, Borrok MJ, Sandlie I, Tucker PW, et al. Aglycosylated IgG variants expressed in bacteria that selectively bind FcgammaRI potentiate tumor cell killing by monocyte-dendritic cells. Proc Natl Acad Sci U S A 2010; 107:604-9; PMID:20080725; http://dx.doi.org/10.1073/pnas.0908590107
13. Niwa R, Hatanaka S, Shoji-Hosaka E, Sakurada M, Kobayashi Y, Uehara A, et al. Enhancement of the antibody-dependent cellular cytotoxicity of low-fucose IgG1 Is independent of FcgammaRIIIa functional polymorphism. Clin Cancer Res 2004; 10:6248-55; PMID:15448014; http://dx.doi.org/10.1158/1078-0432.CCR-04-0850
14. Oganesyan V, Damschroder MM, Leach W, Wu H, Dall'Acqua WF. Structural characterization of a mutated, ADCC-enhanced human Fc fragment. Mol Immunol 2008; 45:1872-82; PMID:18078997; http://dx.doi.org/10.1016/j.molimm.2007.10.042
15. Radaev S, Motyka S, Fridman WH, Sautes-Fridman C, Sun PD. The structure of a human type III Fcgamma receptor in complex with Fc. J Biol Chem 2001; 276:16469-77; PMID:11297532; http://dx.doi.org/10.1074/jbc.M100350200
16. Shields RL, Namenuk AK, Hong K, Meng YG, Rae J, Briggs J, et al. High resolution mapping of the binding site on human IgG1 for Fc gamma RI, Fc gamma RII, Fc gamma RIII, and FcRn and design of IgG1 variants with improved binding to the Fc gamma R. J Biol Chem 2001; 276:6591-604; PMID:11096108; http://dx.doi.org/10.1074/jbc.M009483200
17. Junttila TT, Parsons K, Olsson C, Lu Y, Xin Y, Theriault J, et al. Superior in vivo efficacy of afucosylated trastuzumab in the treatment of HER2-amplified breast cancer. *Cancer Res 2010; 70:4481-9; PMID:20484044;* http://dx.doi.org/10.1158/0008-5472.CAN-09-3704
18. Smith P, DiLillo DJ, Bournazos S, Li F, Ravetch JV. Mouse model recapitulating human Fcγ receptor structural and functional diversity. Proc Natl Acad Sci U S A 2012; 109:6181-6; PMID:22474370; http://dx.doi.org/10.1073/pnas.1203954109
19. Kitazawa T, Igawa T, Sampei Z, Muto A, Kojima T, Soeda T, et al. A bispecific antibody to factors IXa and X restores factor VIII hemostatic activity in a hemophilia A model. Nat Med 2012; 18:1570-4; PMID:23023498; http://dx.doi.org/10.1038/nm.2942
20. Klein C, Sustmann C, Thomas M, Stubenrauch K, Croasdale R, Schanzer J, et al. Progress in overcoming the chain association issue in bispecific heterodimeric IgG antibodies. MAbs 2012; 4:653-63; PMID:22925968; http://dx.doi.org/10.4161/mabs.21379
21. Kontermann R. Dual targeting strategies with bispecific antibodies. MAbs 2012; 4:182-97; PMID:22453100; http://dx.doi.org/10.4161/mabs.4.2.19000
22. Ferrara C, Grau S, Jäger C, Sondermann P, Brünker P, Waldhauer I, et al. Unique carbohydrate-carbohydrate interactions are required for high affinity binding between FcgammaRIII and antibodies lacking core fucose. Proc Natl Acad Sci U S A 2011; 108:12669-74; PMID:21768335; http://dx.doi.org/10.1073/pnas.1108455108
23. Richards JO, Karki S, Lazar GA, Chen H, Dang W, Desjarlais JR. Optimization of antibody binding to FcgammaRIIa enhances macrophage phagocytosis of tumor cells. Mol Cancer Ther 2008; 7:2517-27; PMID:18723496; http://dx.doi.org/10.1158/1535-7163.MCT-08-0201
24. He F, Hogan S, Latypov RF, Narhi LO, Razinkov VI. High throughput thermostability screening of monoclonal antibody formulations. J Pharm Sci 2010; 99:1707-20; PMID:19780136
25. Neri S, Mariani E, Meneghetti A, Cattini L, Facchini A. Calcein-acetyoxymethyl cytotoxicity assay: standardization of a method allowing additional analyses on recovered effector cells and supernatants. Clin Diagn Lab Immunol 2001; 8:1131-5; PMID:11687452
26. Roden MM, Lee KH, Pancelli MC, Marincola FM. A novel cytolysis assay using fluorescent labeling and quantitative fluorescent scanning technology. J Immunol Methods 1999; 226:29-41; PMID:10410969; http://dx.doi.org/10.1016/S0022-1759(99)00039-3

SCIENTIFIC REPORTS

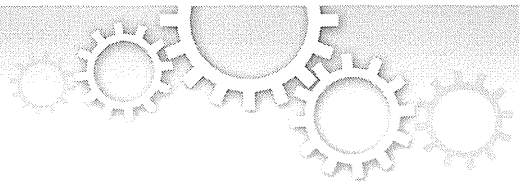

OPEN

SUBJECT AREAS:
GENETIC ENGINEERING
TRANSLATIONAL RESEARCH
EXPERIMENTAL MODELS OF DISEASE
IMMUNOPROLIFERATIVE DISORDERS

Received
14 November 2012

Accepted
15 January 2013

Published
1 February 2013

Correspondence and requests for materials should be addressed to K.-I.J. (jishagekui@chugai-pharm.co.jp)

Novel genetically-humanized mouse model established to evaluate efficacy of therapeutic agents to human interleukin-6 receptor

Otoya Ueda[1], Hiromi Tateishi[2], Yoshinobu Higuchi[1], Etsuko Fujii[1], Atsuhiko Kato[1], Yosuke Kawase[2], Naoko A. Wada[1,2], Takanori Tachibe[2], Mami Kakefuda[2], Chisato Goto[2], Makoto Kawaharada[2], Shin Shimaoka[1], Kunihiro Hattori[1] & Kou-ichi Jishage[1]

[1]Chugai Pharmaceutical Co. Ltd., Research Division, 1-135, Komakado, Gotemba, Shizuoka, Japan, [2]Chugai Research Institute for Medical Science Inc. 1-135, Komakado, Gotemba, Shizuoka, Japan.

For clinical trials of therapeutic monoclonal antibodies (mAbs) to be successful, their efficacy needs to be adequately evaluated in preclinical experiments. However, in many cases it is difficult to evaluate the candidate mAbs using animal disease models because of lower cross-reactivity to the orthologous target molecules. In this study we have established a novel humanized Castleman's disease mouse model, in which the endogenous interleukin-6 receptor gene is successfully replaced by human *IL6R*, and human IL6 is overexpressed. We have also demonstrated the therapeutic effects of an antibody that neutralizes human IL6R, tocilizumab, on the symptoms in this mouse model. Plasma levels of human soluble IL6R and human IL6 were elevated after 4-week treatment of tocilizumab in this mouse model similarly to the result previously reported in patients treated with tocilizumab. Our mouse model provides us with a novel means of evaluating the in vivo efficacy of human IL6R-specific therapeutic agents.

Worldwide trends in the development of therapeutic agents are towards the use of molecularly targeted drugs such as monoclonal antibodies (mAbs), which have revolutionized therapy for many intractable diseases. However, novel issues have emerged when evaluating their preclinical efficacy and safety[1–3]. It is usually difficult to evaluate the efficacy of therapeutic mAbs in animal experiments because, in most cases, they have no or low cross-reactivity to orthologous molecules of animals other than primates (phylogenetically the closest species to human). This means that systems using smaller experimental animals, such as mice and rats, are not applicable despite their obvious advantages. These advantages are that they are well-characterized after a long history of contributing to thousands of studies in various research fields of medical science, and their smaller body sizes require relatively small amounts of candidate agents. This latter advantage is especially useful at the early stage of drug development when a wider variety of drug candidates needs to be screened to select the best agent. As for the use of primates, this has been limited by disease outbreak risks, legislative changes and logistical problems with supply[2]. Moreover, it has also been pointed out that even an examination using primates would not be sufficient to perfectly predict clinical outcomes[4].

Some reviews propose the use of genetically engineered rodents and/or surrogate antibodies in order to predict the efficacy and safety of drug candidate antibodies in preclinical studies[1–3], but various attributes of the two tools need to be taken into account. For example, it will be costly and time-consuming to develop surrogate antibodies only for preclinical animal experiments and, even then, the surrogate antibodies would not necessarily work in the same manner as fully developed therapeutic antibodies. Genetic engineering in mice is a powerful technique to make loss-of-function or gain-of-function mutants for analyzing in vivo gene function and to develop animal models for human diseases, but the type of transgenic mouse established needs to correspond to its end purpose. To evaluate the pharmacokinetics, pharmacodynamics, in vivo efficacy, etc. of a drug, we must produce a genetically humanized mouse by the gene knock-in technique, in which a human target gene would be substituted and controlled to express in a similar spatial and temporal pattern to that of the endogenous orthologous gene. By

using such genetically humanized mice, we can expect to evaluate the in vivo efficacy of the drug candidate antibodies themselves, instead of using surrogate antibodies.

We have previously reported that transgenic mice with human interleukin-6 (hIL6) driven by the major histocompatibility complex class I *H-2L*^{d} gene promoter develop symptoms similar to Castleman's disease in human[4–6] such as lymphadenopathy, massive immunoglobulin G1 plasmacytosis, splenomegaly, mesangial proliferative glomerulonephritis, thrombocytopenia, leukocytosis, anemia and muscle atrophy[7,8]. We also demonstrated that a mAb to mouse IL-6 receptor, the surrogate antibody MR16-1, completely blocked their symptoms[8]. These findings indicate that neutralization of IL-6 signaling by a mAb to IL-6 receptor would be an effective therapeutic strategy for IL-6-related diseases. However, it is not possible to use these transgenic mice to evaluate the in vivo efficacy of drug candidate antibodies directly because they express murine IL-6 receptor (*Il6ra*) instead of human IL-6 receptor (h*IL6R*). A possible solution is to use a double transgenic mouse established by crossing an *H-2L*^{d}-h*IL6* transgenic mouse with an h*IL6R* transgenic mouse. As far as we know, two lines of h*IL6R* transgenic mice were previously reported[9,10]. However, these h*IL6R* transgenic mice cannot be used to evaluate therapeutic mAbs because they express not only hIL6R but also endogenous mouse Il6ra, which is well known as responding to human IL6. Therefore, it is necessary to neutralize or disrupt the endogenous mouse *Il6ra* before evaluating drug efficacy. Moreover, these h*IL6R* transgenic mice express extremely higher levels of hIL6R, driven by relatively stronger promoters. Therefore we predict that using these h*IL6R* transgenic mice to evaluate the therapeutic efficacy of neutralizing antibody to hIL6R would be difficult because the antibody, mediated by antigen, would disappear extremely rapidly from blood.

In this study we have generated a novel Castleman's disease mouse model, in which, in addition to the *H-2L*^{d}-h*IL6* transgene described above, mouse endogenous *Il6ra* gene is successfully replaced by h*IL6R* with the gene knock-in technique to establish a humanized ligand-receptor system for IL6 in mice. We have also demonstrated that symptoms of this model were almost completely blocked by administering tocilizumab, a humanized antibody against hIL6R[11]. These results demonstrate that genetically humanized mice will be powerful tools for directly evaluating in vivo efficacy of not only mAbs but also a wide variety of future therapeutic agents that are highly specific to human target molecules.

Results

Establishing a human IL6R knock-in mouse. The scheme for generating an h*IL6R* gene knock-in mouse is presented in Fig. 1a. Correctly targeted ES cell clones with the targeting vector were microinjected into the blastocysts of C57BL/6J (B6) mouse to make chimera mice. Male chimera mice were crossed with B6 females to obtain offspring with the hIL6R knock-in locus. Genomic PCR analysis of the offspring revealed that the full length of h*IL6R* cDNA with a floxed neomycin resistant gene (*neo*) cassette was correctly inserted in the target region by homologous recombination, and the knock-in allele was transmitted through the germline. To establish the h*IL6R* knock-in allele without the *neo* cassette, the Cre expression plasmid vector was microinjected into the pronuclei of fertilized eggs[12] that were obtained by crossing male heterozygous knock-in mice with C57BL/6J females. PCR product, amplified with the primer set depicted in Fig. 1a, reduced the size from 4.2 kb to 2.7 kb; this difference of 1.5 kb indicates the length of the *neo* cassette excised from the knock-in allele (Fig. 1b). Heterozygous mice without the *neo* cassette were intercrossed to obtain homozygous knock-in mice. This strain of the h*IL6R* knock-in mouse has been named B6;129S6-*Il6ra*$^{tm1(hIL6R)Csk}$. No apparent abnormalities were observed in h*IL6R* knock-in mice.

The results of RT-PCR for h*IL6R* or mouse *Il6ra* cDNA show that each reaction amplified the specific target correctly; that is, in the cDNA samples of homozygous *Il6ra*$^{hIL6R/hIL6R}$ mice, the human-specific *IL6R* target sequence was exclusively amplified and the mouse *Il6ra* sequence was not and, in the cDNA samples of wild-type (*Il6ra*$^{+/+}$) littermates, the mouse-specific *Il6ra* sequence was amplified and the h*IL6R* sequence was not. Signal intensities detected in the same organs were almost similar between h*IL6R* in *Il6ra*$^{hIL6R/hIL6R}$ mice and mouse *Il6ra* in *Il6ra*$^{+/+}$ mice (Fig. 1c).

Plasma soluble hIL6R in homozygous *Il6ra*$^{hIL6R/hIL6R}$ mice was detected at a range of 15 ng/mL–30 ng/mL (Fig. 1d), which is substantially similar to that reported in human[13–15]. Soluble hIL6R levels in heterozygous *Il6ra*$^{hIL6R/+}$ mice were at a range of 8 ng/mL–24 ng/mL, about half of those in homozygous *Il6ra*$^{hIL6R/hIL6R}$ mice, which indicates that soluble hIL6R levels in plasma would be dependent on the gene-dosage of knocked-in h*IL6R*. As determined by the plasma levels of serum amyloid A (SAA), which is produced by the hepatocytes in response to IL6[16], the h*IL6R* knock-in mice can respond to human IL6 but not mouse Il6, whereas wild type mice can respond to both human IL6 and mouse Il6 (Fig. 1e).

Establishing a humanized Castleman's disease model mouse. We have crossed the h*IL6R* knock-in mouse and the *H-2L*^{d}-h*IL6* transgenic mouse to establish a humanized Castleman's disease mouse model, which is named B6(Cg);129-*Il6ra*$^{tm1(hIL6R)Csk}$-Tg(IL6)40Csk. Enlargement of systemic lymph nodes and splenomegaly, typical symptoms of Castleman's disease[4–6], were observed in h*IL6* transgenic mice whether their *Il6ra* gene alleles were wild-type (*Il6ra*$^{+/+}$) (Fig. 2b) or humanized (*Il6ra*$^{hIL6R/hIL6R}$) (Fig. 2c). Histological observation revealed that the number of plasma cells and white pulps were increased in the spleen of both *Il6ra*$^{hIL6R/hIL6R}$-h*IL6* transgenic mice (Table 1, Fig. 3b), as compared to h*IL6* non-transgenic control mice (*Il6ra*$^{hIL6R/hIL6R}$ mice), shown in Fig. 3a.

Treatment with an hIL6R-neutralizing antibody in a humanized Castleman's disease mouse model. We then examined whether this novel humanized Castleman's disease mouse model can be used to evaluate the efficacy of hIL6R-specific therapeutic agents. We treated *Il6ra*$^{hIL6R/hIL6R}$-h*IL6* transgenic mice and *Il6ra*$^{+/+}$-h*IL6* transgenic mice with tocilizumab and MR16-1 (Fig. 2a). As we previously reported, tocilizumab has a neutralizing activity specifically against hIL6R but not against mouse Il6ra, whereas MR16-1 has a specific neutralizing activity to mouse Il6ra but not to hIL6R[17].

The spleen weights (mean ± SD) markedly increased to 0.26 ± 0.03 g in the vehicle-treated *Il6ra*$^{hIL6R/hIL6R}$-h*IL6* transgenic mice. These increased spleen weights were significantly different from those of the hIL6 non-transgenic *Il6ra*$^{hIL6R/hIL6R}$ mice group (0.08 ± 0.01 g). Treatment with tocilizumab markedly prevented the development of splenomegaly in male *Il6ra*$^{hIL6R/hIL6R}$-h*IL6* transgenic mice (Fig. 2c; Supplementary Fig. S1): the spleen weights at the end of 4-week treatment were decreased to 0.14 ± 0.03 g, 0.14 ± 0.02 g and 0.13 ± 0.03 g in groups treated with 0.1, 0.25 and 0.5 mg/body of tocilizumab, respectively. These values were not significantly different to those of the h*IL6* non-transgenic *Il6ra*$^{hIL6R/hIL6R}$ mice group. Spleen weights of the group treated with MR16-1, an antibody to mouse Il6ra (0.34 ± 0.11 g) increased to the same level as the vehicle-treated group.

In contrast, in *Il6ra*$^{+/+}$-h*IL6* transgenic mice tocilizumab treatment does not show preventive effects on the splenomegaly (0.45 ± 0.26 g) observed in the vehicle-treatment group (0.34 ± 0.09 g), whereas MR16-1 markedly prevented splenomegaly at a dose of 0.1 mg/body, with spleen weights decreasing to 0.12 ± 0.01 g. These values were not significantly different to those of h*IL6* non-transgenic *Il6ra*$^{+/+}$ mice (0.08 ± 0.01 g) (Fig. 2b; Supplementary Fig. S1). The spleen weights also displayed great interindividual variability in *Il6ra*$^{+/+}$-h*IL6* transgenic mice treated with tocilizumab (Fig. 2b).

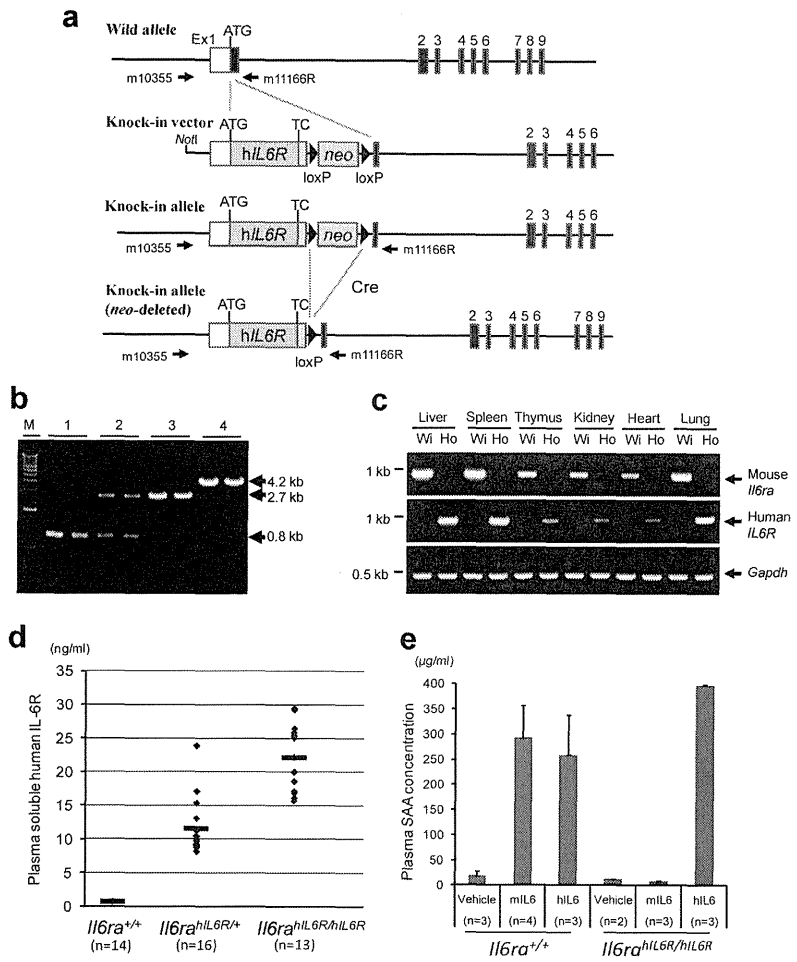

Figure 1 | Generation of human IL6 receptor (*IL6R*) gene knock-in mouse. (a) Schematic representation of the knock-in strategy for the h*IL6R* gene. A knock-in vector was constructed by inserting h*IL6R* cDNA with *neo* cassette flanked by two loxP sites into the mouse *Il6ra* genomic locus in the frame of a BAC genomic clone. A knock-in allele and a *neo*-deleted knock-in allele are also shown. Arrows indicate PCR primers (m10355 and m11166R) for genotyping. TC, terminal codon. (b) A representative result of genotyping to confirm the *neo*-depleted h*IL6R* knock-in allele and homozygosity of the h*IL6R* knock-in allele. Wild-type allele and knock-in allele were detected as signals of 0.8 kb and 4.2 kb, respectively, whereas knock-in allele after removing *neo* cassette was detected as a signal of 2.7 kb. M, DNA molecular marker. Numbers above the gel denote the mouse genotypes, (1) *Il6ra*$^{+/+}$, (2) *Il6ra*$^{hIL6R/+}$, (3) *Il6ra*$^{hIL6R/hIL6R}$ and (4) *Il6ra*$^{hIL6R(neo)/hIL6R(neo)}$. (c) Representative results of RT-PCR analysis for tissue distribution of *Il6ra*$^{+/+}$ (Wi) and *Il6ra*$^{hIL6R/hIL6R}$ (Ho) mice. (d) Plasma levels of soluble hIL6R in *Il6ra*$^{+/+}$ (n = 14), *Il6ra*$^{hIL6R/+}$ (n = 16) and *Il6ra*$^{hIL6R/hIL6R}$ mice (n = 13). (e) Species-specific ligand response was confirmed after intraperitoneal injection of mouse Il6 (mIL6) or human IL6 (hIL6) in *Il6ra*$^{+/+}$ and in *Il6ra*$^{hIL6R/hIL6R}$ mice. Ligand responses were evaluated by the elevation of plasma SAA levels after injection of vehicle (n = 3), mIL6 (n = 4) and hIL6 (n = 3) in *Il6ra*$^{+/+}$ and those of vehicle (n = 2), mIL6 (n = 3) and hIL6 (n = 3) in *Il6ra*$^{hIL6R/hIL6R}$.

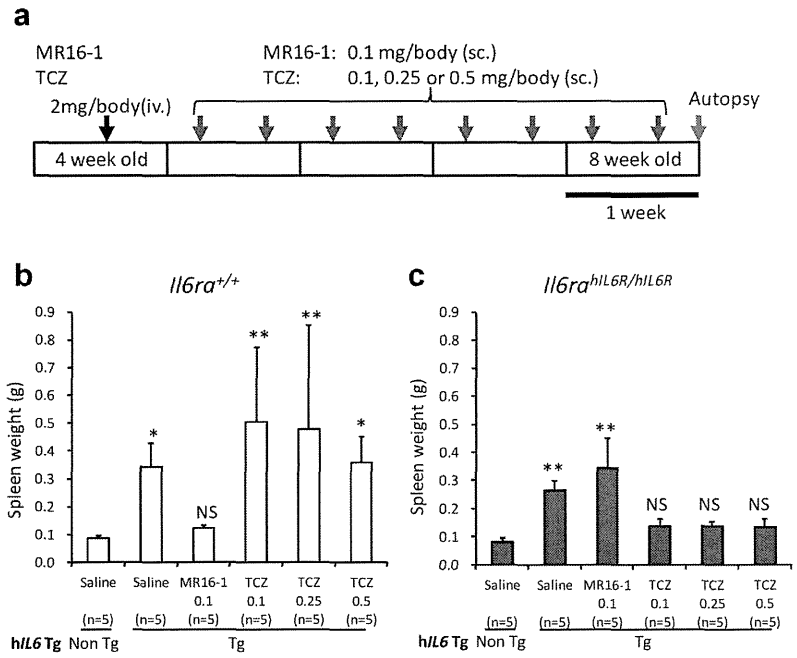

Figure 2 | Treatment with an hIL6R-neutralizing antibody in humanized Castleman's disease model mice. (a) Protocol for 4-week treatment with the anti-mouse Il6ra antibody, MR16-1, or the anti-human IL6R antibody, tocilizumab (TCZ). (iv.), intravenous injection; (sc.) subcutaneous injection. (b) Spleen weights of *Il6ra*$^{+/+}$-h*IL6* transgenic mice and (c) *Il6ra*$^{hIL6R/hIL6R}$-h*IL6* transgenic mice after 4-week treatment (n = 5 per group). Statistical significances were determined by nonparametric comparisons with control using the Dunn method for joint ranking. The data of each treatment group were compared with those of the respective h*IL6* non-transgenic mouse group in each genotype of interleukin-6 receptor, *Il6ra*$^{+/+}$ (b) and *Il6ra*$^{hIL6R/hIL6R}$ (c). *, $p < 0.05$, **, $p < 0.01$ and NS, not significant. Non Tg, h*IL6* non-transgenic mice; Tg, h*IL6* transgenic mice.

An increase in the amount of plasma cells in the marginal zone was observed in all of the saline-treated *Il6ra*$^{hIL6R/hIL6R}$-h*IL6* transgenic mice (Table 1, Fig. 3b) compared to non-transgenic mice (Table 1, Fig. 3a), and aggregates of plasma cells were observed in one of three animals (Table 1, Fig. 3b). Additionally, increased numbers of white pulp was observed in saline-treated *Il6ra*$^{hIL6R/hIL6R}$-h*IL6* transgenic mice (Table 1, Fig. 3e) compared to non-transgenic mice (Table 1, Fig. 3d), which was evidenced by the incidence of white pulp, and this finding was accompanied by enlargement of the total spleen area (Table 1, Fig. 3e). Pathological symptoms of the spleen in tocilizumab-treated *Il6ra*$^{hIL6R/hIL6R}$-h*IL6* transgenic mice were substantially ameliorated upon histological observation at the end of the 4-week treatment (Table 1, Fig. 3, c and f) compared with saline-treated *Il6ra*$^{hIL6R/hIL6R}$-h*IL6* transgenic mice.

Plasma levels of human soluble IL6R and human IL6 were markedly increased at the end of a 4-week tocilizumab treatment in *Il6ra*$^{hIL6R/hIL6R}$-h*IL6* transgenic mice (Fig. 4, a and b). Antibodies to the drug were minimally detected in *Il6ra*$^{hIL6R/hIL6R}$-*hIL6* transgenic mice even after repeated subcutaneous administration of tocilizumab (Fig. 5).

Table 1 | Incidence of histopathological findings of splenic lymphocytes in humanized Castleman's disease model mice with or without tocilizumab treatment

		Il6ra$^{hIL6R/hIL6R}$		
Findings	Severity	Non Tg Saline	h*IL6* Tg Saline	h*IL6* Tg Treated†
*Increased plasma cells	−	3/3	0/3	4/5
	±	0/3	2/3	1/5
	+	0/3	1/3	0/5
**Increased number of white pulp	−	3/3	0/3	1/5
	+	0/3	0/3	4/5
	++	0/3	3/3	0/5

Severity of findings: *±, increased amount of plasma cells in the marginal zone compared to non-transgenic mice; +, aggregates of plasma cells observed in the marginal zone. ** +, increased incidence of white pulp compared to non-transgenic mice; ++, increased incidence of white pulp with enlargement of the total spleen area.
Non Tg, h*IL6* non-transgenic mice; h*IL6* Tg, human *IL6* transgenic mice.
Numerals indicate the number of animals examined.
†, treated with tocilizumab.

Discussion

We have established a line of h*IL6R* knock-in mice, in which endogenous mouse *Il6ra* gene is successfully replaced by h*IL6R* cDNA.

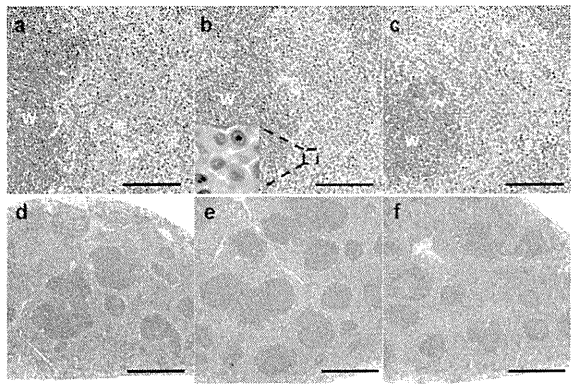

Figure 3 | Spleen tissue of an *Il6ra*$^{hIL6R/hIL6R}$ mouse (a, d), an *Il6ra*$^{hIL6R/hIL6R}$-h*IL6* transgenic mouse (b, e), and a tocilizumab-treated *Il6ra*$^{hIL6R/hIL6R}$-h*IL6* transgenic mouse (c, f). Increase of plasma cells and increased numbers of white pulp in the *Il6ra*$^{hIL6R/hIL6R}$-h*IL6* transgenic mouse (b, e) were ameliorated after 4-week treatment with tocilizumab (c, f). Plasma cells are shown in insert (b). Bars: (a–c), 100 μm; (d–f), 500 μm. W, white pulp.

Results of RT-PCR analysis indicate that tissue distribution of the knocked-in h*IL6R* expression is well-controlled by endogenous transcription mechanisms (Fig. 1c). Membrane-bound hIL6R expressed on the cell surface in these mice would be normally released to the blood as soluble hIL6R, which lacks the transmembrane and cytoplasmic region[18,19], and the plasma levels of soluble hIL6R are revealed to be similar to those reported in Castleman's disease[13,14], rheumatoid arthritis patients[14] and healthy volunteers[14,15]. According to our survey, two lines of h*IL6R* transgenic mice were previously established[9,10]. Both of them were reported to have higher serum levels of soluble hIL6R than healthy humans. Peters *et al.* established a line of hIL6R transgenic mice, driven by *phosphoenolpyruvate carboxykinase* gene promoter, in which serum concentrations of soluble hIL6R were described to range between 4 and 8 μg/mL[9,20], several hundred times higher than those in human. Moreover, these h*IL6R* transgenic mice express only the soluble type of hIL6R, not the membrane-bound type. Another line of h*IL6R* transgenic mice was established to express the membrane bound type of hIL6R, driven by

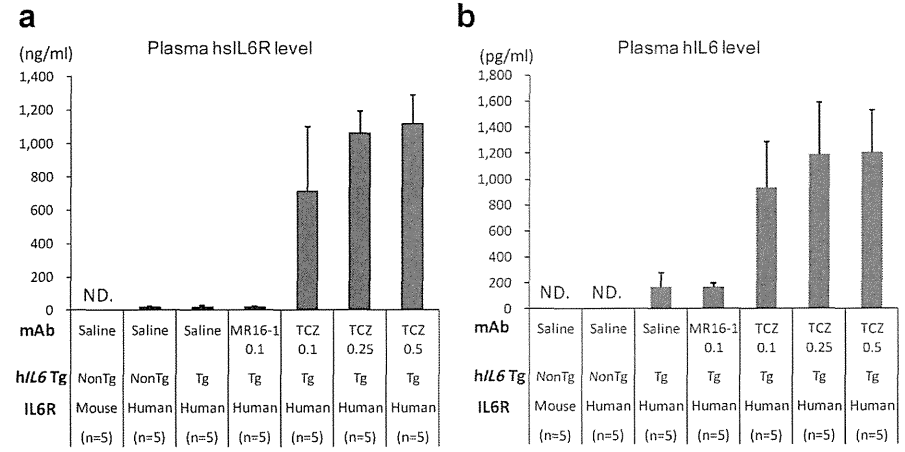

Figure 4 | Plasma levels of soluble hIL6R (a) and hIL6 (b) concentration after 4-week treatment with 0.1, 0.25 and 0.5 mg/body of TCZ in each genotype of mouse (n = 5 per group). (a) Plasma soluble hIL6R concentrations were approximately 21 ng/ml in saline-treated *Il6ra*$^{hIL6R/hIL6R}$-h*IL6* transgenic mice, whereas marked elevation of plasma soluble hIL6R levels, approximately 40–50 times higher than those of vehicle control, was observed after 4 weeks in TCZ-treated *Il6ra*$^{hIL6R/hIL6R}$-h*IL6* transgenic mice. (b) Plasma hIL6 was detected at the level of 163 pg/ml in saline-treated *Il6ra*$^{hIL6R/hIL6R}$-h*IL6* transgenic mice, whereas the hIL6 levels were markedly elevated to the levels of 936–1204 pg/ml after 4-week treatment of TCZ. ND, not detected. Non Tg, h*IL6* non-transgenic mice; Tg, h*IL6* transgenic mice.

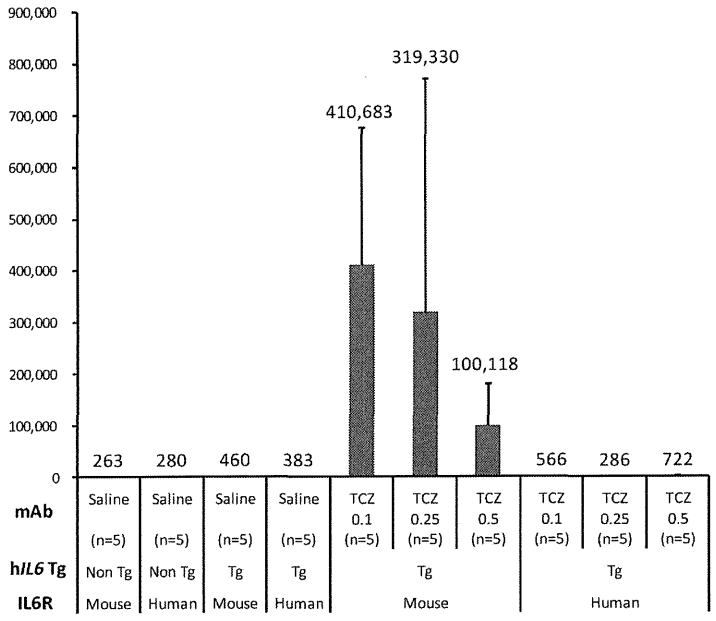

Figure 5 | Titers of plasma anti-drug antibodies after 4-week treatment with 0.1, 0.25 and 0.5 mg/body of TCZ in each genotype of mouse (n = 5 per group). Extremely high levels of plasma anti-TCZ-antibody titers were detected in *Il6ra*$^{+/+}$-h*IL6* transgenic mice, whereas those in TCZ-treated *Il6ra*$^{hIL6R/hIL6R}$-h*IL6* transgenic mice were minimally detected. Non Tg, h*IL6* non-transgenic mice; Tg, h*IL6* transgenic mice.

a strong promoter cassette pCAGGS[21], in which serum concentrations of soluble hIL6R were described to range between 80 and 100 ng/mL[22], about 4–5 times higher than those in human. Taken together, for the first time we have succeeded in genetically humanizing *IL6R* in mice to produce blood levels of soluble hIL6R similar to those in human, with plasma concentrations of soluble hIL6R ranging between 15 and 30 ng/mL (Fig. 1d).

No apparent abnormalities were observed in human *IL6R* knock-in mice, a fact which shows that human *IL6R* expression does not affect animal health under normal breeding conditions. Histological observation revealed that the spleens of *Il6ra*$^{hIL6R/hIL6R}$ mice did not show any abnormalities (Fig. 3a). Homozygous *Il6ra*$^{hIL6R/hIL6R}$ mice deplete the downstream signal from IL6R because human IL6R cannot bind to mouse endogenous Il6[19,23], but this lack of IL6 signaling would not have apparent effects on animal health in normal conditions, as described in several reports that either *Il6* or *Il6ra* gene-disrupted mice are viable and have normal appearance[24–27]. We have detected elevated plasma SAA levels that confirm the species-specific ligand responses after intraperitoneal injection of mouse Il6 or human IL6 to the h*IL6R* knock-in mice. Homozygous *Il6ra*$^{hIL6R/hIL6R}$ mice exclusively respond to human IL6 only, and not to mouse Il6 (Fig. 1e). These responses are compatible with the fact that mouse Il6ra can respond to both mouse Il6 and human IL6, whereas hIL6R can respond to human IL6 only[19,23]. These results strongly suggest that our h*IL6R* knock-in mouse expresses not mouse endogenous Il6ra, but a functional hIL6R molecule that can transduce the downstream signals normally.

Recently, either albumin-expressing hepatocyte-specific or lysozyme M-expressing macrophage/granulocyte-specific *Il6ra* gene knockout mice have been established by crossing mice having floxed alleles of *Il6ra* (*Il6ra*$^{fl/fl}$) with mice expressing Cre recombinase under the control of albumin (*AlbCre*) or lysozyme M promoter (*LysCre*)[27]. McFarland-Mancini *et al.* demonstrated that soluble Il6ra level in plasma was more dependent on immune cell secretion than hepatic production by showing that *AlbCre*$^{+/+}$/*Il6ra*$^{fl/fl}$ mice had higher levels of soluble Il6ra (67.95% of *Cre*$^{-/-}$/*Il6ra*$^{fl/fl}$) than *LysCre*$^{-/-}$/*Il6ra*$^{fl/fl}$ mice (39.95%)[27]. However, SAA production after challenge with turpentine in *AlbCre*$^{+/+}$/*Il6ra*$^{fl/fl}$ mice was severely inhibited, whereas plasma SAA level in *LysCre*$^{-/-}$/*Il6ra*$^{fl/fl}$ mice was similar to that of wild-type mice. Consequently, membrane-bound Il6ra on the hepatocytes makes a critical contribution to hepatic SAA production, meaning that trans-signaling by soluble Il6ra may not have a significant role in SAA production. We have demonstrated that *Il6ra*$^{hIL6R/hIL6R}$ mice can respond to exogenous hIL6 to produce SAA, which strongly suggests that *Il6ra*$^{hIL6R/hIL6R}$ mice express intact membrane-bound hIL6R, at least on the hepatocytes.

The *Il6ra*$^{hIL6R/hIL6R}$-h*IL6* transgenic mouse established in this study showed basically typical Castleman's disease symptoms (enlargement of systemic lymph nodes and splenomegaly) similar to those previously reported in *Il6ra*$^{+/+}$-h*IL6* transgenic mice[7,8]. Histological observation revealed that the number of white pulps is also increased in *Il6ra*$^{hIL6R/hIL6R}$-h*IL6* transgenic mice. White pulp consists of an accumulation of lymphocytes, mostly B-cells; therefore, these results indicate that the knocked-in hIL6R can respond normally to human IL6 to cause B-cell differentiation and proliferation in white pulp in vivo in the same way as endogenous mouse Il6ra in wild-type mice. Extramedullary hematopoiesis was also observed in the spleen of *Il6ra*$^{hIL6R/hIL6R}$-h*IL6* transgenic mice (data not shown) as previously reported in *Il6ra*$^{+/+}$-h*IL6* transgenic mice[7,8].

We have also examined the therapeutic efficacy of an hIL6R-specific neutralizing antibody on the Castleman's disease-like symptoms in this mouse model. As far as we know, this humanized Castleman's disease mouse model is the first small rodent that can be used to evaluate in vivo efficacy of a therapeutic antibody specific to human IL6R. Our results suggest that sufficient efficacy was observed at a low dose, 0.1 mg/body of tocilizumab, when administered to this mouse model in our dosing scheme. Even when we increased the dose of tocilizumab to 0.25 or 0.5 mg/body, further reduction of spleen weights was not observed; therefore, it may be possible to decrease the dose of tocilizumab further to find the minimal dose level. We would like to define the therapeutic window of tocilizumab, as well as the improved antibodies[28] described below, in a future study. Marked elevation of plasma soluble hIL6R and human IL6 levels was also observed in our mouse model similar to that reported by Nishimoto *et al.* in the patients with Castleman's disease or rheumatoid arthritis that had been treated with tocilizumab[14]. Nishimoto *et al.* concluded that it was likely that soluble hIL6R increased because the formation of a tocilizumab/soluble hIL6R immune complex prolonged its elimination half-life, and that free serum IL6 increased because IL6R-mediated consumption of IL6 was inhibited by the lack of tocilizumab-free IL6R[14]. We consider that increased plasma levels of soluble hIL6R and human IL6 in tocilizumab-treated *Il6ra*$^{hIL6R/hIL6R}$-h*IL6* transgenic mice could be caused by a mechanism similar to that in humans, and that our humanized Castleman's disease model would substantially reflect the clinical outcomes seen in the tocilizumab-treated patients.

Nowadays various technologies for optimizing therapeutic antibodies (in other words, antibody-engineering technologies) have been intensively developed by leading researchers, and improving the pharmacokinetics of these expensive therapeutic antibodies to reduce the dose or dosing frequency will be an increasingly important issue[28]. It is necessary to determine the therapeutic window, dosing frequency and route of administration while fully understanding the binding affinity to antigen, the pharmacokinetics and the biodistribution of each antibody modified with various sorts of functions[28]. We propose that our mouse model, expressing a physiological level of hIL6R, will be well-suited for preclinical studies assessing a modified function added to the backbone of new therapeutic antibodies. Our mouse model also has the merit of being smaller in body size than other animal species, such as primates, so smaller amounts of candidate agents would be sufficient for evaluation.

Antibody titers to the drug tocilizumab were only minimally detected, despite the repeated and frequent subcutaneous administration (Fig. 5), so that evaluation of in vivo efficacy of humanized hIL6R-neutralizing antibody was possible after 4-week treatment in this novel Castleman's disease mouse model. Although the cause of these low titer levels remains to be investigated, we are currently considering two possibilities. The first is that tolerance might be successfully induced by relatively higher first dosing (2 mg/body) of humanized antibody intravenously. This possibility is suggested by two recent reports using MR16-1, a rat antibody to mouse Il6ra. Yoshida *et al.* reported that first intravenous dosing (2 mg/body) inhibited the production of antibodies to MR16-1 after repetitive intraperitoneal or subcutaneous injections of MR16-1 in NZB/NZW F1 mice[29]. Sakurai *et al.* also suggested the possibility that tolerance induction would inhibit the production of antibody to drug after finding that antibodies to MR16-1 were detected in some mice treated with 15 mg/kg of MR16-1 intravenously every 3 days but not detected in 50 mg/kg groups[30]. In our study, however, in *Il6ra*$^{+/+}$-h*IL6* transgenic mice expressing only mouse Il6ra, the same doses of tocilizumab produced extremely high titers of anti-tocilizumab antibodies, suggesting that there might be some other mechanism than tolerance induction from a first higher dosing. Therefore we would like to propose a second possibility: that IL6 signal blockade by tocilizumab itself might also suppress the production of antibodies to tocilizumab. In *Il6ra*$^{-/-}$-hIL6 transgenic mice, which express mouse Il6ra but not human IL6R, tocilizumab cannot inhibit IL6 signaling. Therefore, tocilizumab would be treated as nothing more than a foreign substance, not as a therapeutic agent, and might stimulate systemic inflammation induced by hIL6 as well as a strong immune response. As a result, extremely high titers of antibodies to tocilizumab were detected in tocilizumab-treated *Il6ra*$^{-/-}$-hIL6 transgenic mice (Fig. 5). We also speculate that there would be considerable interindividual variability in the exacerbation of systemic inflammatory response, which could cause the large interindividual variation of spleen weights seen in *Il6ra*$^{-/-}$-hIL6 transgenic mice (Fig. 2). In summary, at least two mechanisms, namely tolerance induction (with relatively higher first dosing) and IL6 signal blockade, might be necessary to inhibit the production of antibodies to tocilizumab.

IL6 is a multifunctional cytokine that has a wide range of biological activities in various target cells. Therefore not only Castleman's disease and rheumatoid arthritis but many other diseases and disorders, such as multiple myeloma, sepsis, mesangial proliferative glomerulonephritis, and cancer cachexia, may also be associated with IL6 over-production and subsequent uncontrolled IL6 signaling[18,19,31]. It is predicted that an increasing number of researchers in the future will continue to develop many therapeutic agents molecularly-designed to target hIL6R. Finally, we expect that our mouse model provides a novel system for evaluating in vivo efficacy of the next generation of hIL6R-specific therapeutic agents and also for assessing antibody-engineering technologies to treat patients with Castleman's disease, rheumatoid arthritis, and other diseases caused by abnormalities in IL6 signaling.

Methods

Generation of human IL6R gene knock-in mice. All animal experiments were performed in accordance with the Guidelines for the Care and Use of Laboratory Animals at Chugai Pharmaceutical Co. Ltd.

A line of human *IL6R* gene knock-in mice was established basically by the protocol we reported previously[1,2,32–33]. The methods are briefly described as follows. The targeting vector, constructed by the seamless insertion of human IL6R gene cDNA (GenBank # NM_000565) into the mouse Il6ra genomic locus on the BAC clone with pRed/ET system (Quick and Easy BAC Modification kit, GeneBridges GmbH, Heidelberg) as shown in Fig. 1a, was introduced by electroporation to the 129/SvEv mouse ES cells. The ES cells were selected in a culture medium containing G418. Homologous recombinant ES cell clones were injected into C57BL/6J (B6) mouse (CLEA Japan, Inc., Tokyo) blastocysts to produce chimera mice. Chimera mice were bred with B6 females to generate offspring. After confirmation of germline transmission, *neo* gene cassette was removed from the knock-in allele by pronuclear microinjection of the Cre recombinase expression vector[12]. Removal of the *neo* gene cassette was confirmed by PCR using the primers m10355 (5′-TCTGCAGTAGCCTTCAAAGAGC-3′) and m11166R (5′-AACCAGACAGTGTCACATTCC-3′). *Neo*-deleted allele was determined at 2.7 kb, whereas *neo*-intact allele and wild-type allele were detected at 4.2 kb and 0.8 kb, respectively (Fig. 1b). Heterozygous mice were intercrossed to produce homozygous mice.

RT-PCR analysis was performed to determine tissue distribution of human and mouse IL-6R expression. Total RNA samples extracted from tissue samples with Isogen reagents (Nippon Gene Co. Ltd., Tokyo, Japan) were reverse-transcribed with SuperScript III reverse-transcriptase (Invitrogen) to synthesize cDNA. PCRs were performed with a common forward primer 6RIK-s1 (5′-CCCGGCTGCGGAGCCGCTCTGC -3′) set in 5′ untranslated region and species-specific reverse primers in the coding sequences: 6RI.IcA2 (5′-AGCAACACCGTGAACTCCTTTG-3′) for mouse Il6ra and RLI6-a1 (5′-ACAGTGATGCTGGAGGTCCTT-3′) for human IL6R, respectively. Serum concentrations of soluble-type receptors were determined as described below.

Species-specific ligand-receptor reaction was examined by plasma levels of SAA after intraperitoneal injection of human and mouse IL-6. In this experiment *Il6ra*$^{hIL6R/hIL6R}$ mice and *Il6ra*$^{-/-}$ mice were used. Plasma SAA levels were determined by the commercially available ELISA kit (Invitrogen), according to the manufacturer's protocol.

Establishment of humanized Castleman's disease model mice. The h*IL6R* knock-in mice were crossed with the *H-2L*^{d}-h*IL6* transgenic mice to establish double transgenic mice, that is, *Il6ra*$^{hIL6R/hIL6R}$-h*IL6* transgenic mice, which have homozygous alleles for